1980

Prediction of fatigue failure in steel bridge, August 1980

H. M. Woodward

J. W. Fisher

Lehigh University

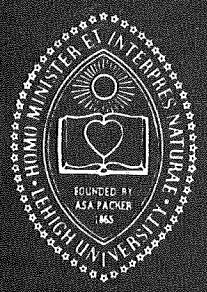

High Cycle Fatigue of Welded Bridge Details

PREDICTIONS OF FATIGUE FAILURE IN STEEL BRIDGES

by

Hugh M. Woodward
John W. Fisher

Fritz Engineering Laboratory

Report No. 386-12(80)

COMMONWEALTH OF PENNSYLVANIA

Department of Transportation

Research Division

Wade L. Gramling - Research Engineer
Istvan Janauschek - Research Coordinator

High Cycle Fatigue of Welded Bridge Details

PREDICTION OF FATIGUE FAILURE IN STEEL BRIDGES

by

Hugh M. Woodward
John W. Fisher

Prepared in cooperation with the Pennsylvania Department of Transportation and the U. S. Department of Transportation, Federal Highway Administration.

LEHIGH UNIVERSITY

Office of Research

Bethlehem, Pennsylvania

August 1980

Fritz Engineering Laboratory Report No. 386-12(80)

TABLE OF CONTENTS

		Page
	ABSTRACT	iv
1.	INTRODUCTION	1
	1.1 Background and Objectives	1
	1.2 Fatigue Failure Criteria	1
	1.3 Objectives of Tests on Lehigh Canal Bridge	5
2.	TESTING OF LEHIGH CANAL BRIDGE	7
	2.1 Description of Bridge	7
	2.2 Tie Plate Cracks	7
	2.3 Phases of Investigation	8
	2.4 Strain Gages	9
	2.5 Data Recording System	10
	2.6 Truck Arrival Time Observations	11
	2.7 Data Reduction	11
3.	CYCLE COUNTING PROCEDURES	15
	3.1 Historical Counting Procedures	15
	3.2 Selection of Cycle Counting Methods	15
	3.3 Compilation of Stress Range Spectra	17
4.	MULTIPLE PRESENCE PARAMETERS	19
	4.1 Truck Headway Model	19
	4.2 Computer Simulation of Multiple Presence	20
	4.3 Cumulative Effect of Multiple Presence	21
	4.4 Multiple Presence Factors	22

		Page
5.	IMPACT AND ELASTIC ADJUSTMENT FACTORS	24
	5.1 Design Impact Factors	24
	5.2 Impact Factors on Lehigh Canal Bridge	24
	5.3 Elastic Analysis Adjustment Factor	26
6.	CYCLE COUNTING PARAMETERS	29
	6.1 Fatigue Category for Tie Plate Details	29
	6.2 Peak to Peak Methods	29
	6.3 Rainflow Methods	35
	6.4 Recommended Cycle Counting Parameters	37
7.	CURRENT PRACTICE	38
	7.1 AASHTO Fatigue Specifications	38
	7.2 Multiple Presence Factors	38
	7.3 Impact and Elastic Adjustment Factors	39
	7.4 Cycle Counting Parameters	40
8.	CONCLUSIONS	41
9.	TABLES AND FIGURES	44
10.	APPENDICES	93
	Appendix A: Data Reduction - Stage 1	93
	Appendix B: Cycle Counting Parameters	98
	Appendix C: Stress Range Spectra for Selected Details by Each Cycle Counting Technique	110
	Appendix D: Derivation of Formula to Compute Effective Fatigue Damage with Multiple Presence	135
11.	REFERENCES	137
12.	ACKNOWLEDGMENTS	140

ABSTRACT

Extensive testing of the Lehigh Canal Bridge is reported with particular emphasis on the tie plate details that experienced fatigue cracking. Three phases of data acquisition - controlled load, measured load and random stress history - are described. The data is analyzed in order to isolate the parameters which a designer could use to predict fatigue failure in the steel details of highway bridge.

The rainflow cycle counting technique is compared to the traditional peak to peak method and the use of these methods at details where severe cracking had occurred indicates that the rainflow method is not substantially more accurate in its prediction than the peak to peak method. Moreover, it is shown that the rainflow method is inherently more complex and costly to apply in either an experimental or a design situation.

The peak to peak method applied to the stress history data is shown to confirm recent evidence that the constant cycle fatigue limit is inappropriate if it is exceeded by any part of the stress range spectrum of a detail subjected to random loading.

Consideration is given to multiple presence and it is shown that although a Poisson process adquately describes truck arrival times that in continuous multiple span bridges the effect of multiple presence can be conservatively ignored.

The primary reasons for this conclusion are that (1) trucks which are very closely spaced travel in different lanes causing an only

slight elevation in stress at selected details accompanied by a reduction in the effective number of cycles, and (2) most concurrently present trucks are more than 1.5 seconds apart, again marginally elevating the stress range but reducing the effective number of cycles.

Impact factors and elastic analysis adjustment factors were measured at several details and although they are expected to vary from bridge to bridge the results for the Lehigh Canal Bridge are reported.

Finally, the results of this investigation are compared with current practice as defined by the American Association of State Highway and Transportation Officials[18].

1. INTRODUCTION

1.1 Background and Objectives

Fatigue cracks have recently been detected on several steel highway bridges in the United States. Among these bridges, all of which occur on heavily trafficked arteries, are the Yellow Mill Pond Bridge on the Connecticut Turnpike, the Lehigh River and Lehigh Canal Bridges on U. S. Route 22 in Pennsylvania and the Allegheny River Bridge on the Pennsylvania Turnpike.

Recent laboratory studies[6,7] indicate that stress range under the action of live load and impact controls the fatigue behavior of structural details. For the purposes of examining further the fatigue behavior of some steel bridge details under traffic loading and correlating the stress range history of these details with laboratory fatigue data, extensive testing of one of the Lehigh Canal Bridges was undertaken.

This report describes the bridge and the test procedure, and summarizes the results.

1.2 Fatigue Failure Criteria

The prediction of fatigue cracking in controlled laboratory tests is now fairly well defined within the limits of the statistical variation, and is described in Refs. 5, 6 and 7. The fatigue life, N_i, is related to the applied stress range, S_{ri}, as follows:

$$N_i = AS_{ri}^{-3} \tag{1.1}$$

where A is a function of the fatigue behavior of a detail.

However, when the stress range applied to a detail varies, the analysis becomes more complicated. Miner[14] suggested that a linear fatigue damage equation, $\Sigma\, n_i/N_i = 1$, defines the failure of a detail, where n_i is the number of cycles of stress range S_{ri}.

If a detail undergoes random loading, then a fatigue damage factor, F, defined by:

$$F = \Sigma \frac{n_i}{N_i} \tag{1.2}$$

can be used to compare the severity of loading at the detail over a finite period of time. It can be seen that failure will occur when

$$F = 1 \tag{1.3}$$

Substituting the expression for N_i in Eq. 1.1 into Eq. 1.2 gives:

$$F = \frac{1}{A} \Sigma\, n_i S_{ri}^{3} \tag{1.4}$$

This equation will be used extensively throughout this report.

However, in the case of a detail situated in a highway bridge, there are no well defined rules as to what to use for N_i and S_{ri} in the fatigue life equation. A further complication is that a designer's knowledge of the service conditions of a bridge is often very limited. This report will examine some of the parameters which

determine these variables and suggest values to be used for bridge structures.

It has been shown by several researchers[2,12] that the relationship between gross vehicle weight (GVW) and stress range can be considered linear, and is usually constant for similar vehicles. Hence, the relationship between actual stress range and (GVW) can be expressed as:

$$S_r = \alpha\beta \ (1 + \gamma I) \ (GVW) \tag{1.5}$$

where I is the design impact factor, γ is the fraction of the design impact factor produced by the vehicle, β is the elastic constant relating load and stress at a particular detail and α is an experimental adjustment factor to account for the unforseen behavior of a bridge. Hence, over a finite period of time, the fatigue damage factor, F, is given by:

$$F = \frac{1}{A} \ \Sigma \ n_i \ (\alpha\beta)^3 \ (1 + \gamma I)^3 \ (GVW)_i^3 \tag{1.6}$$

and if α, β, γ and I are regarded as constants, then

$$F = \frac{1}{A} \ (\alpha\beta)^3 \ (1 + \gamma I)^3 \ \Sigma \ n_i \ (GVW)_i^3 \tag{1.7}$$

The factor $\Sigma \ n_i \ (GVW)_i^3$ is further complicated by the fact that each truck passage causes a random stress excursion. Historically, it has been assumed that each truck passage causes one stress cycle with the stress range being defined as the difference between maximum and minimum stresses. This was based on observations at the

AASHO Road Test where reasonable correlation was provided between laboratory test data and fatigue cracking of several steel bridge beams[8]. However, recent evidence has indicated that this may be in error and that some other method of cycle counting may be more appropriate[16]. Using the peak to peak method of counting, it would be appropriate to put

$$\Sigma\, n_i\, (GVW)_i^3 = N_D\, (GVW)_D \tag{1.8}$$

where $(GVW)_D$ is a weighted average value of (GVW) and N_D is the design life of the bridge. For a constant traffic volume,

$$N_D = \text{ADTT} \times 365 \times \text{life in years} \tag{1.9}$$

where ADTT is the average daily truck traffic. However, it may be more appropriate to write:

$$\Sigma\, n_i\, (GVW)_i^3 = (C_N N_D) \times \{C_s\, (GVW)_D\} \tag{1.10}$$

where C_N and C_s are factors to correct results for cycle counting related errors.

Finally, concern has been expressed by Moses and Pavia[15] that multiple presence of trucks on the bridge may cause greater fatigue damage than that predicted by a single presence model, and that in fact:

$$\Sigma\, n_i\, (GVW)_i^3 = (h_N C_N N_D) \times \{h_s C_s\, (GVW)_D\} \tag{1.11}$$

where h_N and h_s are factors to correct results for errors caused by neglecting the effect of multiple presence.

In summary, fatigue failure will occur at a detail when

$$N S_r^3 = A \tag{1.12}$$

where

$$N = h_N C_N N_D \tag{1.13}$$

and

$$S_r = \alpha\beta\, h_s C_s\, (1 + \gamma I)\, (GVW)_D \tag{1.14}$$

1.3 Objectives of Tests on Lehigh Canal Bridge

The test procedure on the Lehigh Canal Bridge was designed to identify the unknown variables in Eqs. 1.13 and 1.14.

A series of tests using a truck of known weight and axle spacing driven over the bridge at very slow and normal speeds was used to identify the impact factor, γI, in Eq. 1.14. The results of this experiment are outlined in Chapter 5.

Over 200 trucks, which passed over the bridge during the test period, were stopped and weighed. These results were used in conjunction with the design β factor, to estimate the experimental elastic adjustment factor, α, for the Lehigh Canal Bridge. This data is also summarized in Chapter 5.

Two observations of truck spacing times were conducted to identify a model for the statistical variation of this parameter. Using this data and a computer analysis of the bridge behavior the

effect of multiple presence of trucks was estimated and the values of the multiple presence parameters h_N and h_s calculated. A description of this procedure and the results forms Chapter 4 of this report.

Finally, the stress excursions at 56 gages were monitored during the passage of over 8000 trucks. Some of these gages were positioned on tie plates where cracks had occurred and this stress history data was used to give an indication of the cycle counting parameters, C_s and C_N. A summary of the data and results is found in Chapter 3.

2. TESTING OF LEHIGH CANAL BRIDGE

2.1 Description of Bridge

The Lehigh Canal Bridges consist of twin bridges which carry the eastbound and westbound lanes respectively of U. S. Route 22 near Allentown, Pennsylvania. Each bridge is continuous for three spans with small haunches at interior piers. Each bridge has two riveted steel longitudinal girders with a floor beam stringer system and noncomposite concrete deck. An end span of the eastbound bridge was chosen for detailed investigation because of its accessibility, but stresses in details on all spans of the eastbound bridge were monitored in parts of the investigation. A plan and elevation of the bridge is shown in Fig. 1, with a typical cross-section shown in Fig. 2. The bridges were constructed in 1951-53 and opened to traffic in November 1953.

2.2 Tie Plate Cracks

Inspections by Pennsylvania Department of Transportation personnel in the spring of 1972 revealed several cracks in the tie plates in both the Lehigh Canal Bridges and the adjacent Lehigh River Bridges which were of similar design. Most of these cracks were at or near the outside edge of the longitudinal girders and some had cracked across the entire width of the plate. However, all cracks appeared to be through the thickness of the plate and all started at

the edge of the tie plates from a tack weld which was used to connect the tie plates to the outrigger bracket during fabrication. The most severe cracking occurred near piers and abutments.

A more detailed description of the cracking has been given in Refs. 9 and 10.

Annual inspections of cracking in the eastbound Lehigh Canal Bridge have been maintained by Fritz Engineering Laboratory and observations of crack growth recorded. These observations are summarized in Table 1. On some occasions, the cracks were noted but the length was not recorded. In these cases, the presence of a crack is denoted by a "c". Table 1 also records the cracks which were repaired in late 1974 prior to the comprehensive testing in November 1974. Tie plates 1 and 2 on the south girder were replaced in April 1974, during a related investigation[3]. These plates were not attached to the girders and no crack was observed at last inspection in August 1976.

2.3 Phases of Investigation

There were three main phases of data collection during the testing of November 1974. In phase 1 a truck of known weight was allowed to cross the bridge while other traffic was restricted. At least two passes in each lane were made, one of which was very slow and the other at normal driving speed. This procedure was followed four times, so that all gages could be connected into the system at

least once. The dimensions and weight of this truck are shown schematically in Fig. 3. The results of this phase were used to evaluate the impact factor at each detail where a gage existed, and are summarized in Chapter 5.

Phase 2 involved the random selection of 260 trucks which, after passing over the bridge at a measured speed, were stopped and weighed. The objective of this phase was to compare the stress excursions, at selected details, caused by these trucks with the computed influence line for stress at that point. This comparison would then lead to the calculation of the stress adjustment factor for that detail. The results of this analysis are also outlined in Chapter 5.

Phase 3, the major phase of the investigation, involved monitoring 56 of the gages continuously for almost six days. Although the equipment was turned off for light traffic, a recording was made of the effect of every truck during the period. The aim of this phase was to derive a stress histogram for each of these 56 gage positions and perform cycle counting analysis to identify the appropriate cycle counting parameters. This process is outlined in Chapter 3.

2.4 Strain Gages

Two gages were installed on each of the 54 tie plates. In addition, gages were mounted on the brackets, stringers and girders at two cross-sections where tie plate cracking had been severe.

These cross-sections corresponded to the first and second floor beam positions, respectively, from the western end or approach span of the bridge. Figure 4 shows the positioning of gages at the northern end of the second floor beam. Miscellaneous gages were placed on the cantilever brackets at the northern end of the first and second floor beams and on the top and bottom flanges of both girders at positions corresponding to the fourth and seventh floor beams from the western end of the bridge.

All gages were 6 mm long electrical resistance foil gages and were temperature compensated in their connection.

2.5 Data Recording System

The data was recorded simultaneously in both analog and digital forms, using the FHWA automatic data acquisition system and analog trace recorder. The current in the gage was converted to a factored measure of the strain in the detail by a Wheatstone Bridge circuit and following amplification, the impulse was fed simultaneously to an analog trace recorder and to an analog-digital converter. Finally, the digital values were stored on 9-track tape by a tape recorder. A flow diagram of the recording system is shown in Fig. 5.

Throughout the test period, up to 62 gages were continuously sampled, and each of these was sampled at a rate of 20 samples per second. The data were recorded on the tape in blocks of 1013 samples, separated by a 16-digit number which reflected the exact

time of the sampling, the number of channels being sampled and an identity number which was dialed on the front of the machine by the operator.

2.6 Truck Arrival Time Observations

In order to arrive at a model describing the statistical distribution of truck arrival times, or the time elapsed between the arrival of a truck at the bridge abutment and that of the immediate subsequent truck, two observations were made in November and December, respectively, of 1976.

The first observation lasted only twenty minutes, in which time, 79 trucks crossed the bridge. The second observation was for a duration of two hours and involved 400 trucks. On both occasions, the arrival time and number of axles was recorded for every truck. The data obtained and the arrival time model are described in Chapter 4.

2.7 Data Reduction

During the phase 1, or controlled load, tests, no digital values of strains were acquired, so manual measurements of the analog trace was the only possible method of data reduction. Some typical traces are shown in Fig. 6. By comparison of a trace of this type with a standardized calibration record, the maximum stress range for each truck passage on the particular detail can be computed. The

resulting stresses for each of the tie plate gages under static loading are shown in Table 2. The tie plates are numbered from the western end of the bridge, and hence plates numbered 1 and 27 occur over abutments, and plates numbered 9 and 19 occur over piers.

The analog records of the random load tests, or phase 3 were far too voluminous to be reduced manually so a computer program was prepared for automatic manipulation of the recorded samples. In order to allow as much flexibility as possible in the preparation of histograms from the gage readings, the data was reduced in two stages. In stage I, the blocks of 1013 samples were sorted into channels and each stationary point in the strain-time curve was recorded. In stage II the summarized values were used to calculate the stress ranges during a truck passage, by several cycle counting techniques, and these were assembled into a complete histogram for that detail.

The computer program for stage I was designed to identify calibration recordings, calculate the calibration value for each gage and store these values separately from the rest of the data. For the truck passages, the stationary points were recorded according to the following criteria:

1. Threshold levels were set for each channel, and all stress excursions within the threshold levels were ignored. These threshold levels were set at such a value that the number of stationary points during a truck passage did not exceed 18, in most cases. This criteria was only established for

computer storage and cost considerations. The actual threshold levels used averaged about 9 MPa, and are listed in Table 3.

2. Each time the recorded stress either exceed the upper threshold level or was less than the lower threshold level, only one stationary point was recorded either until the stress remained within the threshold levels for a period in excess of one second or until stress reversal occurred with a subsequent value outside the threshold levels.

Some examples of the use of these criteria are described in Appendix A.

The stage II computer program used the results of stage I to construct stress range spectra. This compilation was done using four methods of cycle counting:

1. The peak to peak method based on the assumption that each stress excursion record was the result of a single truck passage across the bridge,
2. The peak to peak method with the effect of closely spaced trucks included in the analysis,
3. The "rainflow" counting technique, and
4. A modified form of the rainflow counting technique.

These stress cycle counting methods are more fully explained in Chapter 4 along with a summary of the resulting stress range spectra.

The phase 2 records, containing all the stress excursion data for the trucks which were stopped and weighed, were analyzed as part of phase 3. However, additional data was obtained in the form of peak to peak stresses at certain details for each truck passage. These values were used in conjunction with an elastic analysis of the bridge to compute the elastic adjustment factor (α). The results of this phase are presented in Chapter 5.

3. CYCLE COUNTING PROCEDURES

3.1 Historical Counting Procedures

In the United States, almost all previous field investigation of cyclic stress has been performed using the peak to peak method of cycle counting. That is, each truck was considered to produce one cycle of a stress range computed by subtracting the minimum stress from the maximum stress[8,11].

Although the peak to peak method gave good results[8] it has never been established that the method is analytically correct. In recent years, several other methods have been developed including the peak count, the mean-crossing peak count, the range count, the range-mean count, the range-pair count, the level-crossing count, and the rainflow count methods. Of these, the rainflow count method is the most popular because it is based on a consideration of the stress-strain characteristics of the material. These methods are described in detail by Matsuiski and Endo[13], by Watson and Dabell[17], Schijve[19], and Webber[20]. A brief description is given in Appendix B.

3.2 Selection of Cycle Counting Methods

A sample of 55 trucks was used to thoroughly investigate the cycle counting methods available, four of which were selected for detailed study. The first two of these methods were:

1. The peak to peak method without separation of multiple presence, and

2. The peak to peak method with separation of multiple presence. During the data acquisition, many of the stress excursion records were created by the passage of more than one truck. The first peak to peak method assumes one truck per record and reflects the simplest way of applying the peak to peak method in an experimental analysis. The second method separated the effects of multiple trucks present on the bridge, although very close spacing could not be identified and the record was treated as a single truck. This method, therefore, more accurately reflects a design analysis.

The other methods adopted for detailed study were:

3. The rainflow method which was chosen for its popularity and its theoretical basis. This method assumes plasticity at the crack tip and actually counts hysteresis loops on the stress-strain diagram for the material in the plastic zone.

4. A modified form of the rainflow method which counted each reversal as a half-cycle without reference to hysteresis considerations. It is, in fact, the rainflow method applied to an elastic crack tip. It was not expected to give good results but was chosen to isolate the effect of this simplification.

Among other methods investigated and discarded was one which defined an increase in tensile stress or a decrease in compressive stress as one cycle of a stress range equal to the algebraic

difference between the maximum and minimum stress. However, the fatigue damage factor for this method varied considerably with the threshold level and in fact, could show a significant decrease as the threshold was lowered. For example, the stress excursion shown in Fig. 7 has a fatigue damage factor of $3.43 \times 10^5/A$ using the peak to peak method, and $2.38 \times 10^5/A$ for the rainflow method irrespective of whether the threshold level is set at 5 or 10 MPa (0.75 or 1.5 ksi). However, the increase in tensile stress method gives a fatigue damage factor of $1.33 \times 10^5/A$ if the threshold level is 10 MPa (1.5 ksi) and only $3.5 \times 10^4/A$ if the threshold level is 5 MPa (0.75 ksi). In addition, computation of fatigue damage factor by this method for the sample of 55 trucks gave very erratic results and the method was finally abandoned.

3.3 Compilation of Stress Range Spectra

A subroutine for use on Lehigh University's CDC 6400 computer was developed to compile stress range spectra by each of the four cycle counting procedures adopted. These were assembled into a computer program and spectra compiled for 56 gages. The gage names and positions are listed in Table 3.

To facilitate programming simplicity and effect economy of storage, all the spectra were compiled using identical stress range levels, selected to compromise between the relatively low stresses in the girder and stringer details and the high stresses in the tie plates. A listing of the stress range levels used is given in Table 4.

Spectra for some of the details have been included in this report under Appendix C. A comparison of the cycle counting methods and results is included in Chapter 6.

4. MULTIPLE PRESENCE PARAMETERS

4.1 Truck Headway Model

It was suspected that truck headways or the spacing between successive trucks along a roadway could be described by a Poisson process, at least to an accuracy of one second. Moses and Pavia[15] claimed that this model overpredicted the number of closely spaced trucks but their data concerned headways in the 0.00 - 0.20 second category.

The Poisson model for the spacing between successive trucks along a roadway gives:

$$F(t) = 1 - e^{-ut}$$

where F(t) is the probability that the time between successive trucks is less than t, and u is the truck volume in vehicles per unit time.

The truck headway times observed at the Lehigh Canal Bridge in late 1976 have been plotted in Figs. 8 and 9. Figure 8 represents the twenty minute observation and Fig. 9 represents the hundred and twenty minute observation. In both cases, the measured distribution is compared with the exponential distribution of the Poisson model.

As the Poisson curve was found to be reasonably close to the measured distribution, and noted to be a better estimate when the sample space was greater, it was concluded that truck headways could be described by a Poisson model. Very short headways of up to 0.20 second were not measured so the findings of Moses and Pavia

could not be verified for the Lehigh Canal Bridge, but this question did not affect the subsequent analysis.

4.2 Computer Simulation of Multiple Presence

The effect of multiple presence on the fatigue damage to the bridge was studied by summation of influence lines for two single trucks. The static influence line for stress at four selected details for the truck in either lane was retrieved from the phase I tests. This is effectively the static influence line for the AASHTO HS20 truck.

For each of these details, the influence lines were summed to represent two trucks on the bridge separated by distances of 0, 22.4, 44.8, 67.2, 89.6, 112.0 and 134.4 meters respectively, representing one second increments of time at 80 kilometers per hour. The calculations were done for the second truck in the right-hand lane and in the left-hand lane for all cases except the 0 meter separation.

For each case studied, the effective fatigue damage factor,

$$F = \frac{1}{A} \Sigma \; n_i S_{ri}^{\;3}$$

was compared with the factor for the two trucks crossing the bridge separately, using both the peak to peak and rainflow cycle counting techniques. The results of this analysis are summarized in Tables 5, 6, 7 and 8.

In almost every case, except for closely spaced trucks, the factor is less than 1.0. This reflects the fact that the trucks are not on the same span together so the maximum stress range is not greatly increased, but the number of stress cycles is 1 for the peak to peak counting method instead of 2 as would be assumed for separate passages. The number of stress cycles is similarly reduced using the rainflow counting method. The net effect of a small increase in stress range and a significant decrease in number of cycles is to reduce the fatigue damage factor. The girder flanges have an influence line indicating little effect due to a load more than half the bridge length away, especially if the load is the lane on the opposite side of the centerline. For large truck separations, the stress excursions become distinct leading to a factor ratio of 1.0 for the peak to peak method and close to 1.0 for the rainflow method.

4.3 Cumulative Effect of Multiple Presence

The ratios of fatigue damage factors were combined with truck headway model to calculate the total effect of multiple presence on the Lehigh Canal Bridge. It was assumed that the leading truck was in the right-hand lane, and that the second truck would be in the right-hand lane unless the separation was less than 1.5 second or 33.6 meter (110 feet) at 80 kilometers per hour (50 mph). This assumption is not entirely true due to the presence of cars on the bridge, but visual observation showed that it held for most passages. If the multiple presence parameters had been critical, a more accurate analysis would have been made.

The calculation of effective fatigue damage was done with a theory based on the cumulative damage law proposed by Miner[14]. The derivation of the formula is outlined in Appendix D. The ratios of total fatigue damage to fatigue damage calculated by ignoring the effects of multiple presence are summarized in Table 9 for each of the four details considered.

4.4 Multiple Presence Factors

The fatigue damage ratios, as shown in Table 9 are all significantly less than 1.0. The major reasons for this are:

1. Trucks which are very closely spaced travel in different lanes, elevating the stress only slightly at the selected details but reducing the effective number of cycles.
2. Most of the trucks which are concurrently present are separated by more than 1.5 seconds, and again, only elevate the stress range marginally but reduce the effective number of cycles.

Since these facts will be true of all bridges with two lanes and two or more continuous spans, the results can be extended. In fact, for bridges of this type it will be conservative to ignore the effect of multiple presence. Hence, in Eqs. 1.13 and 1.14,

$$h_s = 1.0 \text{ and } h_N = 1.0 \tag{4.1}$$

for two lane bridges with two or more continuous spans.

Moses and Pavia[15] suggested that the magnification on moment due to multiple presence should be 1.2, which in Eqs. 1.13 and 1.14 would reduce to

$$h_s = 1.2 \text{ and } h_N = 1 \tag{4.2}$$

However, this value was quoted in conjunction with a proposal to reduce the girder distribution factor to S/11 where S is the girder spacing. If this distribution factor remains at its current value of S/5.5 it would be appropriate to ignore the effect of multiple presence.

If the girder distribution factor is reduced, the currently available data would suggest that the appropriate multiple presence factors are:

$$h_N = 1.0$$

$$h_s = 1.0 \text{ (for multi-span continuous bridges)}$$

$$h_s = 1.2 \text{ (for simple span bridges)} \tag{4.3}$$

Further research may indicate that a reduction in h_s could be effected for single lane simple span bridges in view of the physical impossibility of trucks crossing side by side.

5. IMPACT AND ELASTIC ADJUSTMENT FACTORS

5.1 Design Impact Factors

The impact value given in the AASHTO code is a function of span length for the detail being considered. Hence the design impact factors for the Lehigh Canal Bridge vary with position but can be calculated to be 0.186 for details on the girders in the end spans, 0.164 for details on the girders in the center span and 0.300 anywhere on the floor beams or stringers.

Moses and Pavia[15] measured impact factors on ten bridges in Ohio and found that the values did not bear any relationship to span length. The average value observed was 0.11, but no attempt was made to correlate impact with vehicle velocity, type or axle spacing.

A study by Csagoly, Campbell and Agarwal[1] of the Ontario Ministry of Transportation and Communications showed that the recorded impact factor is related to the degree of vehicle-bridge interaction which depends in turn on the vibratory motions of the bridge and truck as the truck enters the bridge. Hence they claim that impact is a function of the roughness conditions of the bridge deck and the pavement adjacent to it.

5.2 Impact Factors on Lehigh Canal Bridge

The impact factors on the Lehigh Canal Bridge were calculated from the results of the phase 1 or controlled-load tests. For

each gage, a record was available of the stress excursion caused by a truck crossing the bridge at a very slow speed giving virtually the static influence line, and by a passage at normal driving speed creating the dynamic influence line. This process was carried out in both the north and south lanes. A comparison of the stress excursions under the static and dynamic passages was used to measure the impact factor. In contrast to the measurements by Moses and Pavia, these measurements do not involve a range of truck velocity, type or axle spacing.

The measured impact factors were averaged for generalized sections of the bridge and the results are summarized in Table 10, both for a truck on the same side of the centerline as the detail and for a truck in the opposite lane.

The results are seen to be generally higher than the values measured by Moses and Pavia, but are similar to the values measured by Csagoly et al. In all positions except floor beams, the impact value is much higher in details on the opposite side of the centerline to that in which the truck is traveling. This is explained by the fact that the bridge is fairly flexible and while a truck traveling in the north lane has relatively small static effect on details under the south lane and vice versa, as demonstrated in Table 11, the dynamic loading sets up a strong vibrational motion in all parts of the bridge. However, the floor beams which span from north to south and hence are equally affected by trucks in either lane do not exhibit this characteristic.

The high impact values should not be a cause of concern however, because they are associated with small live loads. The larger live loads occurring at details on the same side of the centerline as the truck passage are increased by an impact factor which is always less than the value given by the AASHTO code.

The impact in the center span is much lower than that on equivalent details on the end span, probably reflecting the impact caused by the truck crossing the rough surface near the abutment.

The values obtained from a truck passage on the same side of the centerline as the detail are the appropriate values to use in design, because the total stress at these details is greater. Since the maximum average value for any detail is 0.89, it would appear that a value of γ equal to 0.90 would give a conservative design for any bridge similar to the Lehigh Canal Bridge.

5.3 Elastic Analysis Adjustment Factor

A complete analysis of the Lehigh Canal Bridge to derive stresses in the tie plates under the action of live load would be complex and was not attempted in this phase of study. However, two gages in use during the phase 3 or weighed sample tests were on details at which the computation of stress is possible with basic beam theory. These gages were G7TS on the top flange of the south girder near floor beam 7 and G4TN on the top flange of the north girder near floor beam 4.

An elastic analysis to find the influence line for stress under the action of a unit axle was performed at both these positions. Because the elastic analysis adjustment factor, α, is a correction factor to the elastic constant, β, relating load and stress at the relevant detail, the requirements of the AASHTO Code for lane loading were considered. The Code requires that in a two-lane bridge, both lanes should be equally loaded and no reduction of stress is allowed for the statistical improbability of simultaneous loading. Hence, each girder must be designed to carry the weight of an entire truck. The common practice in a design office would be to ignore the lateral bracing system and the interaction of the slab stringer system, and this practice was adopted in the analysis.

As a simplifying assumption, the effect of the haunches at the piers was ignored and a moment of inertia of 0.0515 m^4 was used for the entire length of the bridge. The influence lines for a 1.0 kN (225 lb.) axle are shown in Fig. 10.

The influence lines were summed for 198 of the trucks which were weighed and the peak to peak stress range calculated. This was compared to the measured peak to peak stress range in each case and histograms of the ratio compiled. These histograms are presented in Fig. 11 for gage G7TS and Fig. 12 for gage G4TN.

The effective ratio was calculated by computing the total fatigue damage factor for the measured peak to peak stress ranges and dividing by the fatigue damage factor derived from the design

influence lines. The results are presented in Table 12 with the average ratio from all the relevant truck passages.

The ratios are relatively low. However, the comparison is of the real loading to a design loading consisting of two trucks side by side. In the calculations, it was assumed that the trucks occur only singly and, in fact, multiple presence has been accounted for by the multiple presence parameters, h_s and h_N. The lower value for gage G4TN reflects the lower probability of a truck crossing in the north lane.

These ratios are not the elastic analysis adjustment factors. Since a dynamic passage has been compared to a static influence line, the effect of impact has been included in the ratios. At these details, design impact factor, I, is 0.186 and if γ is taken to be 0.90, then

$$\alpha = 0.30 \text{ (for north details)} \tag{5.1}$$

$$\text{and } \alpha = 0.37 \text{ (for south details)} \tag{5.2}$$

However, it is probably simpler to choose a constant conservative value for $\alpha\ (1 + \gamma I)$ for use in Eq. 2.14. Hence, for the Lehigh Canal Bridge -

$$\alpha\ (1 + \gamma I) = 0.35 \text{ (for north details)} \tag{5.3}$$

$$\alpha\ (1 + \gamma I) = 0.43 \text{ (for south details)} \tag{5.4}$$

6. CYCLE COUNTING PARAMETERS

6.1 Fatigue Category for Tie Plate Details

Erb[4] showed that Category D as defined in the AASHTO Highway Bridge Design Code is a good lower bound for cracks initiating at the tack weld in the tie plates, when submitted to a constant amplitude sinusoidal load.

The 95% lower confidence limit for Category D is defined by:

$$N = 6.56 \times 10^{11} S_r^{-3} \quad \text{(stress range in MPa)} \qquad (6.1)$$

$$N = 2.00 \times 10^{9} S_r^{-3} \quad \text{(stress range in ksi)}$$

and using a standard elevation of 0.864 being the average value for the two types of 100 mm (4 inch) attachments reported by Fisher, et al.[6], the 95% upper confidence limit can be calculated to be:

$$N = 1.45 \times 10^{12} S_r^{-3} \quad \text{(stress range in MPa)} \qquad (6.2)$$

$$N = 4.42 \times 10^{9} S_r^{-3} \quad \text{(stress range in ksi)}$$

Category D was believed to have a constant cycle fatigue limit of 48 MPa (7 ksi).

6.2 Peak to Peak Methods

The high volume of truck traffic on the Lehigh Canal Bridge induces a high percentage of multiple presence. Using the Poisson model of arrival times proposed in Chapter 4 and the estimated ADTT for 1974 of 4050 it is apparent that approximately 27 percent of truck arrivals will occur while the preceding truck is still wholly

or partially supported by the bridge. However, the stress excursion records were acquired by activating the system at all times when a truck was present on the bridge so many of these records will contain multiple presence. The above figures indicate that 37 percent of the stress excursion records are likely to reflect the passage of more than one truck across the structure.

In addition many light trucks which are included in the ADTT count do not produce sufficiently large stresses at some details to exceed the threshold levels. For some gages monitored during the stress history phase of the investigation almost 50 percent of the records contained stress ranges which failed to exceed the threshold. While some of these reflect the passage of light trucks other reasons are:

1. That multiple presence can cause compensatory addition with a smaller total stress range, and
2. That a truck in one lane only induces small stresses in the the details on the other side of the bridge.

In Chapter 5 it was shown that although the static effect of a truck on details on the opposite side of the bridge was low, the impact factor was high and hence these stresses tend to be vibratory in nature. As the threshold levels were deliberately chosen to eliminate small vibrational stresses, it is reasonable to assume that only on rare occasions would stresses have been recorded for a truck passage in the opposite lane.

In the light of this reasoning, it is obvious that the number of stress cycles per truck passage recorded at any one detail is very sensitive to the choice of threshold level for stresses at that detail. However, the stress cycles which are eliminated are small in magnitude and since the fatigue damage factor is a function of the cube of the stress range it is not affected significantly. Hence, in the typical S-N plot of stress range versus number of cycles, the point representing the fatigue damage at a detail will vary along a line defined by

$$N S_r^3 = \text{constant} \qquad (6.3)$$

with a change in threshold level but its relative position with respect to the AASHTO fatigue failure curves which are also described by Eq. 6.3 will not be greatly affected.

The fatigue damage factors were calculated for each detail monitored using the peak to peak counting technique and the Miner cumulative damage rule[14] and are plotted in Figs. 13 and 14. For clarity the details which had cracks exceeding 10 mm (0.4 inch) in September 1974 are shown in Fig. 13 and those which had not cracked by the date are shown in Fig. 14. It was assumed in this calculation that each stress excursion record was generated by one truck passage. The Category D design line and the 48 MPa (7 ksi) fatigue limit have also been plotted. The estimated cumulative truck traffic (Σ ADTT) in the twenty-one year life of the bridge to November, 1974, was 21.9×10^6.

Figures 15 and 16, similarly show the fatigue damage factors calculated using the computer subroutine which separated the effects of trucks concurrently present on the structure. In this case, the number of trucks recorded was greater but it was assumed that the number of trucks which actually crossed the bridge during the sampling period was increased by the same ratio so the points are plotted at the same number of cycles but obviously the stress levels are different.

In both sets of figures, four points represent details which cracked prior to November 1974 but their fatigue damage factors plot below the Category D design limit. All of these gages were placed at positions where large cracks had existed in September 1974 and which were repaired by gouging and welding prior to testing in November of that year. The tie plates represented by gages T26NE, T26NW and T27SW had actually broken completely. A 125 mm (5 inch) crack was repaired at position T6SE.

It was assumed that the repair operation would restore the tie plates to their original condition but the stresses measured at T26NE and T26NW seem to cast doubt on this assumption. Of course, these gages were placed on a north side tie plate and there were probably occasions during the life of the bridge when the south lane was closed, resulting in periods of much higher stress levels in north side details. The detail labeled T27SW was a tie plate on the south side which had already recracked before the stress history data was recorded. A crack of 175 mm (7 inch) was observed prior to testing and

the tie plate had completely broken by the time it was next inspected in August 1975. A crack of this magnitude would inevitably induce stress relief at the gage position and the results at this detail were not considered reliable.

Aside from these four gage positions, the Category D design limit is shown to give a reliable prediction for the possible onset of severe fatigue damage by either of the peak to peak counting methods. Figure 15 indicates that some of the details may have cracked as early as 1960 but there is no way to verify this except that severe cracking was found at first inspection in November 1973. In fact, five tie plates had completely broken by this date, as summarized in Table 1.

Figures 14 and 16 show several details which exhibited no visual cracking even though the fatigue damage factor exceeded the upper 95% confidence limit as measured in laboratory tests. However, these tests reported by Erb[4] and replotted in Fig. 17 show that although Category D forms a reasonable lower bound, there was a large amount of scatter above the mean regression line and some details had not failed even at 10 million cycles. If these details had been included in the calculation of the upper confidence limit, the line would lie at even higher stress levels. Consequently, it can be concluded that the peak to peak counting methods give results which are consistent with the laboratory tests.

Where tie plate stresses were monitored on the north and south end of the same floor beam the fatigue damage factor in the

south end plate was generally higher than that at the north end, as would be expected from a consideration of the concentration of heavy traffic in the south lane. For example, at floor beam 7 using the data obtained with separation of multiple presence, a total of 6085 cycles with Miner's stress range of 57 MPa (8.3 ksi) was recorded at the north end. At the south end during the same period 6458 cycles had a Miner's stress range of 76 MPa (11 ksi) to give a fatigue damage factor ratio over the north end of 2.5. Similar results for other floor beam positions are given in Table 13.

Recent evidence gathered from the Yellow Mill Pond Bridge, Bridgeport, Conn., and from laboratory tests[16] indicates that when the fatigue limit, currently given by AASHTO as 48 MPa (7 ksi) for Category D is exceeded by stress cycles in the stress spectrum, all stress cycles must be considered in estimating damage. In order to compare the Lehigh Canal Bridge data with this evidence the fatigue damage factors plotted in Figs. 13 and 15 were replotted under the assumption that 21.9×10^6 stress cycles occurred, but that those which were too small to exceed the threshold levels did not significantly affect the cumulative fatigue damage factor. The results are shown in Figs. 18 and 19. As some of these points plot below the fatigue limit, it can be concluded that for the Lehigh Canal Bridge, all stress cycles in a spectrum which contains cycles with a magnitude exceeding the fatigue limit are required for an accurate prediction of fatigue damage. Research which examines the fatigue strength of welded details as a function of the frequency of occurrence of stress cycles above the constant cycle fatigue limit is currently being initiated.

It was pointed out in Chapter 3 that the peak to peak method without separation of multiple presence represents the simplest application of that method to an experimental situation, and that the peak to peak method taking account of multiple presence is closer to the results that would be obtained from an analytic analysis. Hence, it has been shown that for the case of the Lehigh Canal Bridge, either application gives a conservative prediction of the onset of fatigue failure.

6.3 Rainflow Methods

Fatigue damage factors were compiled for the rainflow methods in a similar fashion to those for the peak to peak methods, and the results are plotted in Figs. 20 to 23. Figures 20 and 21 are the S-N values for cracked and uncracked details respectively using the rainflow counting technique and Figs. 22 and 23 give the same results for the modified rainflow method.

A comparison of Figs. 22 and 23 with the peak to peak methods reveals that the prediction of the modified rainflow method, as suspected, does not give reliable results. However, Figs. 20 and 21 show that in this case, the rainflow method can be used for satisfactory prediction of fatigue failure, with the same condition on the fatigue limit as proposed for the peak to peak methods. Insufficient evidence was available in this study to identify whether or not the rainflow method was more accurate than the peak to peak method, but it should be noted that it is much more complex to apply.

In an experimental situation it is far more expensive to reduce the results by the rainflow method and during the design phase it is virtually impossible to use unless the designer can be supplied with the vibrational characteristics of the bridge and the vehicles using it.

In order to more fully investigate the relationship of the rainflow method to the peak to peak method, the ratio of the number of cycles of the rainflow technique to the number of cycles of the peak to peak method without separation of multiple presence was compared for each detail studied. The ratios which are essentially the C_N values of Eq. 1.13 are listed in Table 14. The mean value of these ratios is given by:

$$C_N = 2.28 \text{ (standard deviation = 0.36)} \tag{6.4}$$

Similarly, the ratios of stress range were calculated and are presented in Table 14. The mean value is given by:

$$C_S = 0.76 \text{ (standard deviation = 0.06)} \tag{6.5}$$

The combined effect of these factors on the fatigue damage factor, using the Miner cumulative damage rule is found from:

$$C_F = C_N C_S^{\,3} \tag{6.6}$$

where C_F is the ratio of fatigue damage factor calculated by the rainflow method to the fatigue damage factor calculated by the peak to peak method. Therefore,

$$C_F = 1.00 \tag{6.7}$$

Hence, for an average detail the rainflow method gives a result which is very close to that of the peak to peak method.

Throughout this chapter, it was assumed that the effect of truncation of small stress cycles on the fatigue damage factor was insufficient to significantly affect the results. To confirm this hypothesis, the fatigue damage factors for details which had failed were recalculated by both of the peak to peak methods and the rainflow technique by applying a truncation of stress cycles at 48 MPa. The results have been plotted in Figs. 24, 25 and 26 and a comparison of these plots with Figs. 13, 15 and 20 respectively reveal that the assumption was justified.

6.4 Recommended Cycle Counting Parameters

The results of the stress history study on the Lehigh Canal Bridge have shown that within the accuracy of data available to both a designer or a researcher, the peak to peak cycle counting technique is at least as accurate as the rainflow method. However, it is much cheaper and simpler to use in either the experimental or design phase and the information on which it is based is more readily available.

Hence, the peak to peak method is recommended as a satisfactory technique in fatigue analysis. The appropriate factors in Eqs. 1.13 and 1.14 are thus given by:

$$C_S = 1.0 \qquad C_N = 1.0 \tag{6.8}$$

7. CURRENT PRACTICE

7.1 AASHTO Fatigue Specifications

The current AASHTO Highway Bridge Design Specification[18] limits conditions conducive to fatigue crack growth by specifying a maximum allowable fatigue stress range for each stress category. The theory summarized in Eqs. 1.12 through 1.14 is reflected in the Specification by requiring smaller stress ranges for longer expected life. In addition, the catastrophic collapse which can be caused by a single fracture in a nonredundant structure is accounted for by specifying a higher factor of safety for such structures.

This chapter examines the parameters outlined in this report and the value which is assigned to them in the AASHTO Specification.

7.2 Multiple Presence Factors

The Lehigh Canal Bridge study demonstrated that if the girder distribution factor remains at its current value based on bridge geometry as per the AASHTO Specifications that the effect of multiple presence in multiple lane spans can be conservatively ignored. In addition, it is suspected that further research will indicate that a reduction in actual stress range is possible for single lane simple spans.

The AASHTO Specification ignores the effect of multiple presence and consequently, gives a conservative estimate of fatigue strength.

7.3 Impact and Elastic Adjustment Factors

The Lehigh Canal Bridge study showed that the maximum impact factor adjustment in the same lane as the stress point under consideration was 0.80 for longitudinal members (tie plates) and 0.89 for transverse members (floor beams). The elastic analysis adjustment factor was found to be 0.37 for details on the right side of the bridge and 0.30 for details on the left side, reflecting the lower probability of a truck crossing in this lane.

Using the design impact factors of 0.30 for the floor beams and 0.19 for details on the girders in the end spans, the following values of the factor $\alpha\ (1 + \gamma I)$ can be determined -

0.43 (for longitudinal members on the right side)

0.47 (for transverse members on the right side)

0.43 (for longitudinal members on the left side)

0.38 (for transverse members on the left side)

Reference 5 reports that the AASHTO Specification uses a value for this combined factor of 0.8 for transverse members and 0.7 for longitudinal members. Hence, for two lane unidirectional bridges, it can be concluded that the AASHTO Specification is conservative. However, the Lehigh Canal Bridge factors were derived using the design assumptions that

(1) Each lane simultaneously carries maximum load, and that

(2) No reduction of stress is allowed for the statistical improbability of simultaneous loading.

It should be noted that the results cannot be directly extrapolated to situations where the design assumptions are invalid, that is, to bridges with more than two lanes. A conservative result would develop.

7.4 Cycle Counting Parameters

The results of this study indicate that the peak to peak count method gives results which are as accurate as the more sophisticated methods. It has the additional advantage that it is much simpler to incorporate into design specifications. The AASHTO Specification reflects this finding by assuming that cycle counting will be done by the peak to peak method.

8. CONCLUSIONS

1. The Poisson model was found to give an adequate description of truck arrival times on the Lehigh Canal Bridge. However, the bridge configuration along with the observations that very closely spaced trucks must travel in different lanes and most concurrently present trucks are separated by at least 1.5 seconds combine to reduce the damaging effect of simultaneously present trucks. The effect of multiple presence can conservatively be ignored on bridges of two or more continous spans. Currently available data indicates that the stresses should be increased by 1.2 in simple span multiple beam bridges when used together with a distribution factor of S/11. Alternatively, a distribution factor of S/7 results in a multiple presence factor on stresses of about 1.0.
2. Impact factors were found to vary widely with the detail being considered. However, the larger values were always associated with the passage of a truck on the opposite side of the center line to the detail and as these impact factors were associated with small stresses they do not contribute significantly to fatigue damage. For trucks in the same lane the measured impact factor was always less than 90% of the Code value which, consequently, forms a conservative estimate.
3. The elastic analysis adjustment factor was calculated for several details and found to have a larger value on south side details due to the higher probability that a truck will cross in that

lane. The average factors, incorporating the effect of impact, were found to be 0.35 for the north details and 0.43 for south details.

4. A correlation of stress history data with crack growth history at 56 details showed that the peak to peak cycle counting method, with or without separation of multiple presence, gave results which were as reliable as laboratory experiments on the same details. The rainflow technique did not improve the correlation. In view of the complexity of using the rainflow method, it is recommended that the peak to peak method be used, as it is satisfactory for both experiment and design.

5. The stress history data at several details on the Lehigh Canal Bridge confirms recent evidence that if some stresses in the stress spectrum at a detail exceed the fatigue limit then the whole spectrum should be included in the computation of fatigue damage factor to adequately predict the onset of failure in the detail.

6. The combined evidence of tests at the Lehigh Canal Bridge indicate that failure is possible at a detail when

$$NS_r^3 = A$$

where A is defined by the fatigue category, $N = \Sigma$ (ADTT) for the design life of the bridge, and

$$S_r = \beta \{\alpha (1 + \gamma I)\} (GVW)_D$$

In this equation, β is the elastic constant relating gross vehicle weight to stress range, $(GVW)_D$ is the weighted average of gross vehicle weight using the truck weight spectrum for the relevant area and $\alpha (1 + \gamma I)$ is a constant which for the Lehigh Canal Bridge was found to be 0.35 for the north details and 0.43 for the south details.

TABLE 1a: TIE PLATE CRACKING ON LEHIGH CANAL BRIDGE

SOUTH GIRDER
CRACK LENGTH (mm)

Floor Beam Position	Date of Inspection: Nov. 1973 West	Nov. 1973 East	Sep. 1974 West	Sep. 1974 East	Nov. 1974 West	Nov. 1974 East	Aug. 1975 West	Aug. 1975 East	Aug. 1976 West	Aug. 1976 East
1	Broken		New plate							
2	Broken		New Plate							
3		C		200	Repaired			194	39	200
4										
5										
6		C		125	Repaired					
7		C		50	Repaired					
8		C		17	Not inspected			28		50
9										44
10										
11										
12										
13										
14										
15										
16										
17										
18										
19										
20		C		175	Repaired					
21										
22										
23										
24										
25		C		200	Repaired		70		83	
26	Broken		Broken		Repaired		Broken		Broken	
27		C		200	Repaired		225		225	

TABLE 1a: (CONTINUED)

NORTH GIRDER
CRACK LENGTH (mm)

Floor Beam Position	Date of Inspection: Nov. 1973 West	Nov. 1973 East	Sep. 1974 West	Sep. 1974 East	Nov. 1974 West	Nov. 1974 East	Aug. 1975 West	Aug. 1975 East	Aug. 1976 West	Aug. 1976 East
1		C		175	Repaired					
2										
3				63	Repaired					
4										
5										
6										
7				19		20		22		44
8		C		200	Repaired			133		146
9										
10				50	Repaired			137		159
11				75	Repaired					
12										
13										
14										
15										
16										
17										
18										
19	C	C	175	50	Repaired		159		175	44
20	Broken		Broken		Repaired		44		44	
21										
22										
23										
24										
25										
26	Broken		Broken		Repaired					
27										

TABLE 1b: TIE PLATE CRACKING ON LEHIGH CANAL BRIDGE

SOUTH GIRDER

CRACK LENGTH (inches)

Floor Beam Position	Date of Inspection: Nov. 1973 West	Nov. 1973 East	Sep. 1974 West	Sep. 1974 East	Nov. 1974 West	Nov. 1974 East	Aug. 1975 West	Aug. 1975 East	Aug. 1976 West	Aug. 1976 East
1	Broken		New plate							
2	Broken		New plate							
3		C		8.0	Repaired			7.6	1.5	8.0
4										
5										
6		C		5.0	Repaired					
7		C		2.0	Repaired					
8		C		0.7	Not inspected			1.1		2.0
9										1.7
10										
11										
12										
13										
14										
15										
16										
17										
18										
19										
20	C		7.0		Repaired					
21										
22										
23										
24										
25	C		8.0		Repaired		2.8		3.2	
26	Broken		Broken		Repaired		Broken		Broken	
27	C		8.0		Repaired		9.0		9.0	

TABLE 1b: (CONTINUED)

North Girder

CRACK LENGTH (inches)

Floor Beam Position	Date of Inspection: Nov. 1973 West	Nov. 1973 East	Sep. 1974 West	Sep. 1974 East	Nov. 1974 West	Nov. 1974 East	Aug. 1975 West	Aug. 1975 East	Aug. 1976 West	Aug. 1976 East
1		C		7.0	Repaired					
2										
3				2.5	Repaired					
4										
5										
6										
7				0.75	0.9		0.9		1.7	
8		C		8.0	Repaired		5.2		5.8	
9										
10				2.0	Repaired		5.4		6.3	
11				3.0	Repaired					
12										
13										
14										
15										
16										
17										
18										
19	C	C	7.0	2.0	Repaired		6.3		7.0	1.7
20	Broken		Broken		Repaired		1.7		1.7	
21										
22										
23										
24										
25										
26	Broken		Broken		Repaired					
27										

TABLE 2a: SUMMARY OF STRESS RANGES IN THE TIE PLATES UNDER HS20 STATIC LOADING

(TRUCK IN SOUTH LANE)

Floor Beam Position	Stress Range (MPa) North Side Plates West	North Side Plates East	South Side Plates West	South Side Plates East
1	29.2	10.8		
2	24.0	29.8		
3				74.7
4	32.1	23.4	79.6	69.8
5	10.1	24.0	54.9	47.4
6			43.2	
7			138.6	
8				103.8
9				
10				126.0
11			124.1	
12			85.2	99.4
13				
14			74.7	
15			76.4	
16			119.1	123.1
17	16.8	15.1	126.9	103.0
18	4.6	9.3	135.3	127.5
19		8.3		156.1
20				88.9
21			92.8	96.9
22	9.5		61.7	50.5
23			61.4	53.4
24				
25	16.5	18.4	115.1	82.9
26		16.3	52.7	156.8
27	14.9	15.1		

TABLE 2a: (CONTINUED)

(TRUCK IN NORTH LANE)

Floor Beam Position	Stress Range (MPa) North Side Plates West	North Side Plates East	South Side Plates West	South Side Plates East
1	100.7	75.1		
2	126.6	146.8		
3				11.0
4	98.3	79.2	18.4	15.1
5	50.4	79.1	9.3	10.3
6			4.9	
7	133.1			3.1
8				2.7
9				
10				5.8
11			11.0	
12	83.9	110.3		11.8
13				
14			11.0	
15	124.3		9.3	
16				8.7
17	152.3	136.1	11.8	9.5
18	175.5	183.2	9.1	6.2
19	25.5	154.2		9.1
20				3.5
21	132.2	132.8	7.2	
22	57.6		8.9	5.0
23			19.4	9.3
24				
25	90.5	90.3	14.9	15.1
26		81.1	15.5	31.6
27	115.2	91.0		

TABLE 2b: SUMMARY OF STRESS RANGES IN THE TIE PLATES UNDER HS20 STATIC LOADING

(TRUCK IN SOUTH LANE)

Floor Beam Position	Stress Range (ksi) North Side Plates West	North Side Plates East	South Side Plates West	South Side Plates East
1	4.23	1.57		
2	3.48	4.32		
3				10.80
4	4.66	3.39	11.50	10.10
5	1.46	3.48	7.96	6.87
6			6.27	
7			20.10	
8				15.10
9				
10				18.30
11			18.30	
12			12.40	14.40
13				
14			10.80	
15			11.10	
16			17.30	17.90
17	2.44	2.19	18.40	14.90
18	0.67	1.35	19.60	18.50
19		1.20		22.60
20				12.90
21			13.50	14.10
22	1.38		8.95	7.32
23			8.91	7.74
24				
25	2.39	2.67	16.70	12.00
26		2.36	7.64	22.70
27	2.16	2.19		

TABLE 2b: (CONTINUED)

(TRUCK IN NORTH LANE)

Floor Beam Position	Stress Range (ksi) North Side Plates West	North Side Plates East	South Side Plates West	South Side Plates East
1	14.60	10.9		
2	18.40	21.3		
3				1.60
4	14.30	11.5	2.67	2.19
5	7.31	11.5	1.35	1.49
6			0.71	
7	19.30			0.45
8				0.39
9				
10				0.84
11			1.60	
12	12.20	16.0		1.71
13				
14			1.60	
15	18.00		1.35	
16				1.26
17	22.10	19.7	1.71	1.38
18	25.50	26.6	1.32	0.90
19	3.70	22.4		1.32
20				0.51
21	19.20	19.3	1.04	
22	8.35		1.29	0.73
23			2.81	1.35
24				
25	13.10	13.1	2.16	2.19
26		11.8	2.25	4.58
27	16.70	13.2		

TABLE 3a: THRESHOLD VALUES FOR DATA REDUCTION (STAGE I)

Gage Position	Floor Beam Number	Gage Name	Threshold Stress (MPa)	Gage Position	Floor Beam Number	Gage Name	Threshold Stress (MPa)
Girder	7	G7TS	3.0	Tie Plate	15	T15SW	10.6
Tie Plate	5	T5SE	5.7	Stringer	2	ST18	2.0
Tie Plate	6	T6SE	8.2	Tie Plate	16	T16SW	11.3
Tie Plate	26	T26NW	9.9	Tie Plate	25	T25NE	8.0
Tie Plate	4	T4NE	5.8	Bracket	1	BW1S	2.2
Tie Plate	3	T3NE	6.7	Bracket	2	BW2S	2.2
Tie Plate	27	T27SW	4.5	Tie Plate	18	T18SW	15.0
Tie Plate	27	T27NE	15.8	Tie Plate	21	T21SE	7.7
Tie Plate	1	T1NW	10.4	Tie Plate	1	T1SW	15.1
Tie Plate	2	T2NW	13.6	Tie Plate	2	T2SW	9.0
Tie Plate	8	T8NE	8.4	Tie Plate	18	T18NW	10.1
Tie Plate	4	T4SW	5.9	Stringer	Between 1 and 2	ST23	2.2
Tie Plate	3	T3SW	5.9	Tie Plate	19	T19NE	16.9
Tie Plate	8	T8SW	10.0	Stringer	Between 1 and 2	ST24	2.2
Tie Plate	7	T7NE	12.0	Tie Plate	20	T20NE	19.4
Tie Plate	7	T7SW	15.1	Tie Plate	17	T17SE	13.4
Stringer	1	ST1	1.6	Tie Plate	21	T21NE	14.1
Tie Plate	14	T14SW	9.9	Tie Plate	22	T22SE	8.1
Stringer	1	ST2	2.2	Bracket	1	BW1N	4.3
Tie Plate	13	T13SW	6.9	Bracket	2	BW2N	4.3
Tie Plate	12	T12SE	9.7	Tie Plate	23	T23SW	6.0
Tie Plate	10	T10NW	8.3	Tie Plate	24	T24SE	10.8
Tie Plate	11	T11NW	9.5	Girder	4	G4TN	2.5
Tie Plate	25	T25NW	32.0	Tie Plate	27	T27NW	8.0
Tie Plate	9	T9NW	10.7	Tie Plate	27	T27SE	17.1
Tie Plate	9	T9SE	14.5	Tie Plate	26	T26NE	11.7
Tie Plate	10	T10SE	6.2	Tie Plate	25	T25SE	9.8
Tie Plate	11	T11SE	9.3	Floor Beam	1	FB1-16	5.0

TABLE 3b: THRESHOLD VALUES FOR DATA REDUCTION (Stage I)

Gage Position	Floor Beam Number	Gage Name	Threshold Stress (ksi)	Gage Position	Floor Beam Number	Gage Name	Threshold Stress (ksi)
Girder	7	G7TS	0.44	Tie Plate	15	T15SW	1.54
Tie Plate	5	T5SE	0.83	Stringer	2	ST18	0.29
Tie Plate	6	T6SE	1.19	Tie Plate	16	T16SW	1.64
Tie Plate	26	T26NW	1.44	Tie Plate	25	T25NE	1.16
Tie Plate	4	T4NE	0.84	Bracket	1	BW1S	0.32
Tie Plate	3	T3NE	0.97	Bracket	2	BW2S	0.32
Tie Plate	27	T27SW	0.65	Tie Plate	18	T18SW	2.18
Tie Plate	27	T27NE	2.29	Tie Plate	21	T21SE	1.12
Tie Plate	1	T1NW	1.51	Tie Plate	1	T1SW	2.19
Tie Plate	2	T2NW	1.97	Tie Plate	2	T2SW	1.31
Tie Plate	8	T8NE	1.22	Tie Plate	18	T18NW	1.46
Tie Plate	4	T4SW	0.86	Stringer	Between 1 and 2	ST23	0.32
Tie Plate	3	T3SW	0.86	Tie Plate	19	T19NE	2.45
Tie Plate	8	T8SW	1.45	Stringer	Between 1 and 2	ST24	0.32
Tie Plate	7	T7NE	1.74	Tie Plate	20	T20NE	2.81
Tie Plate	7	T7SW	2.19	Tie Plate	17	17SE	1.94
Stringer	1	ST1	0.23	Tie Plate	21	T21NE	2.04
Tie Plate	14	T14SW	1.44	Tie Plate	22	T22SE	1.17
Stringer	1	ST2	0.32	Bracket	1	BW1N	0.62
Tie Plate	13	T13SW	1.00	Bracket	2	BW2N	0.62
Tie Plate	12	T12SE	1.41	Tie Plate	23	T23SW	0.87
Tie Plate	10	T10NW	1.20	Tie Plate	24	T24SE	1.57
Tie Plate	11	T11NW	1.38	Girder	4	G4TN	0.36
Tie Plate	25	T25NW	4.64	Tie Plate	27	T27NW	1.16
Tie Plate	9	T9NW	1.55	Tie Plate	27	T27SE	2.48
Tie Plate	9	T9SE	2.10	Tie Plate	26	T26NE	1.70
Tie Plate	10	T10SE	0.90	Tie Plate	25	T25SE	1.42
Tie Plate	11	T11SE	1.35	Floor Beam	1	FB1-16	0.73

TABLE 4a: STRESS RANGE LEVELS ADOPTED FOR STRESS RANGE SPECTRA

Stress Range Level No.	Stress Ranges (MPa) Minimum	Maximum
1	0	3.45
2	3.45	5.17
3	5.17	6.90
4	6.90	13.79
5	13.79	20.69
6	20.69	27.58
7	27.58	34.48
8	34.48	41.37
9	41.37	48.27
10	48.27	55.16
11	55.16	62.06
12	62.06	68.95
13	68.95	75.85
14	75.85	82.74
15	82.74	89.64
16	89.64	96.53
17	96.53	103.43
18	103.43	110.32
19	110.32	117.22
20	117.22	∞

TABLE 4b: STRESS RANGE LEVELS ADOPTED FOR STRESS RANGE SPECTRA

Stress Range Level No.	Stress Ranges (ksi) Minimum	Maximum
1	0	0.50
2	2.50	0.75
3	0.75	1.00
4	1.00	2.00
5	2.00	3.00
6	3.00	4.00
7	4.00	5.00
8	5.00	6.00
9	6.00	7.00
10	7.00	8.00
11	8.00	9.00
12	9.00	10.00
13	10.00	11.00
14	11.00	12.00
15	12.00	13.00
16	13.00	14.00
17	14.00	15.00
18	15.00	16.00
19	16.00	17.00
20	17.00	∞

TABLE 5: RATIO OF FATIGUE DAMAGE FACTORS DUE TO MULTIPLE PRESENCE

TIE PLATE - NORTH SIDE

Truck Separation (sec)	Fatigue Damage Factor Ratios for Second Truck in- Right Lane		Left Lane	
	Peak to Peak	Rainflow	Peak to Peak	Rainflow
0	---	---	1.59	1.54
1	1.88	0.48	1.18	1.15
2	0.37	0.38	0.64	0.64
3	0.45	0.83	0.77	0.84
4	0.76	1.58	0.97	1.07
5	0.62	1.38	1.06	1.18
6	0.50	1.19	0.93	1.03

TABLE 6: RATIO OF FATIGUE DAMAGE FACTORS DUE TO MULTIPLE PRESENCE

TIE PLATE - SOUTH SIDE

Truck Separation (sec)	Fatigue Damage Factor Ratios for Second Truck in-			
	Right Lane		Left Lane	
	Peak to Peak	Rainflow	Peak to Peak	Rainflow
0	---	---	1.15	1.15
1	0.64	0.62	1.04	1.02
2	0.56	0.92	0.87	0.92
3	0.49	0.88	0.88	0.93
4	0.49	0.79	1.01	1.00
5	0.50	0.84	0.88	0.93
6	0.49	0.89	1.00	1.00

TABLE 7: RATIO OF FATIGUE DAMAGE FACTORS DUE TO MULTIPLE PRESENCE

GIRDER FLANGE - NORTH SIDE

Truck Separation (sec)	Fatigue Damage Factor Ratios for Second Truck in-			
	Right Lane		Left Lane	
	Peak to Peak	Rainflow	Peak to Peak	Rainflow
0	---	---	1.45	1.44
1	1.00	0.75	0.98	0.96
2	0.50	0.63	0.91	0.95
3	0.50	0.88	0.96	1.02
4	0.50	1.13	1.00	1.06
5	1.00	1.13	1.00	1.06
6	1.00	1.13	1.00	1.06

TABLE 8: RATIO OF FATIGUE DAMAGE FACTORS DUE TO MULTIPLE PRESENCE

GIRDER FLANGE - SOUTH SIDE

Truck Separation (sec)	Fatigue Damage Factor Ratios for Second Truck in- Right Lane		Left Lane	
	Peak to Peak	Rainflow	Peak to Peak	Rainflow
0	---	---	1.26	1.27
1	0.98	0.93	0.97	0.98
2	0.55	0.63	0.94	0.97
3	0.50	0.82	0.99	1.00
4	0.50	0.89	1.00	1.00
5	0.50	0.89	1.00	1.00
6	0.50	0.91	1.00	1.00

TABLE 9: MULTIPLE PRESENCE FACTORS FOR LEHIGH CANAL BRIDGE

Position of Detail	Fatigue Damage Ratios	
	Peak to Peak Method	Rainflow Method
Girder Flange - south	0.68	0.83
Tie Plate - south	0.68	0.85
Girder Flange - north	0.55	0.55
Tie Plate - north	0.58	0.58

TABLE 10: AVERAGE IMPACT VALUES UNDER AASHTO HS20 TRUCK LOADING

Detail Position	AASHTO Design Factor, I	Measured Impact, γI		Ratio of Measured to Design Impact, γ	
		Same	Opposite	Same	Opposite
Tie plates - end span	0.186	0.15	0.92	0.80	4.92
Tie plates - center span	0.164	0.04	2.41	0.23	14.71
Cantilever brackets	0.186	0.14	0.77	0.74	4.16
Girder - end span	0.186	0.05	0.36	0.29	1.91
Floor beams	0.300	0.27	0.28	0.89	0.94

TABLE 11: STRAINS IN ANTITHETIC DETAILS UNDER AASHTO HS20 STATIC LOADING

Floor Beam Position	Truck Lane	Strain Ranges ($x10^6$) North Tie Plate	South Tie Plate
4	North	423	134
4	South	81	353
5	North	313	82
5	South	47	247
12	North	469	0
12	South	28	446
22	North	279	46
22	South	29	284
26	North	392	79
26	South	83	470

TABLE 12: RATIOS OF REAL TO DESIGN STRESS RANGES

Gage Name	Stress Range Ratio Fatigue Damage Factor Analysis	Average Ratio
G4TN	0.35	0.35
G7TS	0.43	0.46

TABLE 13a: COMPARISON OF FATIGUE DAMAGE FACTORS ON TIE PLATES AT OPPOSITE ENDS OF SAME FLOOR BEAM

Floor Beam Position	Tie Plate Position	No. of Cycles	Stress Range (MPa)	Ratio of Fatigue Damage Factors
3	S	4952	77	3.3
	N	6223	48	
4	S	6045	51	1.2
	N	6075	48	
7	S	6458	76	2.5
	N	6085	57	
8	S	6317	66	2.5
	N	6276	49	
9	S	6447	74	1.7
	N	5768	64	
10	S	5671	72	1.8
	N	6337	57	
11	S	5358	78	1.9
	N	5899	61	

TABLE 13b: COMPARISON OF FATIGUE DAMAGE FACTORS ON TIE PLATES AT OPPOSITE ENDS OF SAME FLOOR BEAM

Floor Beam Position	Tie Plate Position	No. of Cycles	Stress Range (ksi)	Ratio of Fatigue Damage Factors
3	S	4952	11	3.3
	N	6223	7.0	
4	S	6045	7.4	1.2
	N	6075	7.0	
7	S	6458	11	2.5
	N	6085	8.3	
8	S	6317	9.6	2.5
	N	6276	7.1	
9	S	6447	11	1.7
	N	5768	9.3	
10	S	5671	10	1.8
	N	6337	8.3	
11	S	5358	11	1.9
	N	5899	8.8	

TABLE 14: C_S AND C_N FACTORS FOR RAINFLOW COUNTING METHOD

Gage	C_S	C_N	Gage	C_S	C_N
67TS	0.82	2.24	T15SW	0.74	2.03
T5SE	0.76	2.90	ST18	0.74	2.83
T6SE	0.81	2.02	T16SW	0.74	2.07
T26NW	0.88	1.76	T25NE	0.68	2.92
T4NE	0.69	2.71	BW1S	0.71	2.13
T3NE	0.69	2.69	BW2S	0.73	1.89
T27SW	0.81	1.59	T18SW	0.76	2.25
T27NE	0.74	2.09	T21SE	0.72	2.45
T1NW	0.71	2.36	T1SW	0.69	2.33
T2NW	0.72	2.25	T2SW	0.70	2.50
T8NE	0.69	2.34	T18NW	0.77	2.30
T4SW	0.69	2.54	ST23	0.89	2.11
T3SW	0.68	2.89	T19NE	0.75	2.12
T8SW	0.70	2.36	ST24	0.89	2.65
T7NE	0.73	2.37	T20NE	0.79	2.01
T7SW	0.75	2.27	T17SE	0.77	2.09
ST1	0.91	1.67	T21NE	0.78	2.03
T14SW	0.77	2.78	T22SE	0.85	1.72
ST2	0.87	2.15	BW1N	0.84	1.45
T13SW	0.74	2.33	BW2N	0.83	1.63
T12SE	0.75	2.48	T23SW	0.76	2.51
T10NW	0.72	2.33	T24SE	0.74	2.17
T11NW	0.76	2.39	G4TN	0.78	2.08
T25NW	0.83	2.36	T27NW	0.71	3.19
T9NW	0.72	2.49	T27SE	0.78	1.83
T9SE	0.70	2.28	T26NE	0.82	1.84
T10SE	0.71	2.43	T25SE	0.75	2.60
T11SE	0.76	2.52	FB1-16	0.80	2.27

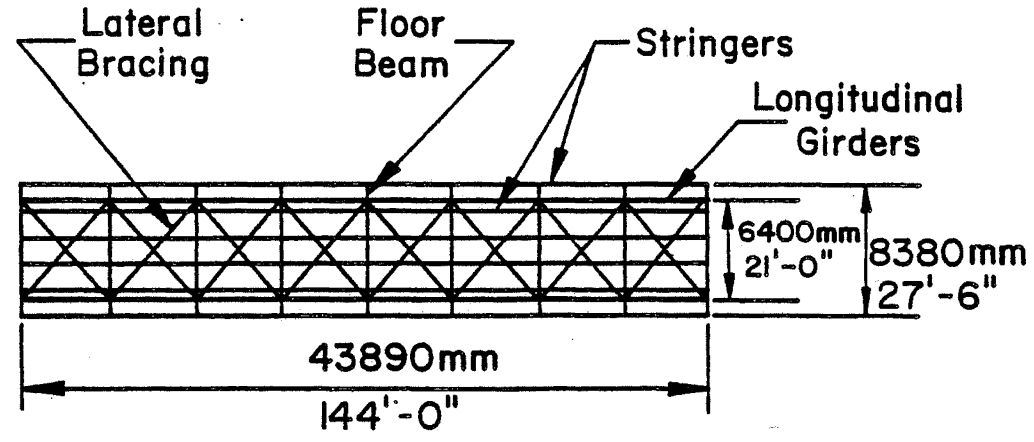

PLAN

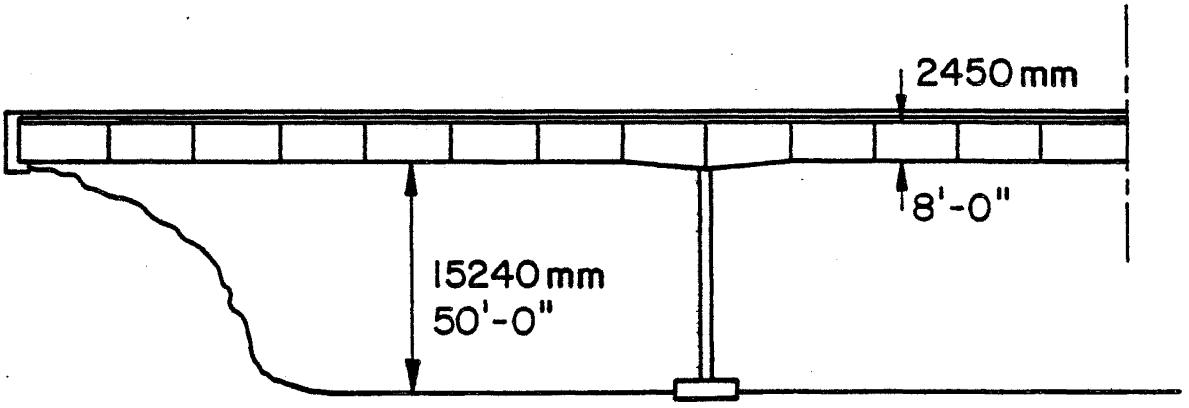

ELEVATION

Fig. 1 Plan and Elevation of Lehigh Canal Bridge

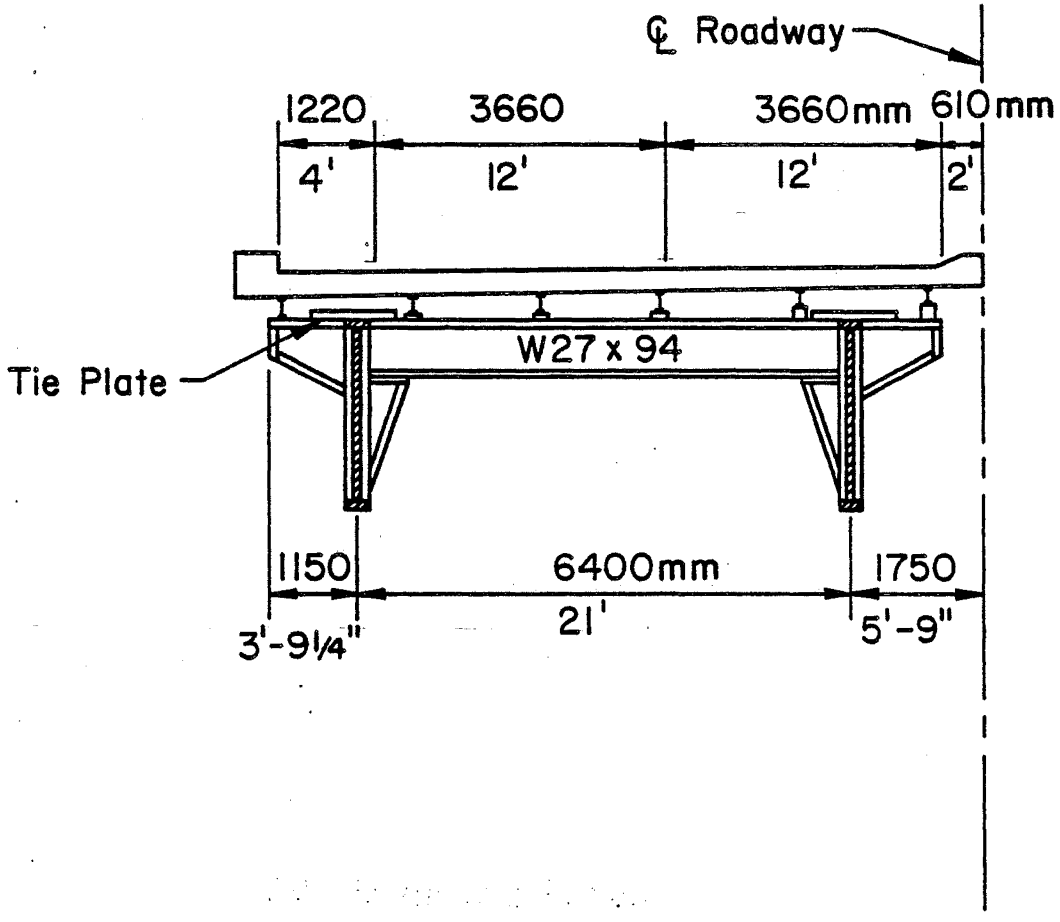

Fig. 2 Cross-Section of Lehigh Canal Bridge

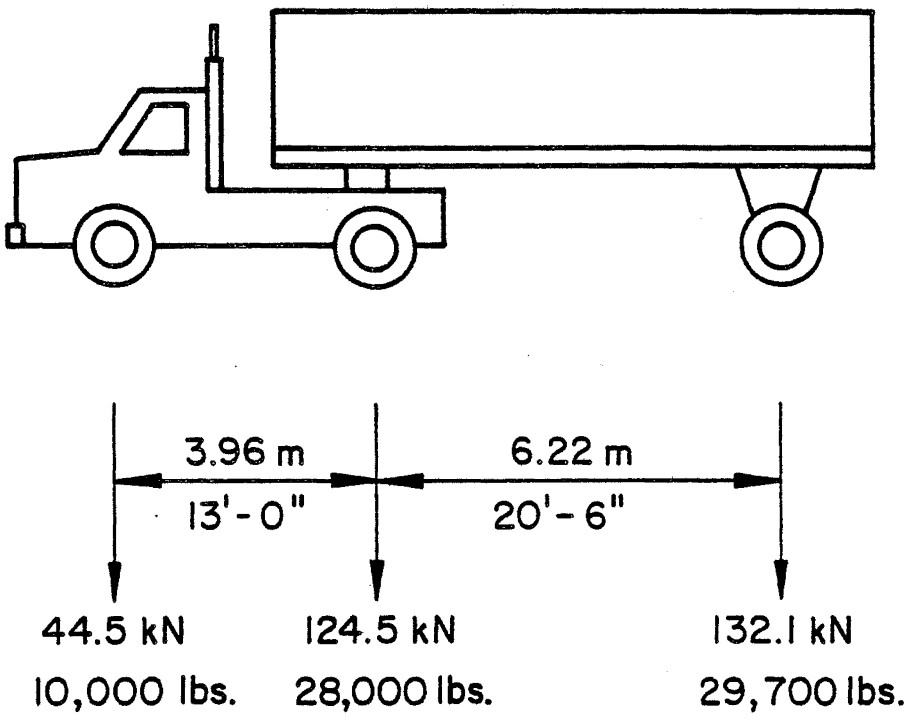

Fig. 3 Dimensions of FHWA Test Truck

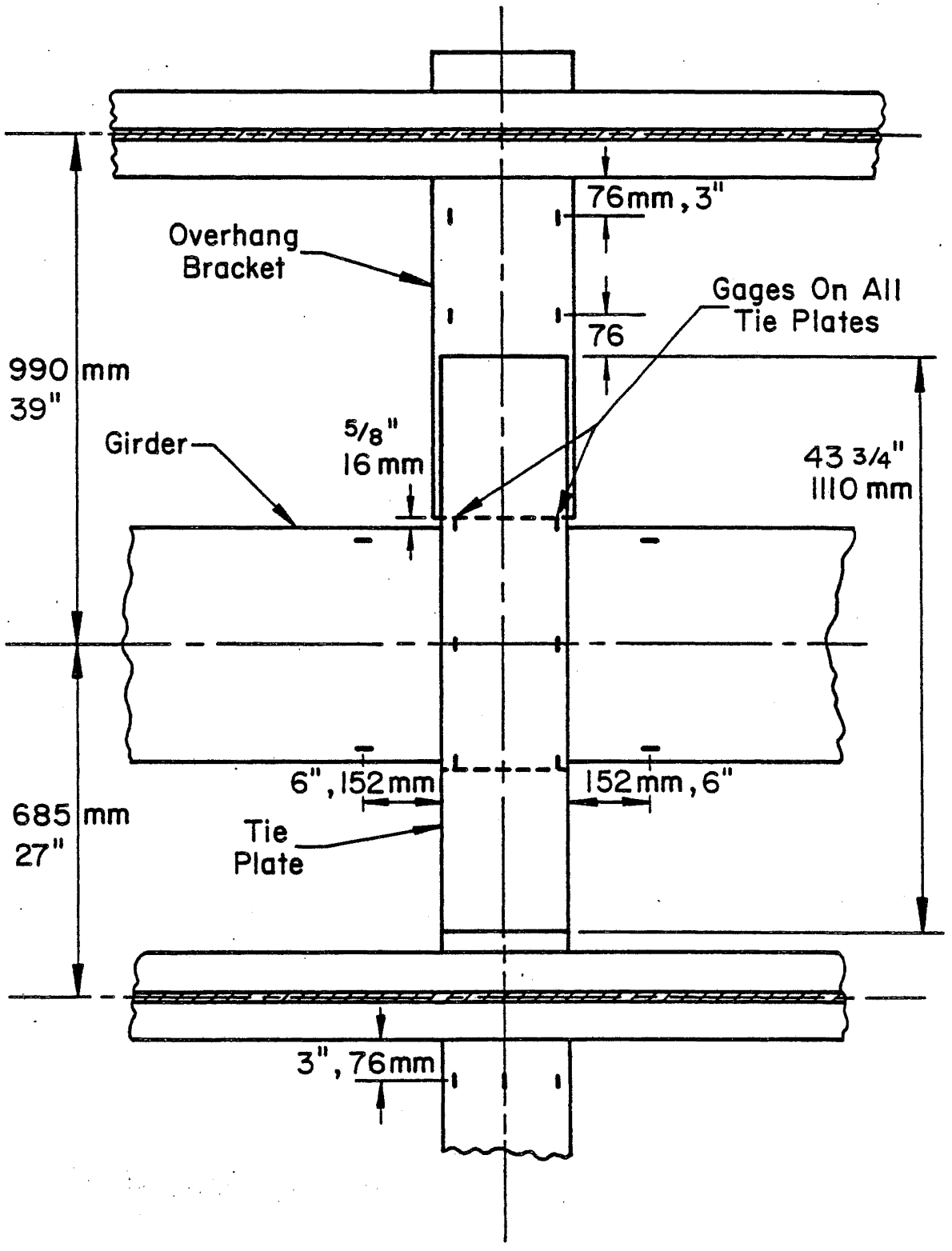

Fig. 4 Arrangement of Gages at Tie Plate of Floor Beam 2

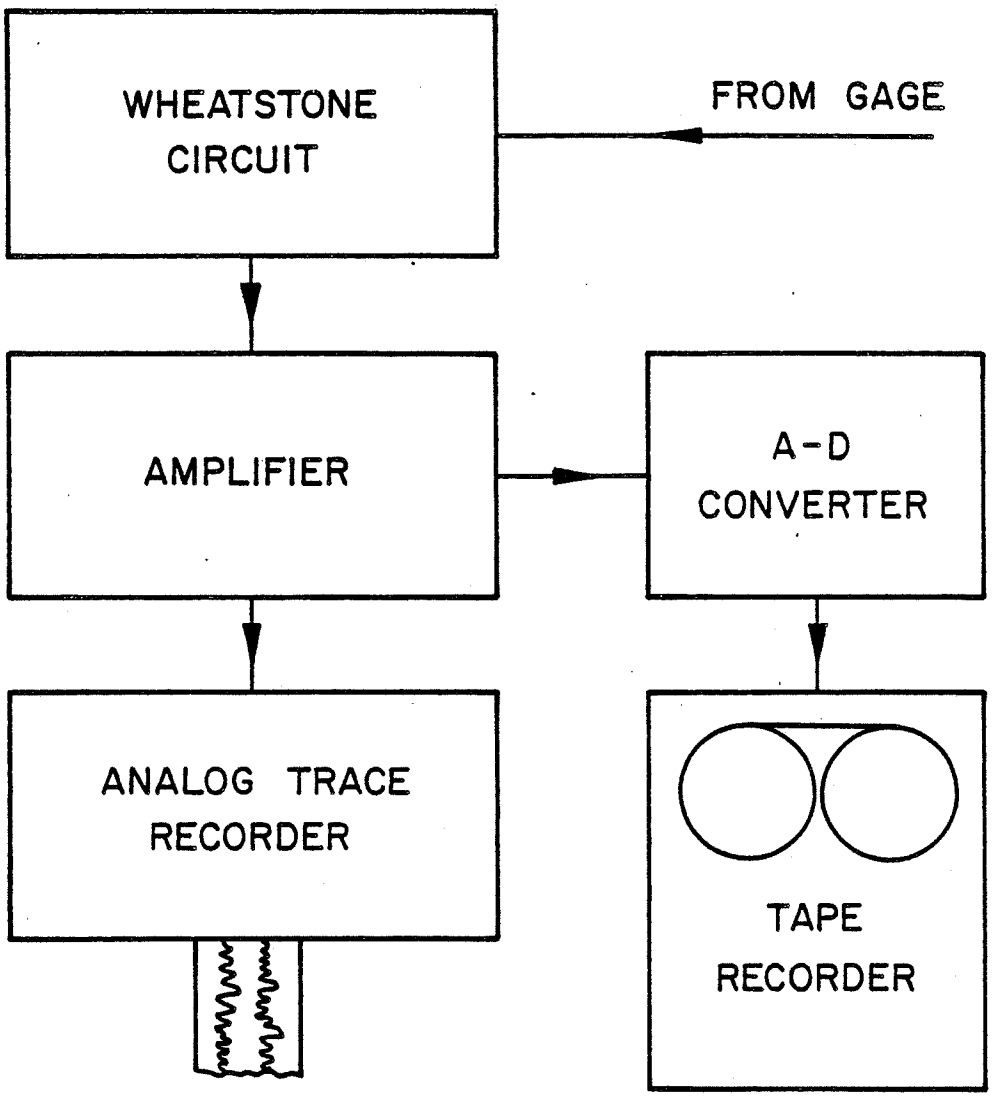

Fig. 5 Data Acquisition System

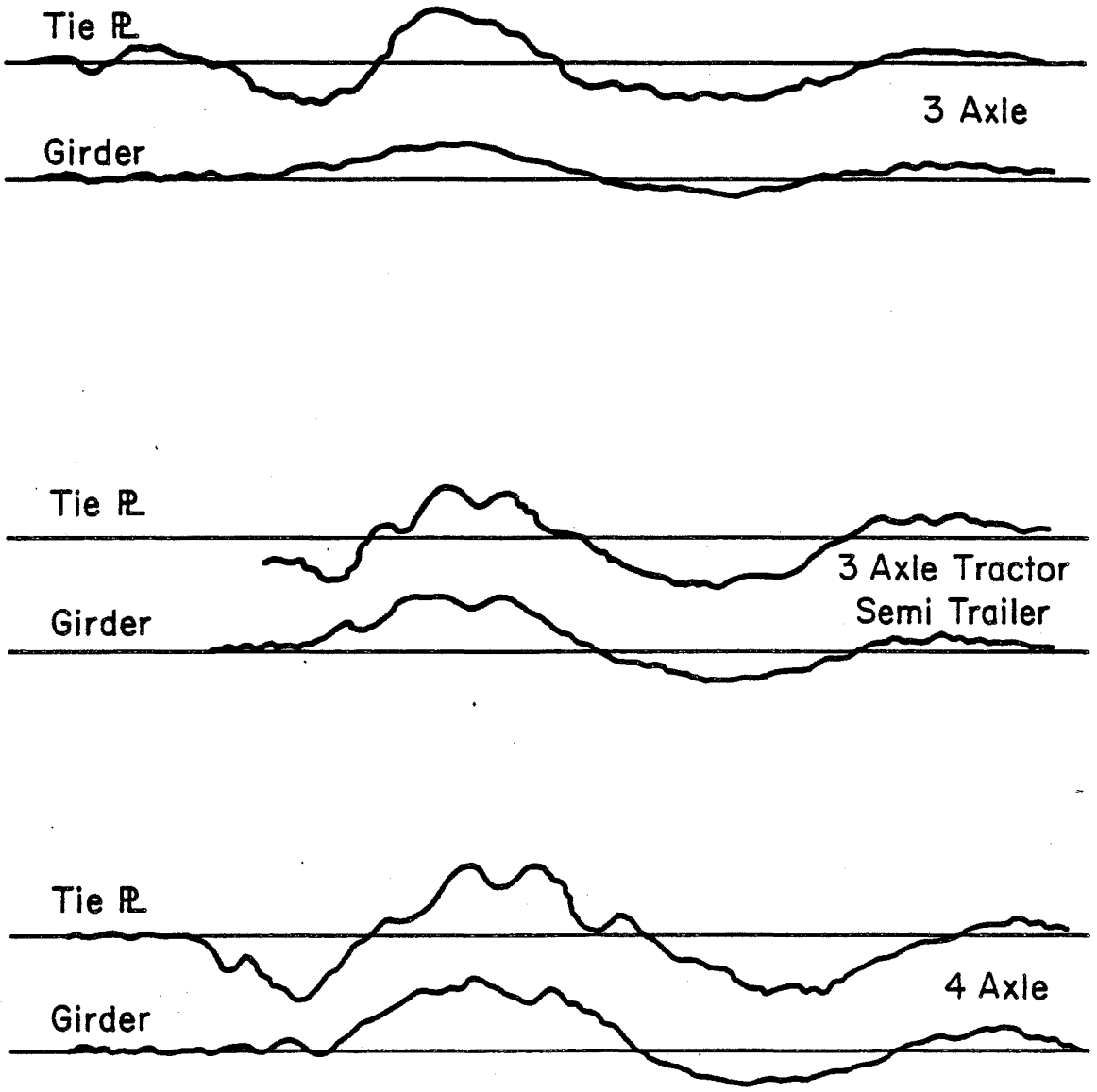

Fig. 6 Typical Analog Traces

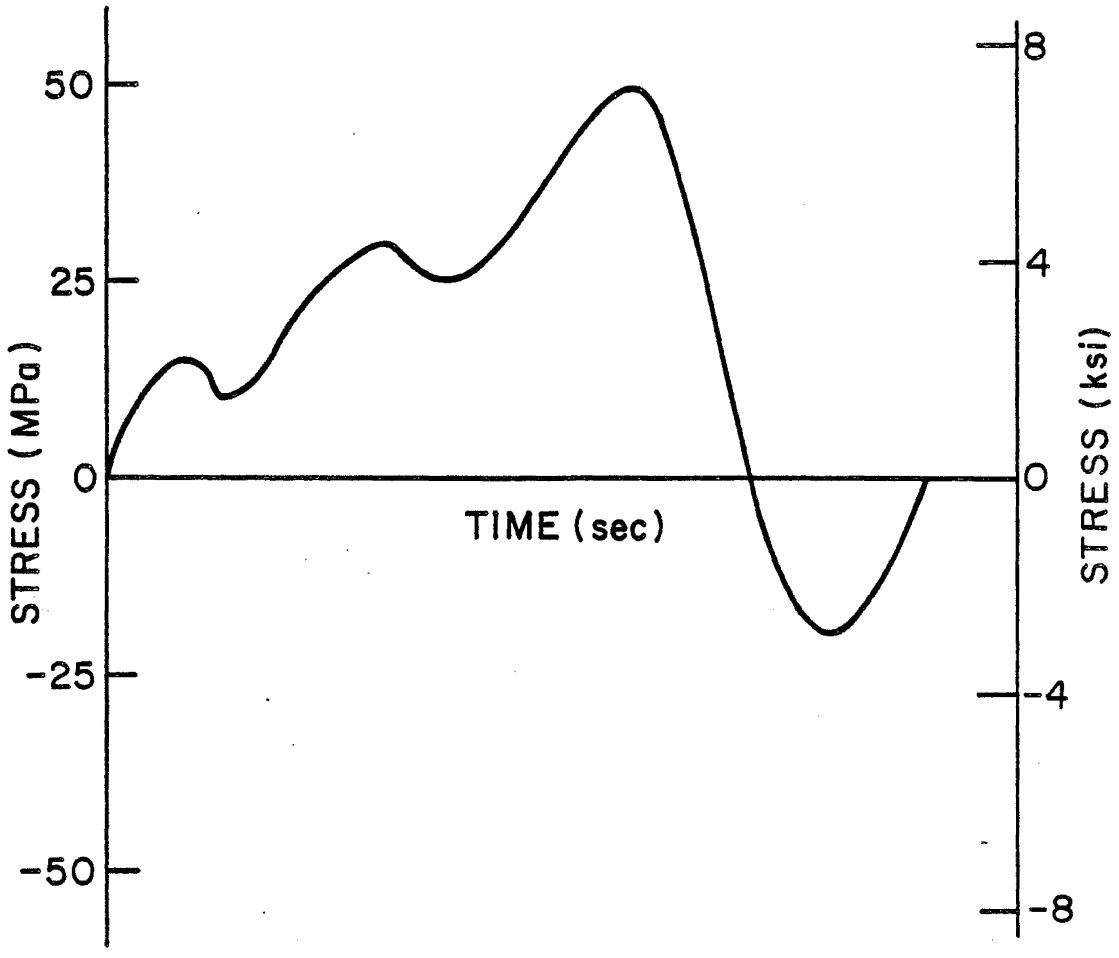

Fig. 7 Stress Time Curve for Comparison Purposes

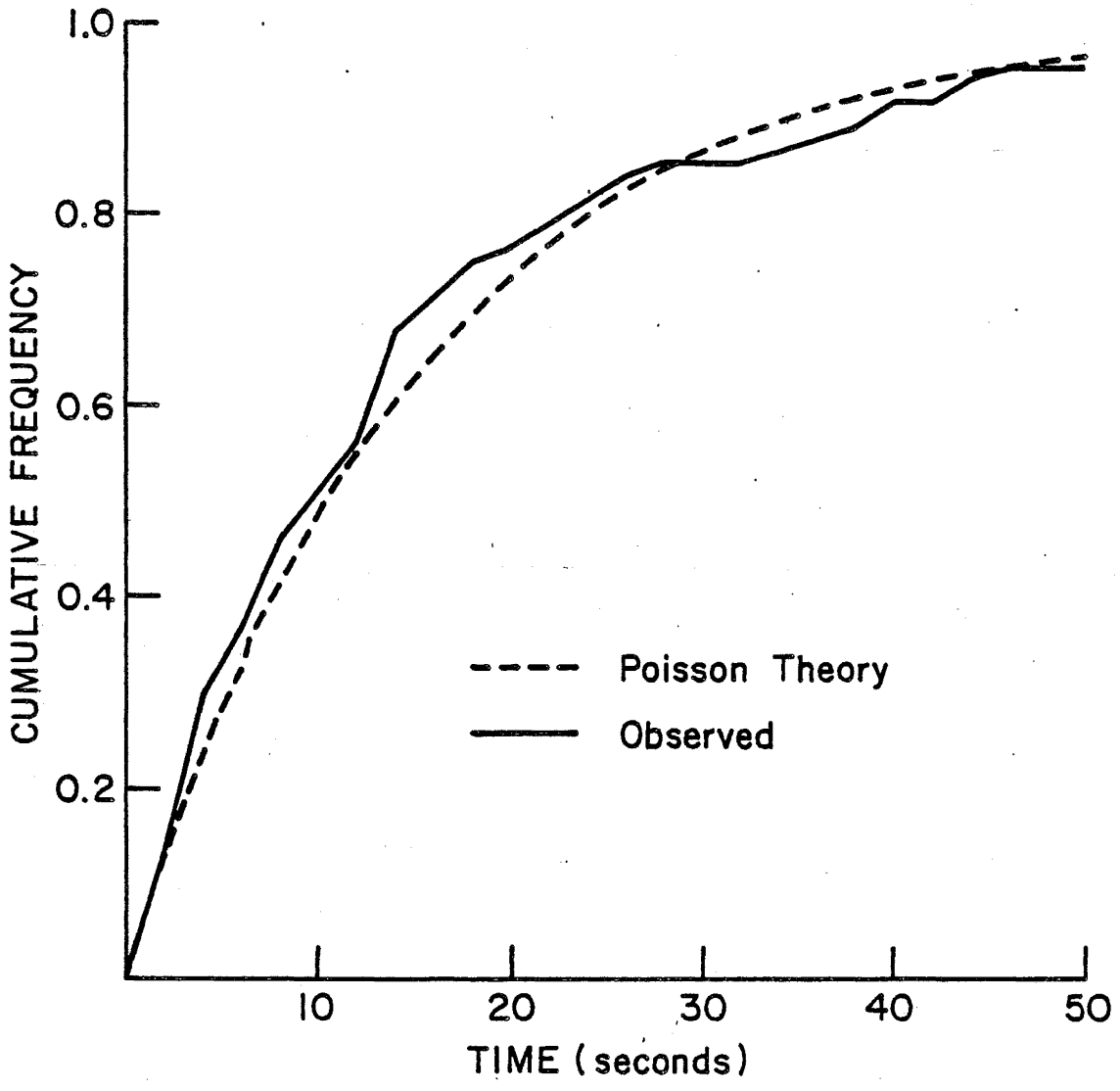

Fig. 8 Truck Headway Distribution

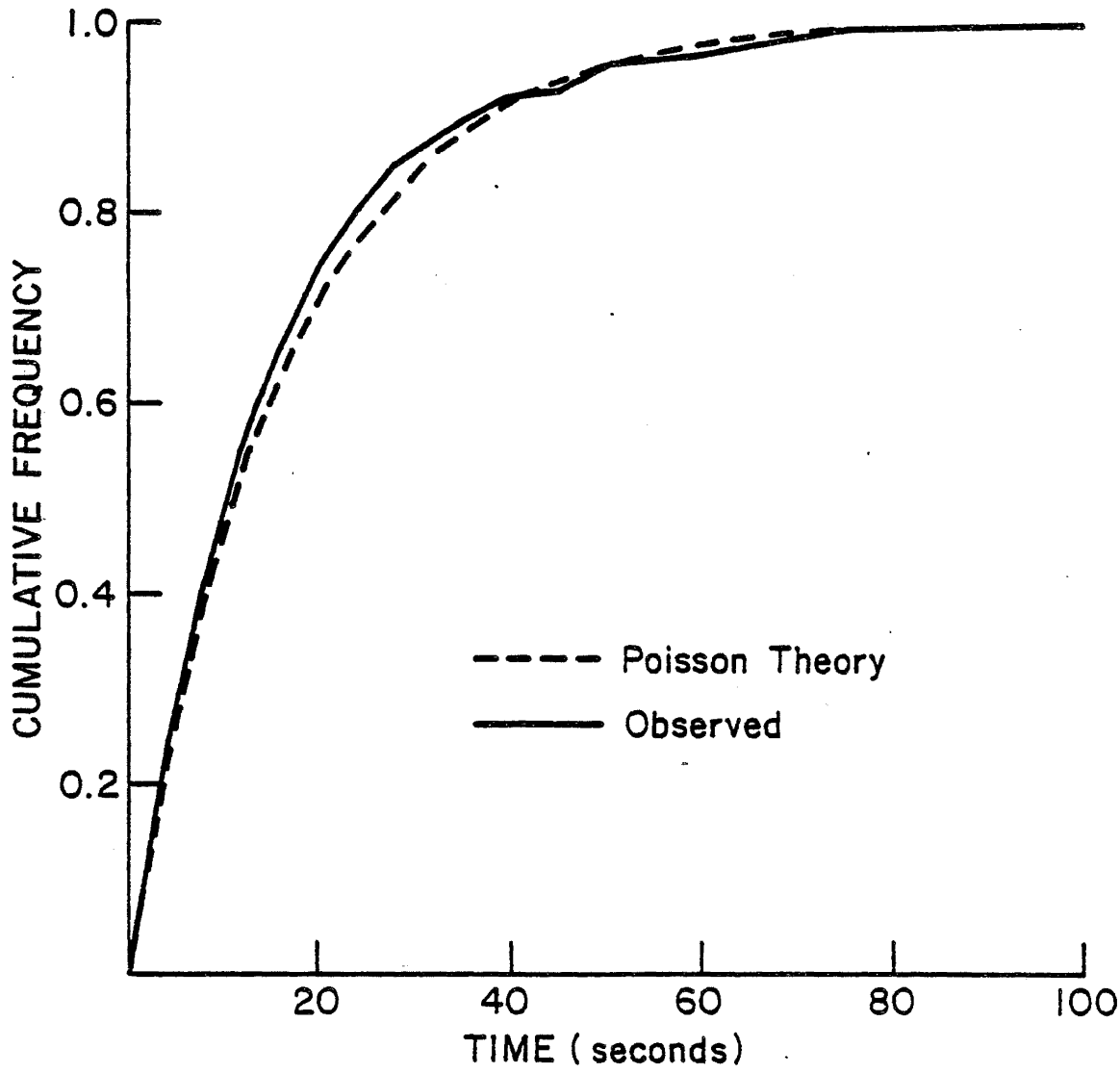

Fig. 9 Truck Headway Distribution

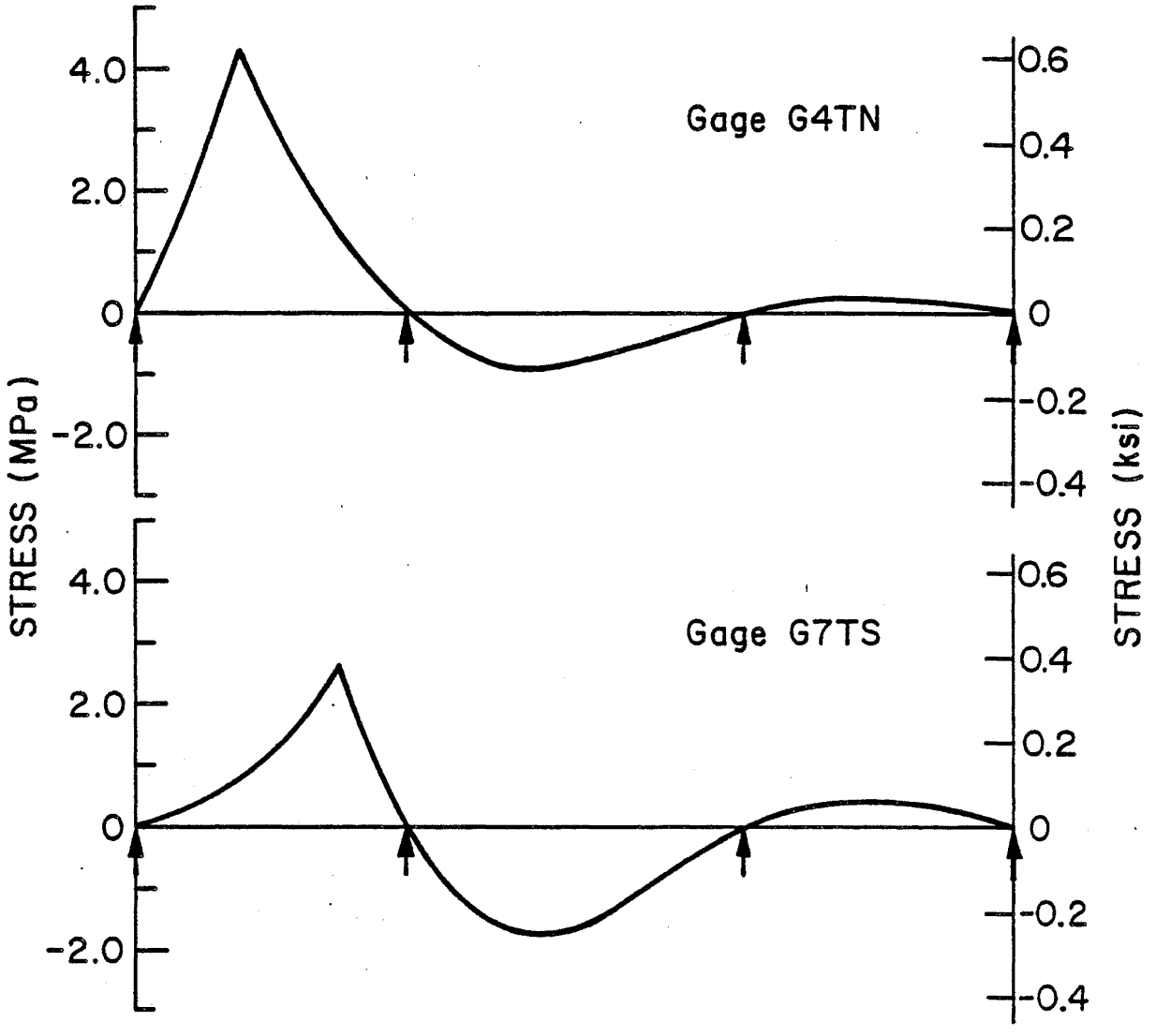

Fig. 10 Influence Lines for Stress at Girder Details

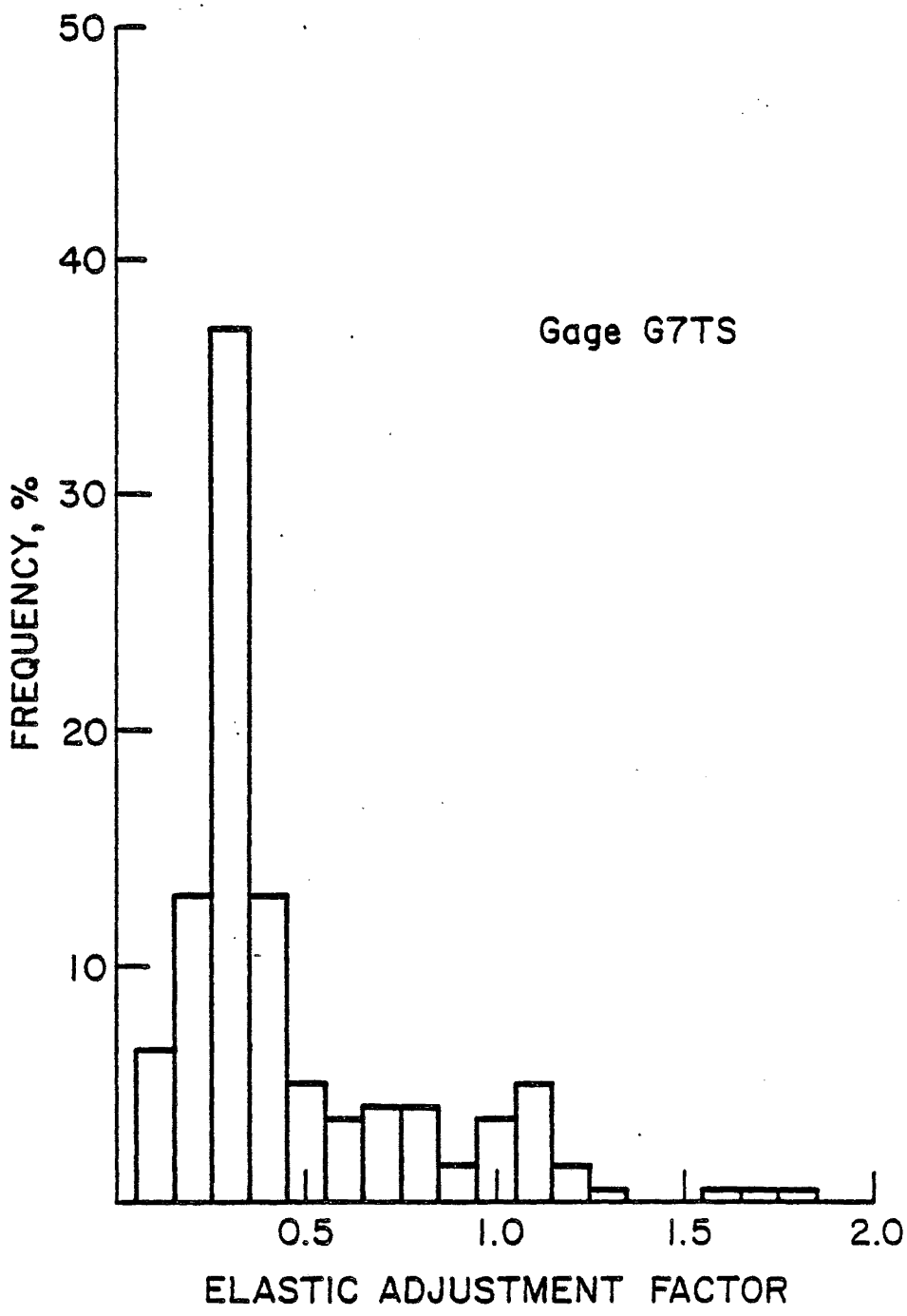

Fig. 12 Distribution of Elastic Adjustment Factor

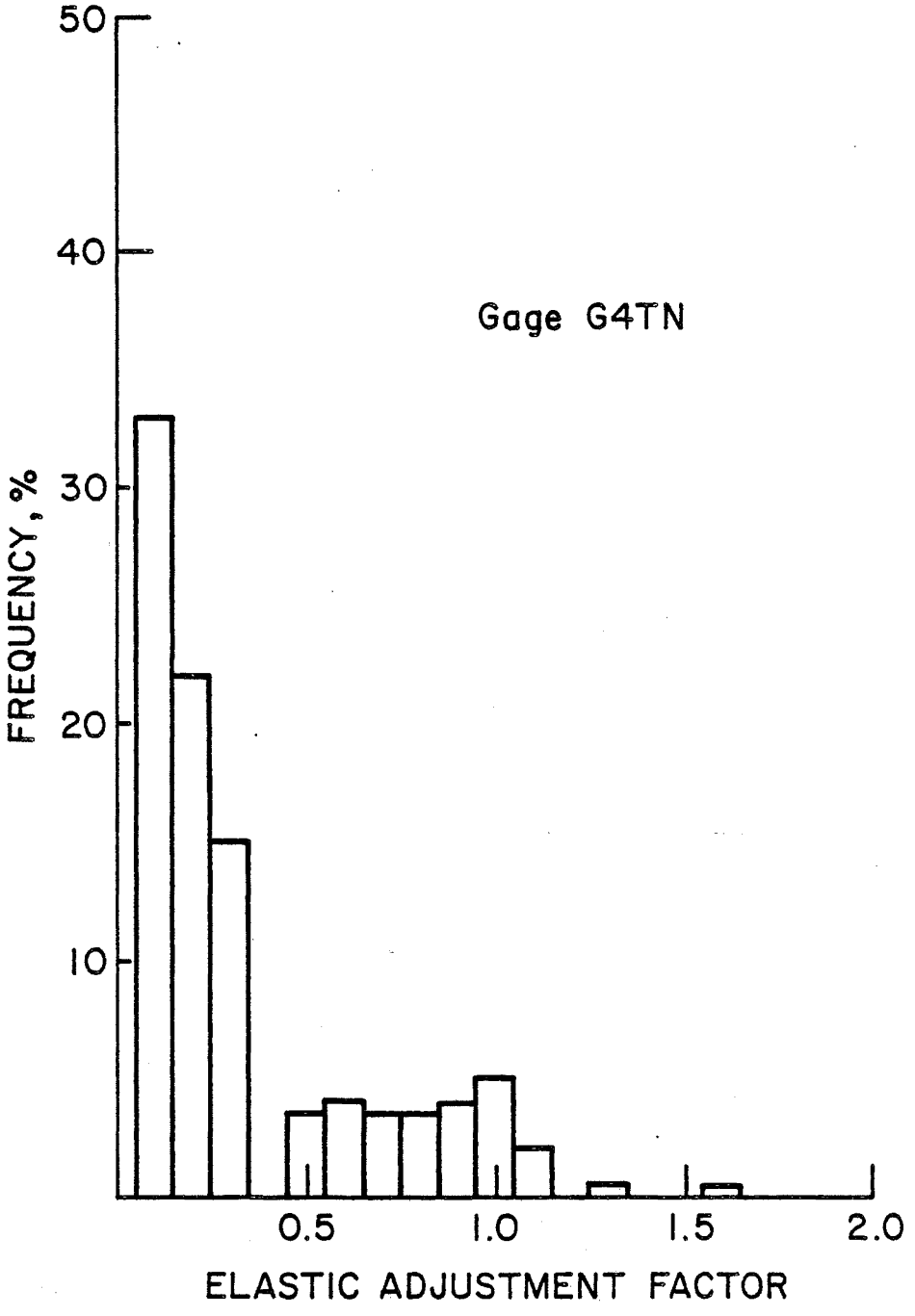

Fig. 12 Distribution of Elastic Adjustment Factor

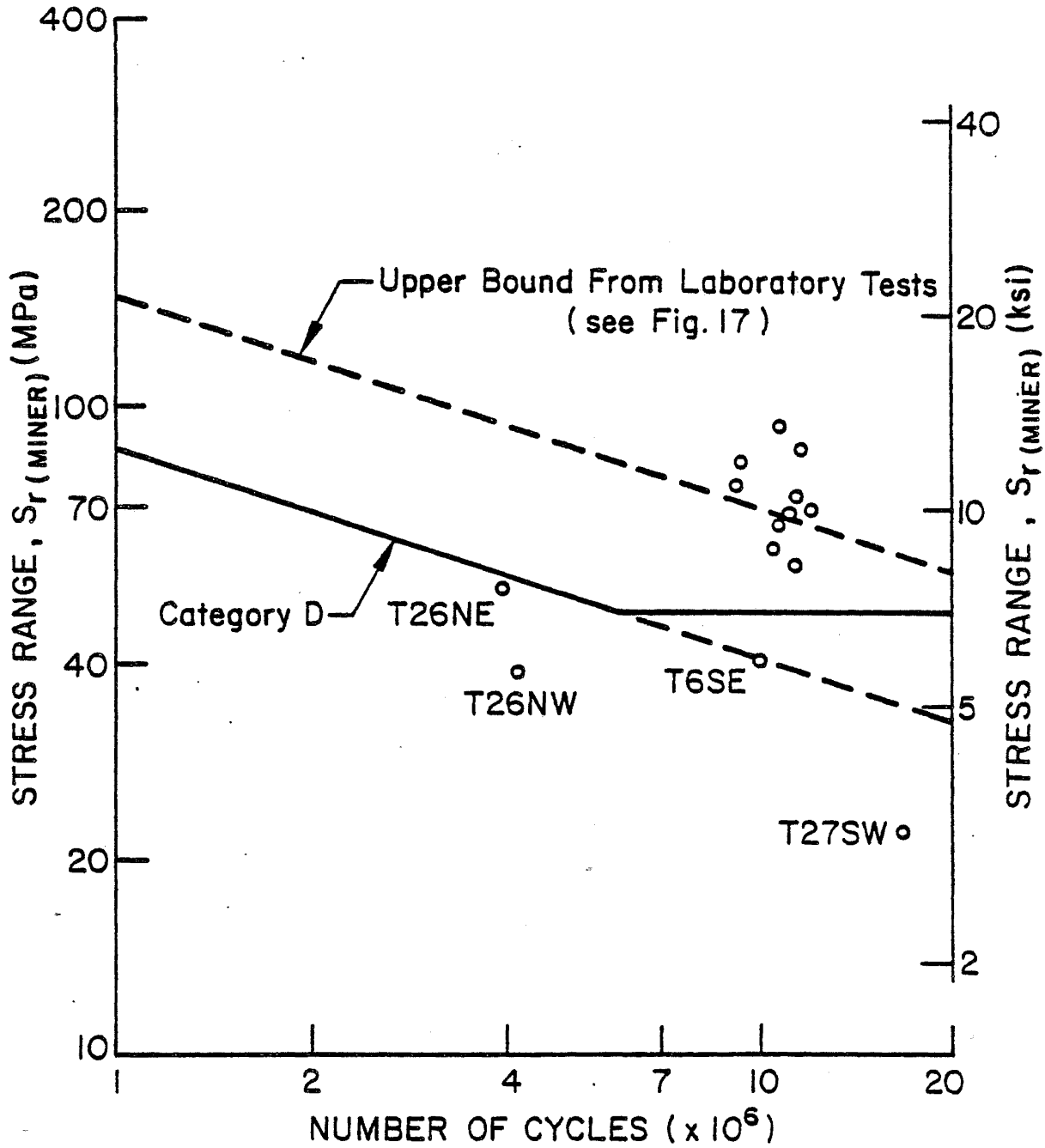

Fig. 13 S-N Values Using Peak to Peak Method without Multiple Presence Separation (Cracked Details)

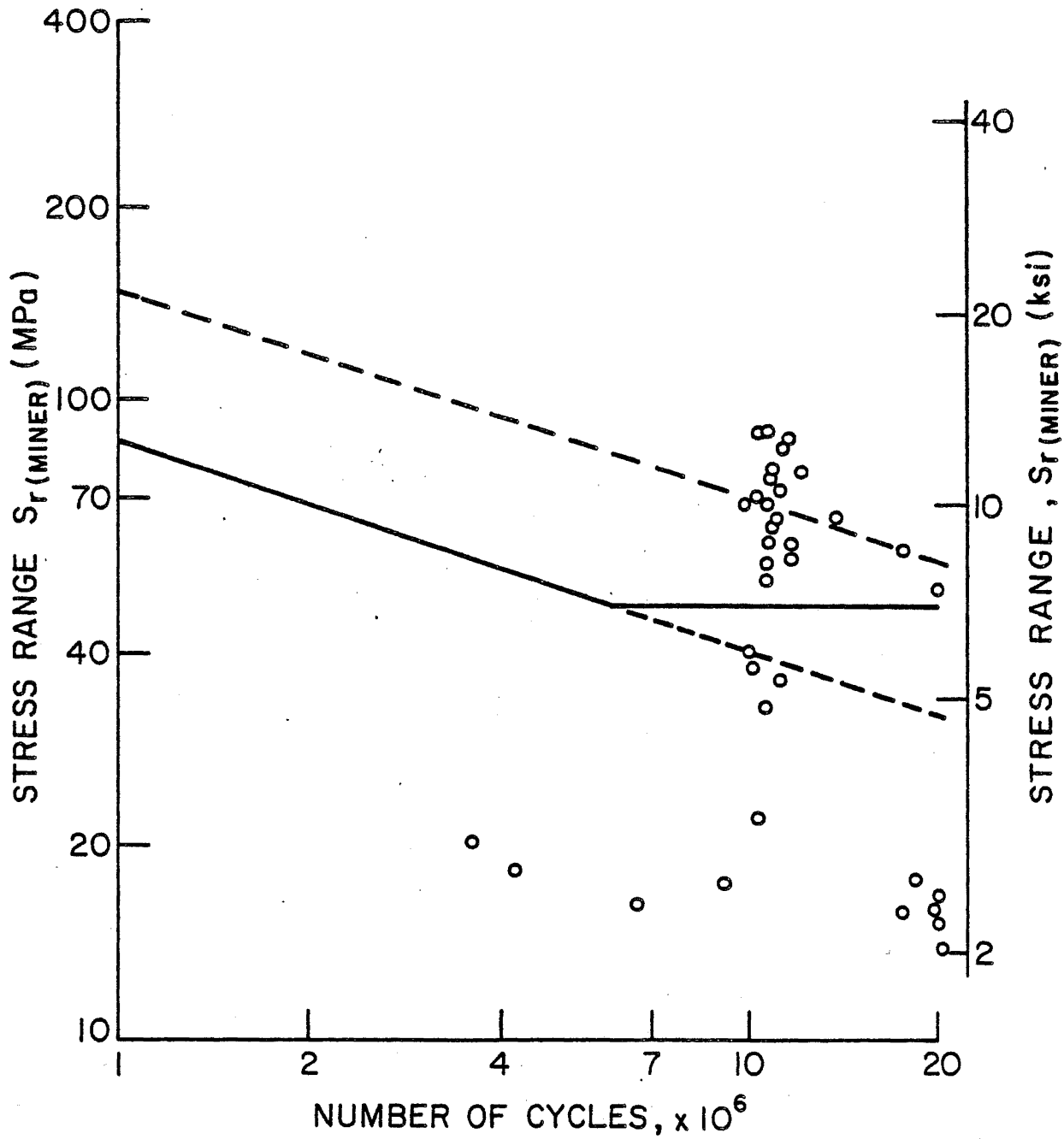

Fig. 14 S-N Values Using Peak to Peak Method Without Multiple Presence Separation (Noncracked Details)

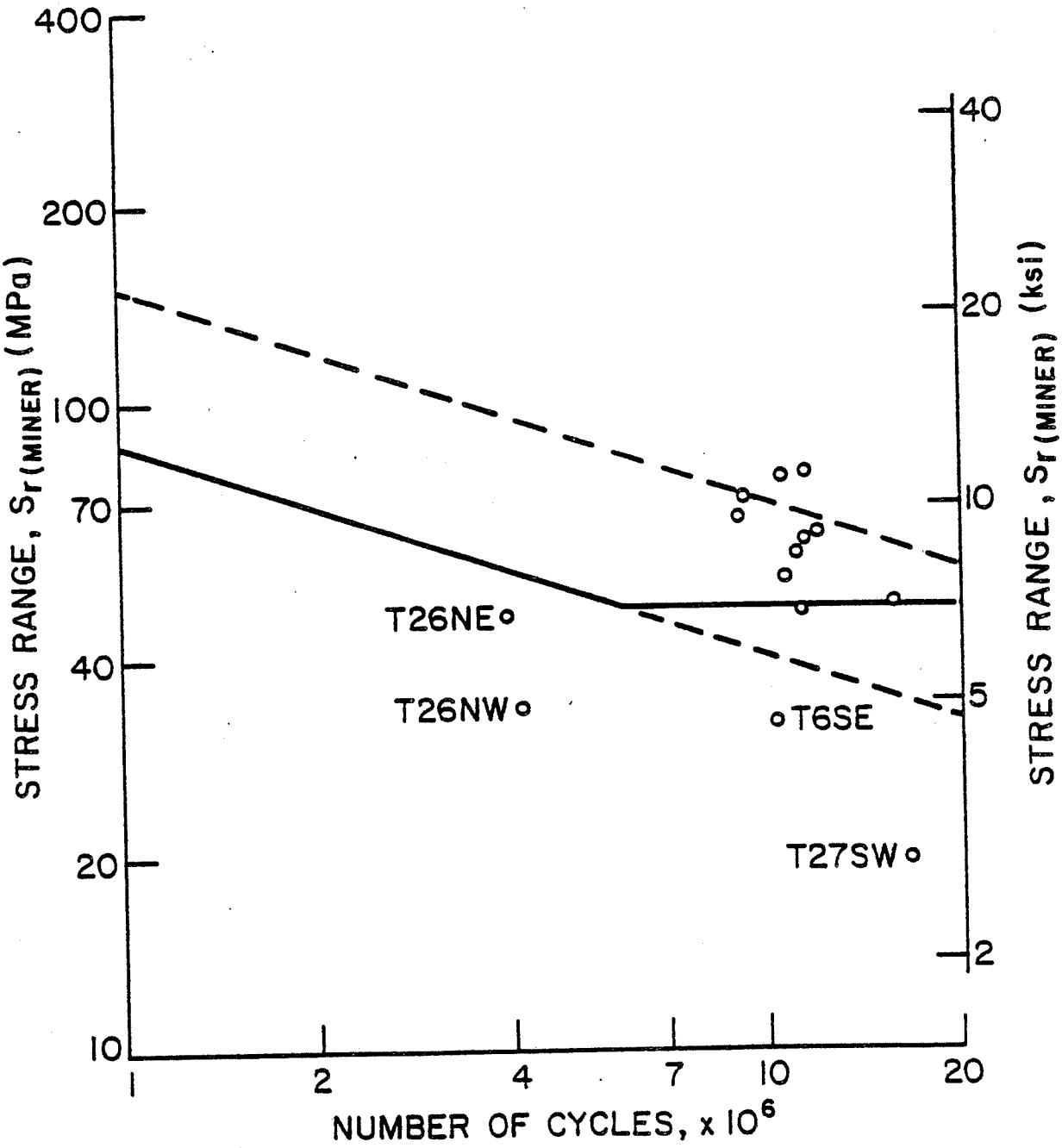

Fig. 15 S-N Values Using Peak to Peak Method with Multiple Presence Separation (Cracked Details)

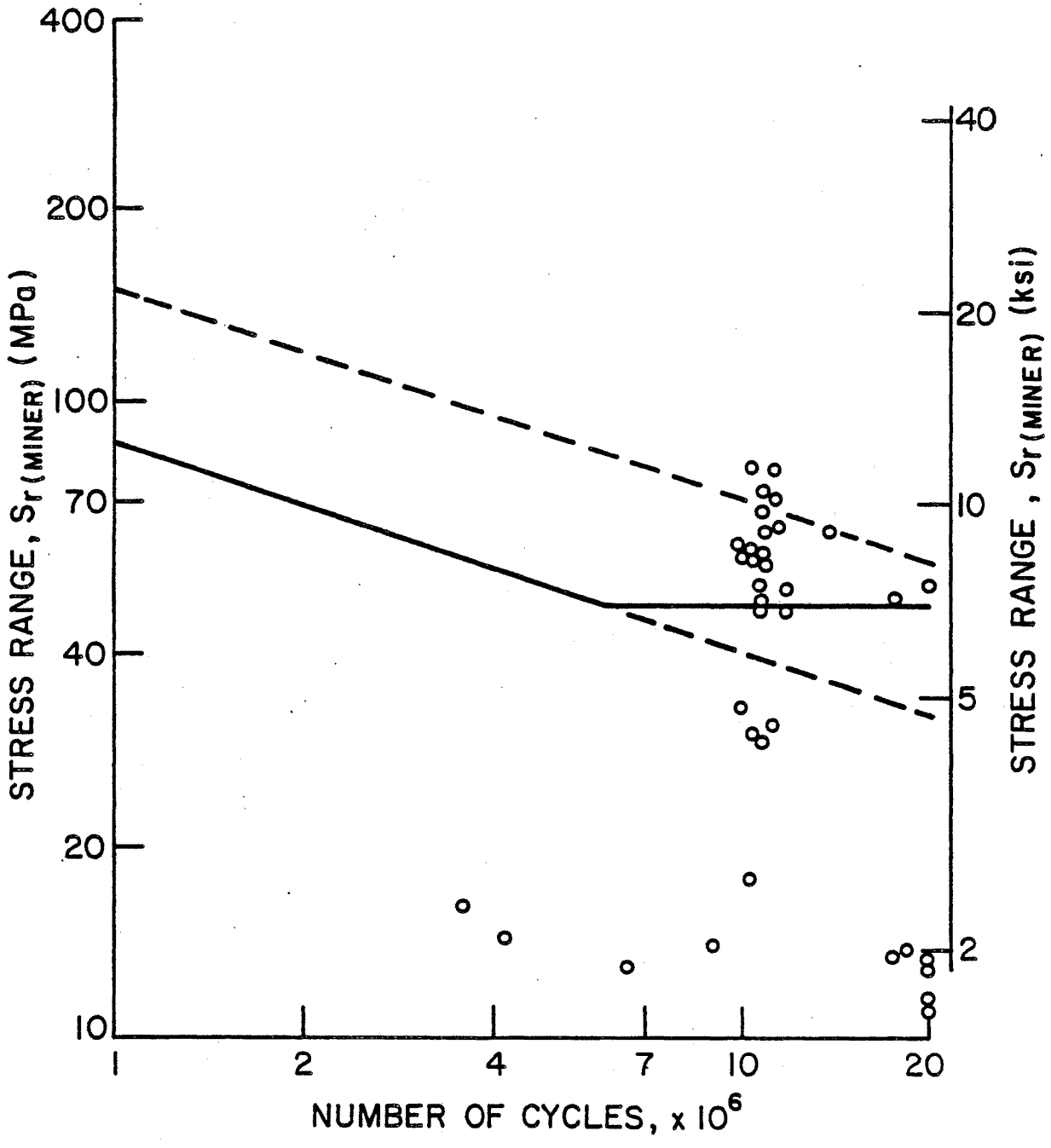

Fig. 16 S-N Values Using Peak to Peak Method with Multiple Presence Separation (Noncracked Details)

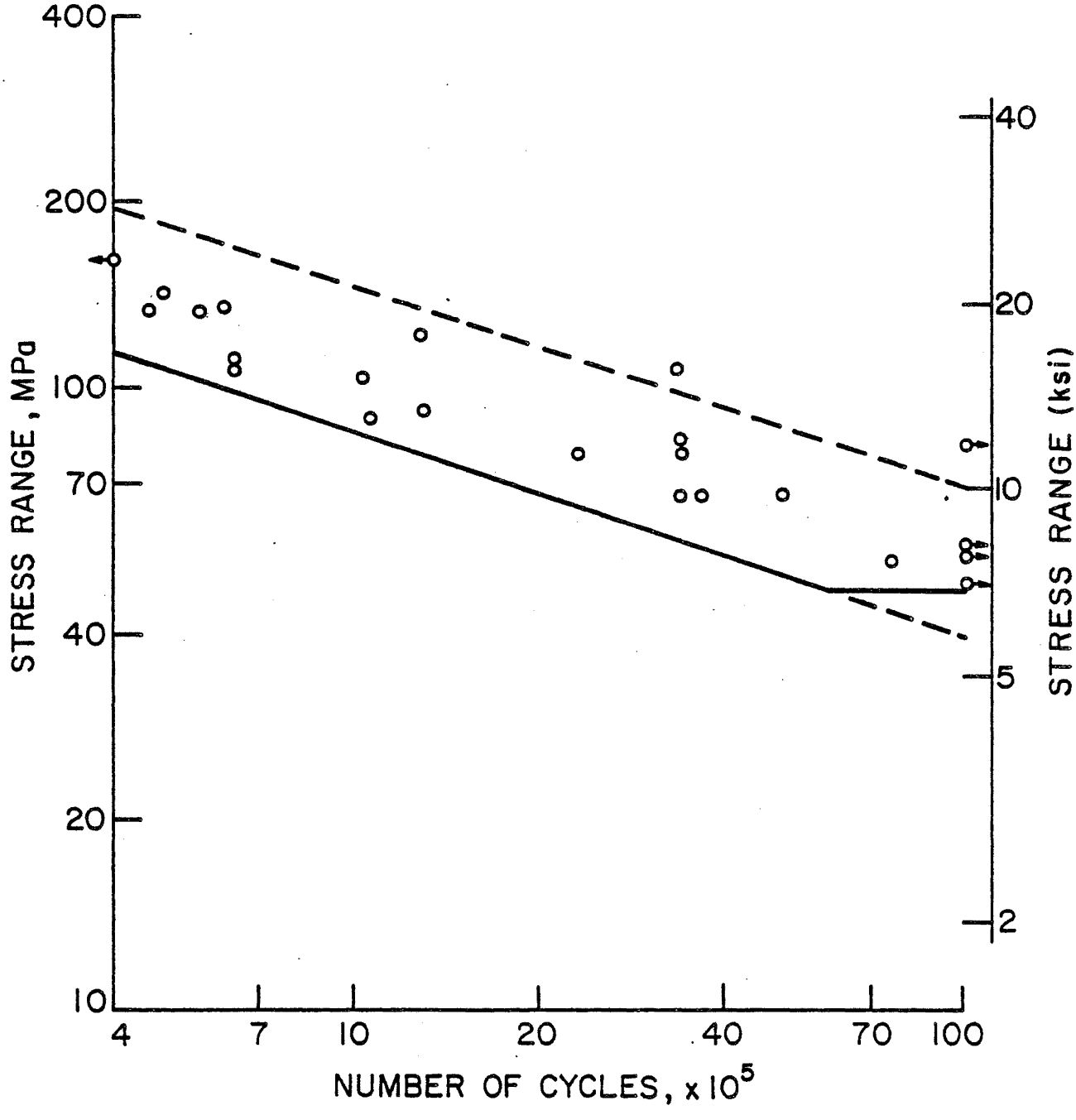

Fig. 17 S-N Values from Laboratory Experiments on Tie Plates

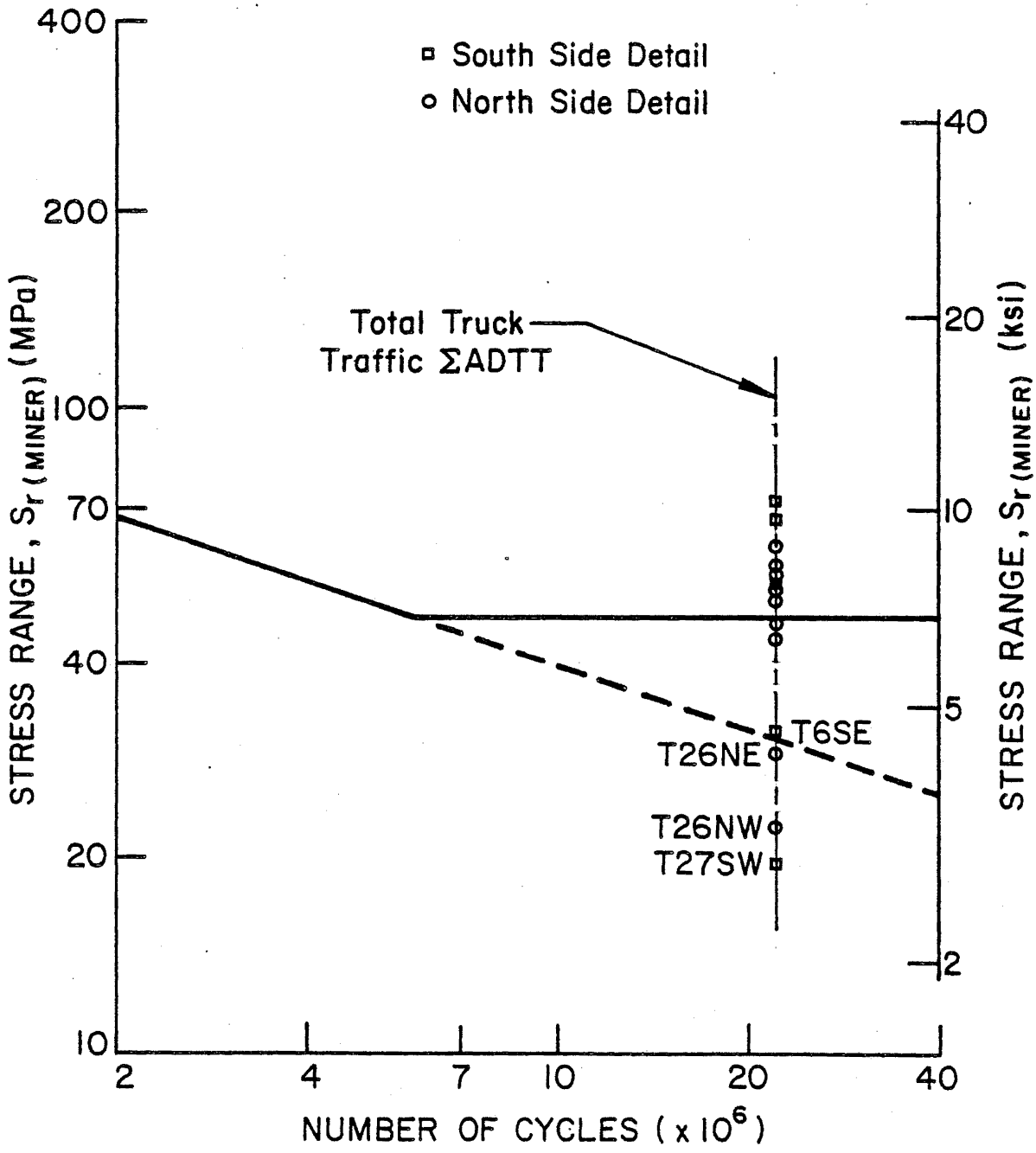

Fig. 18 S-N Values Using Peak to Peak Method Without Multiple Presence Separation, Evaluated at Total Truck Traffic (Cracked Details)

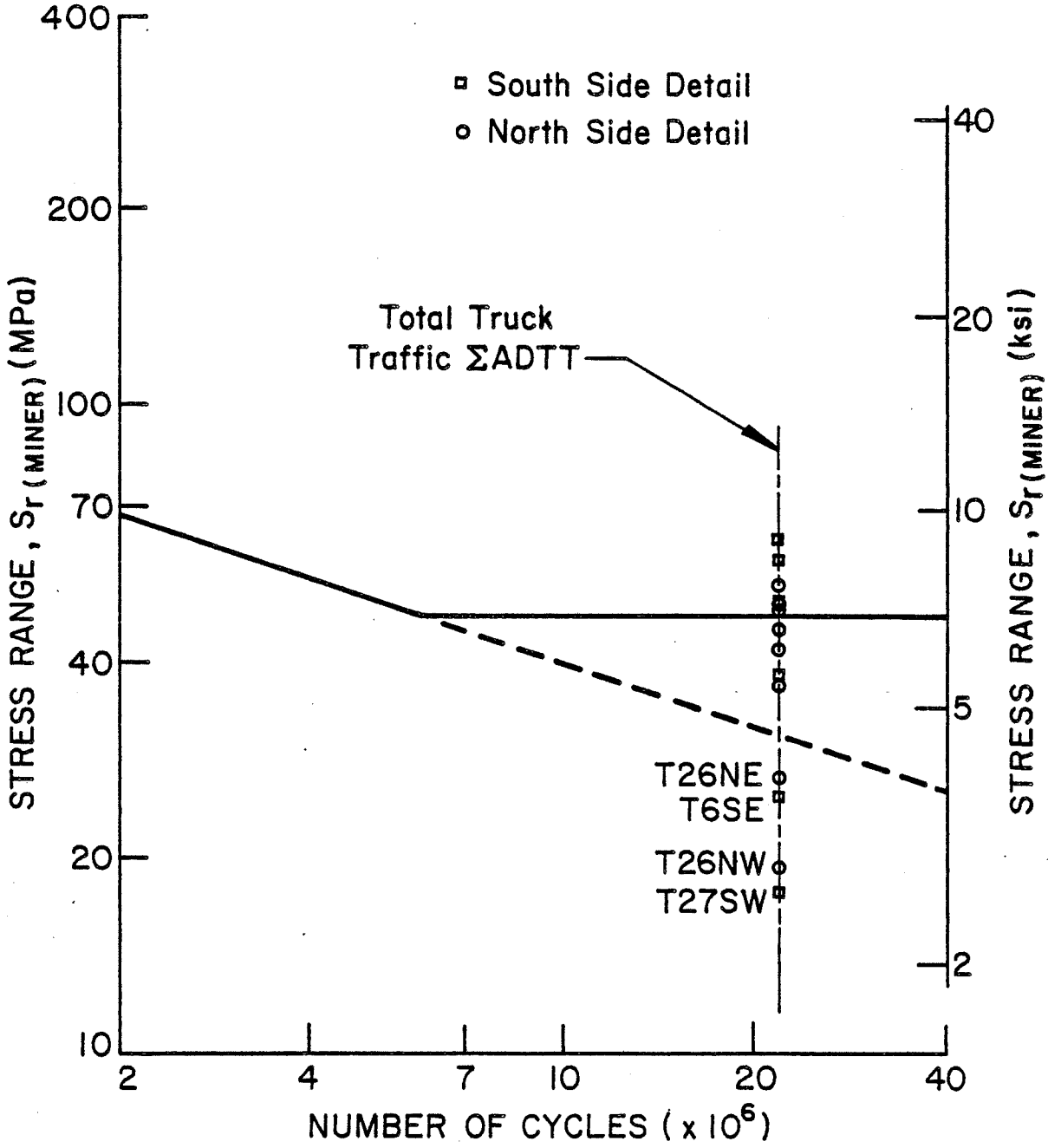

Fig. 19 S-N Values Using Peak to Peak Method with Multiple Presence Separation, Evaluated at Total Truck Traffic (Cracked Details)

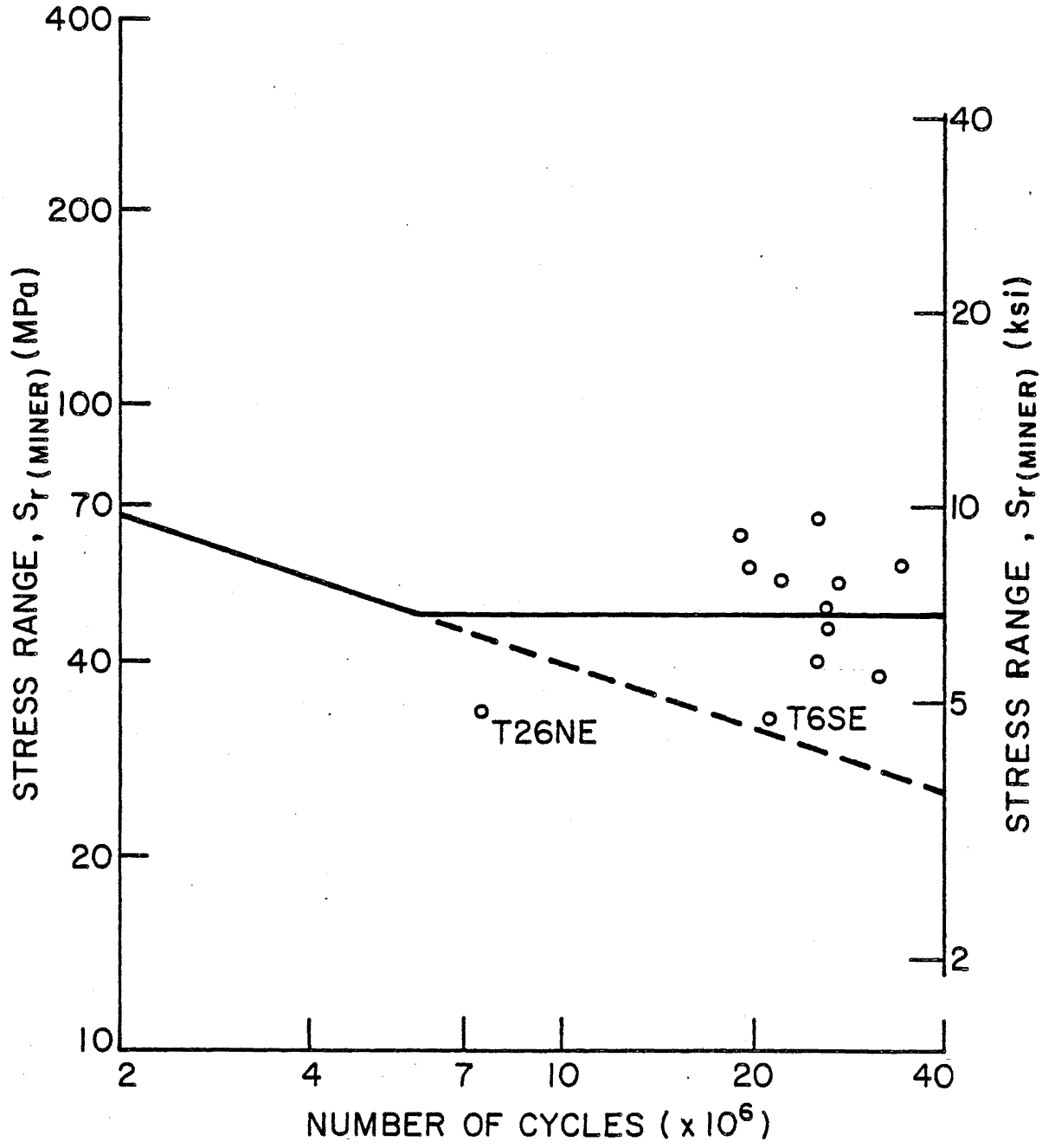

Fig. 20 S-N Values Using Rainflow Counting (Cracked Details)

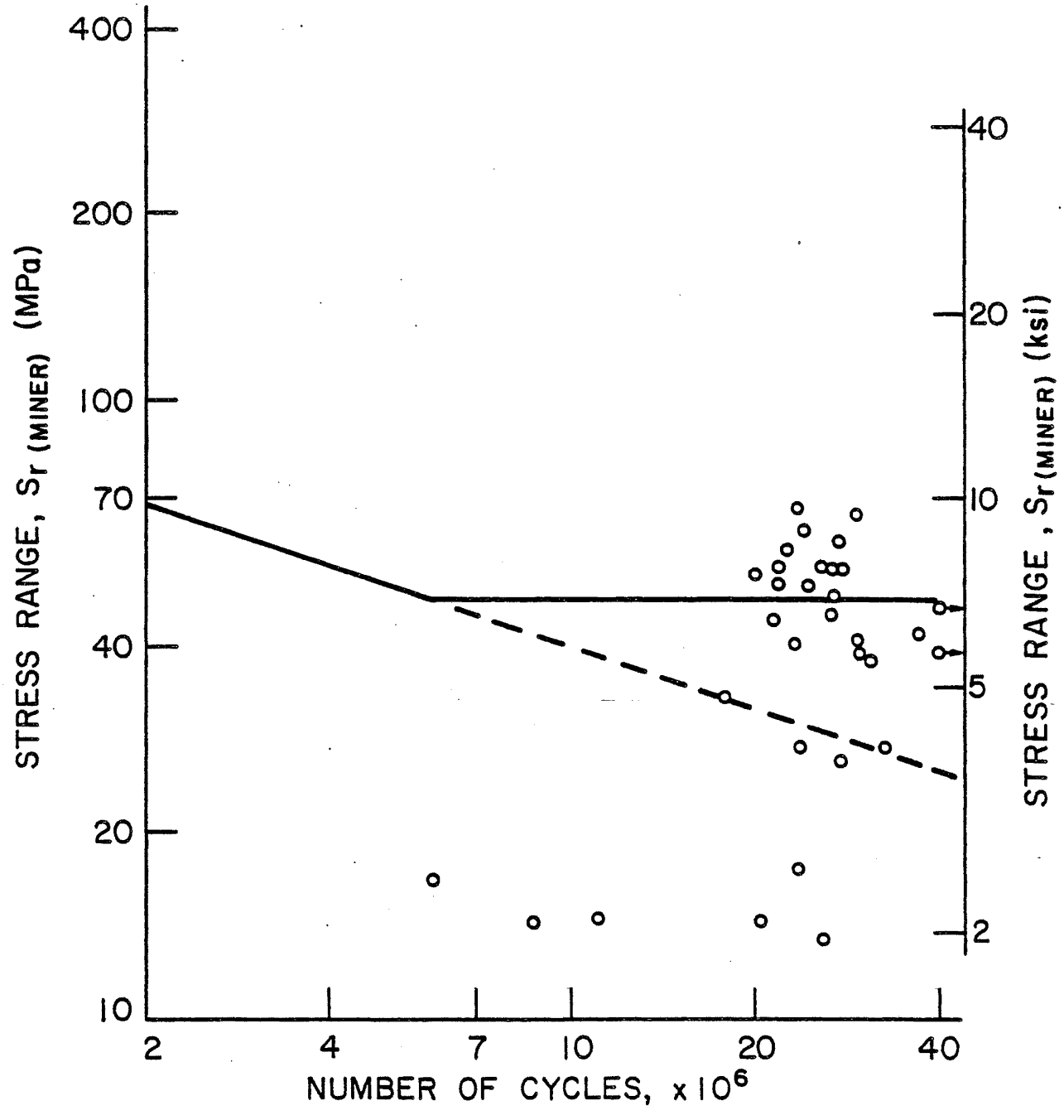

Fig. 21 S-N Values Using Rainflow Counting (Noncracked Details)

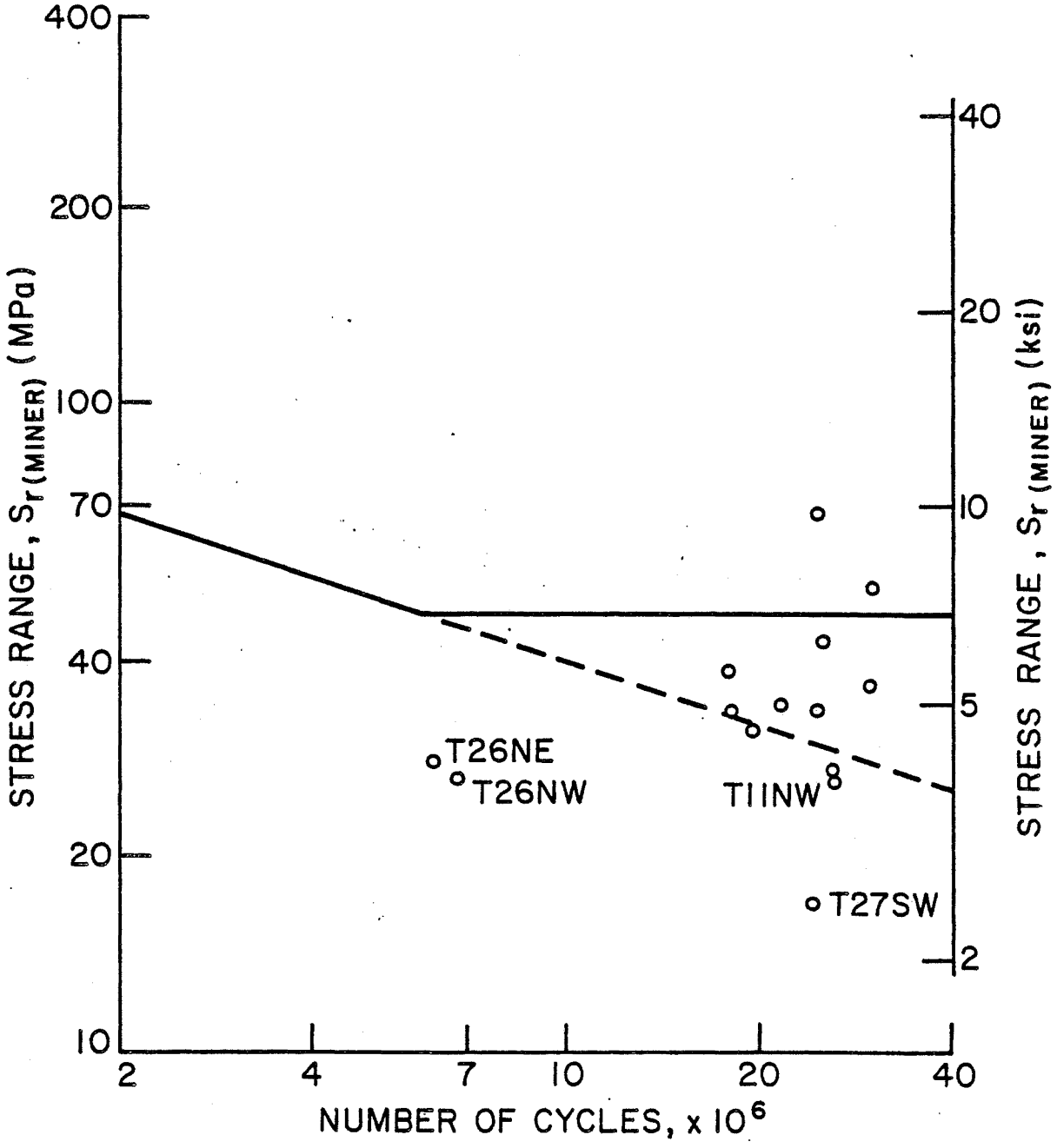

Fig. 22 S-N Values Using Modified Rainflow Counting (Cracked Details)

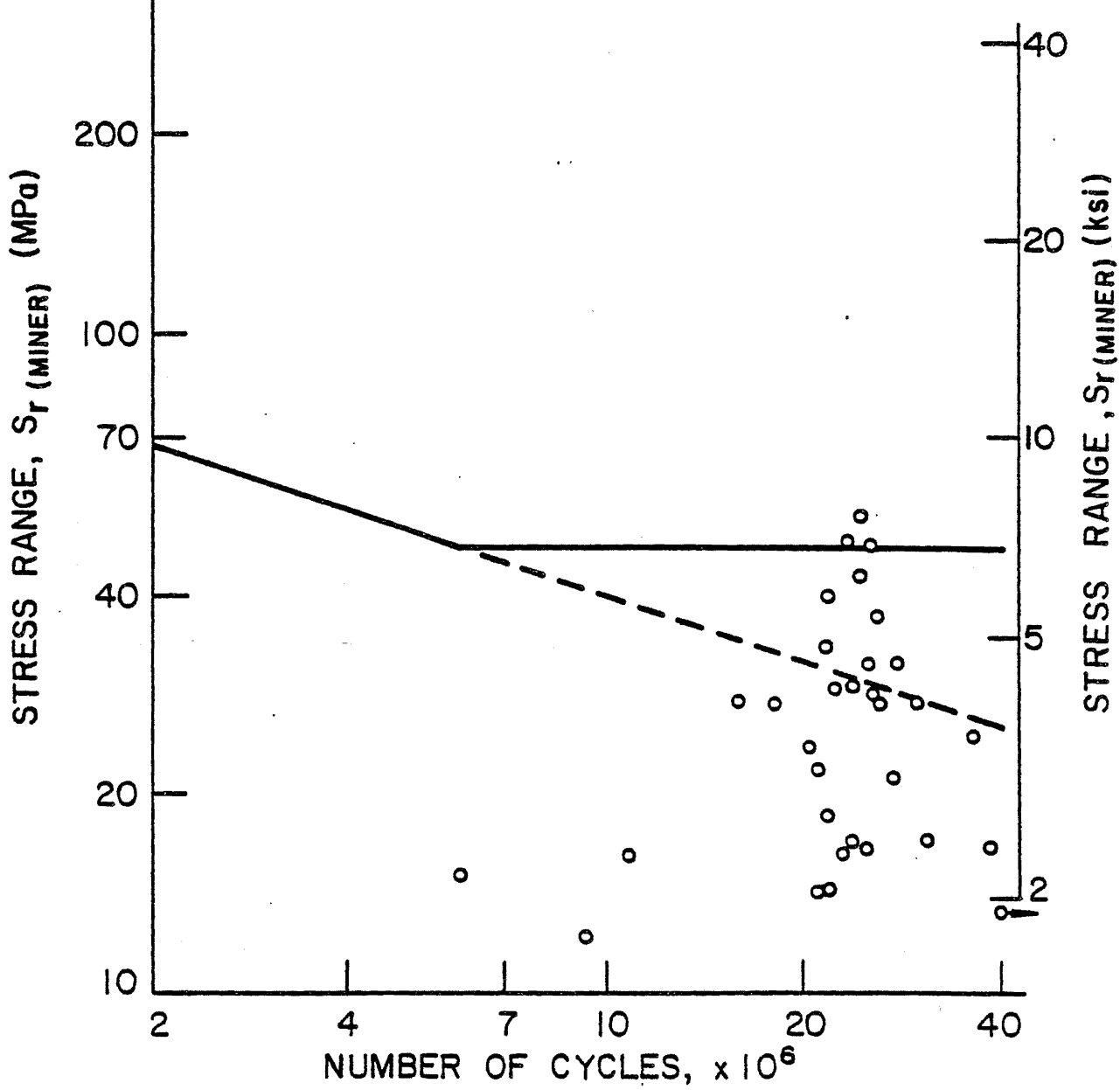

Fig. 23 S-N Values Using Modified Rainflow Counting
(Noncracked Details)

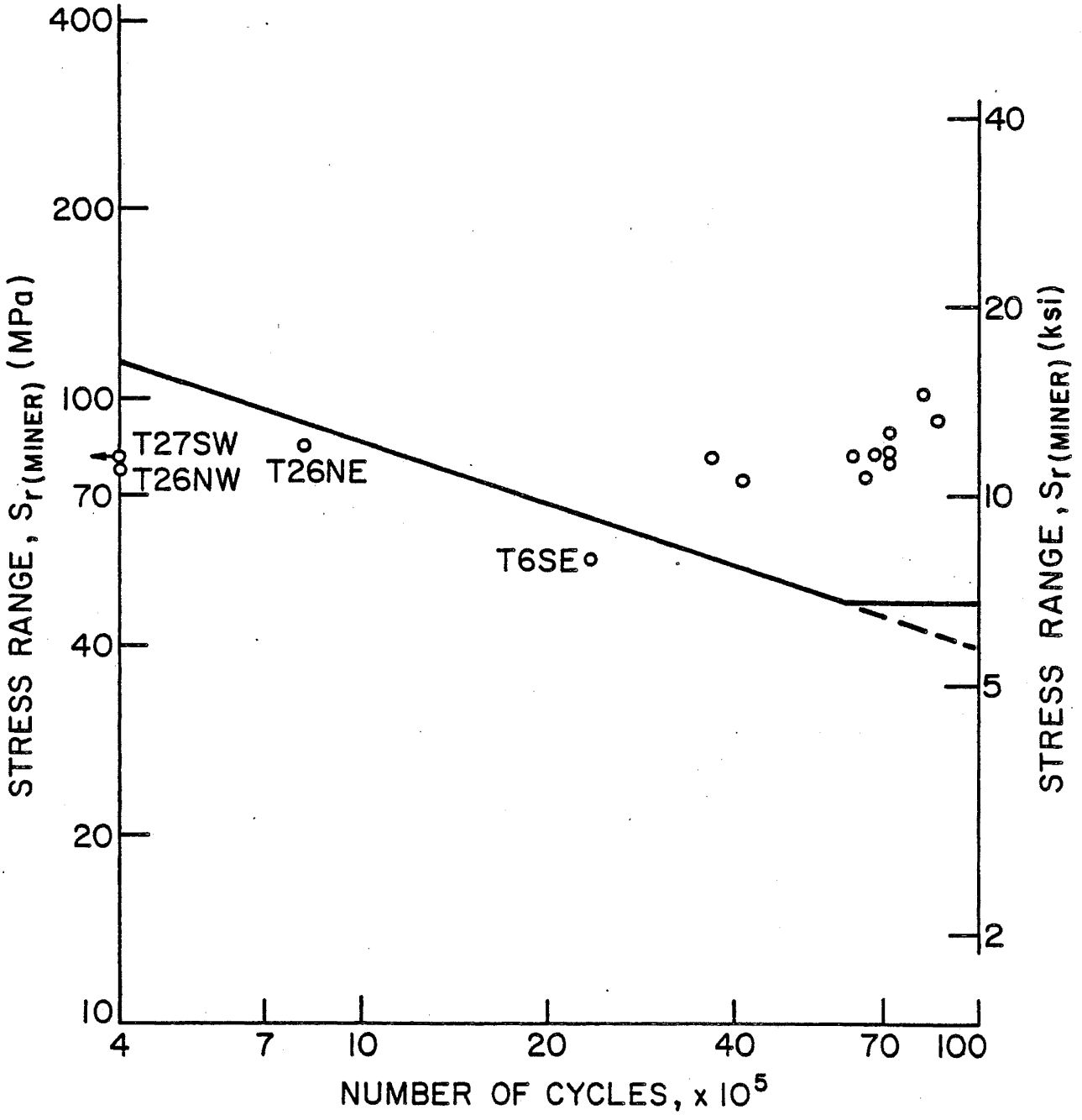

Fig. 24 S-N Values Using Peak to Peak Method Without Multiple Presence Separation and Truncating Stresses at 48 MPa (Cracked Details)

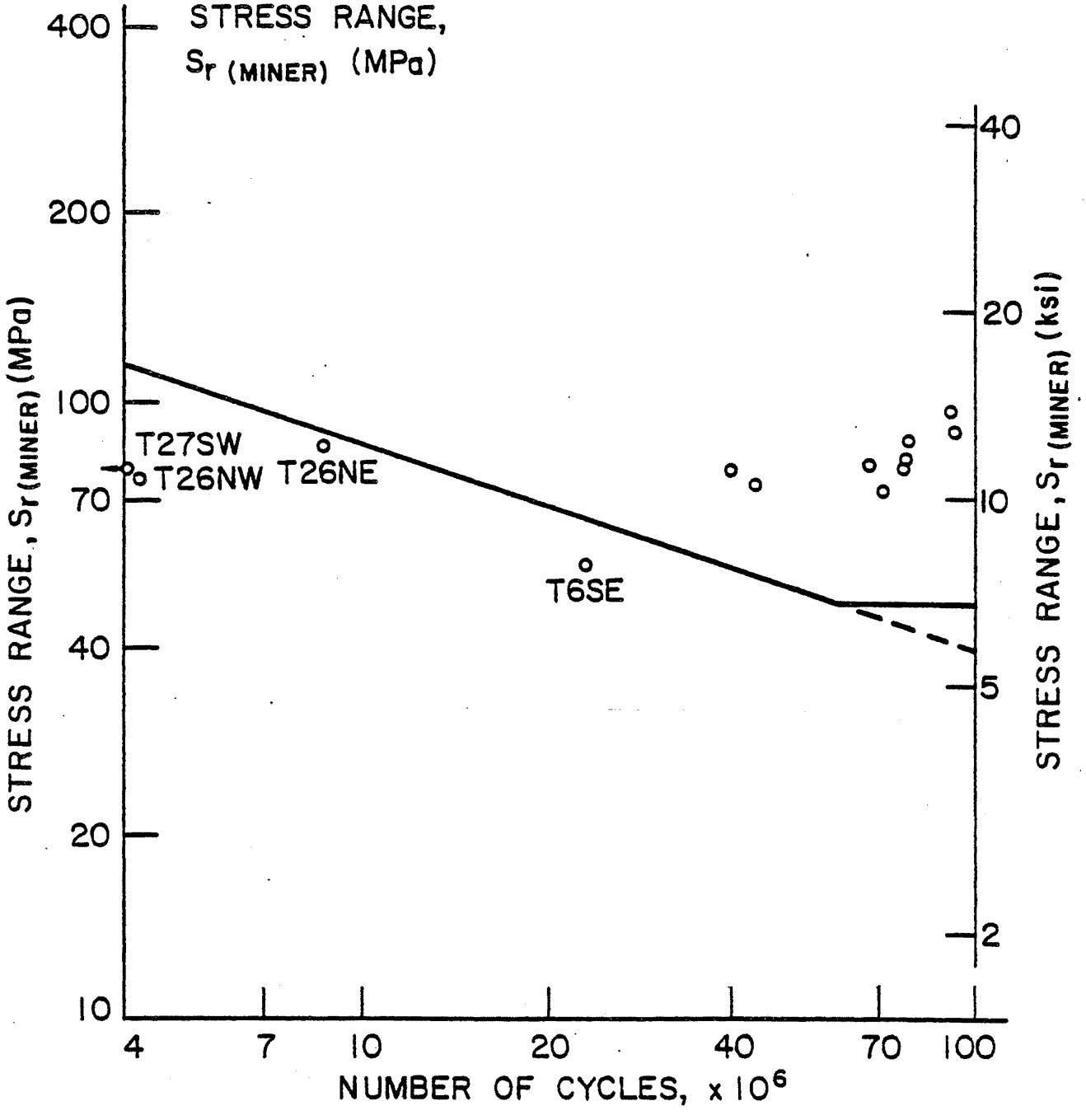

Fig. 25 S-N Values Using Peak to Peak Method with Multiple Presence Separation and Truncating Stresses at 48 MPa (Cracked Details)

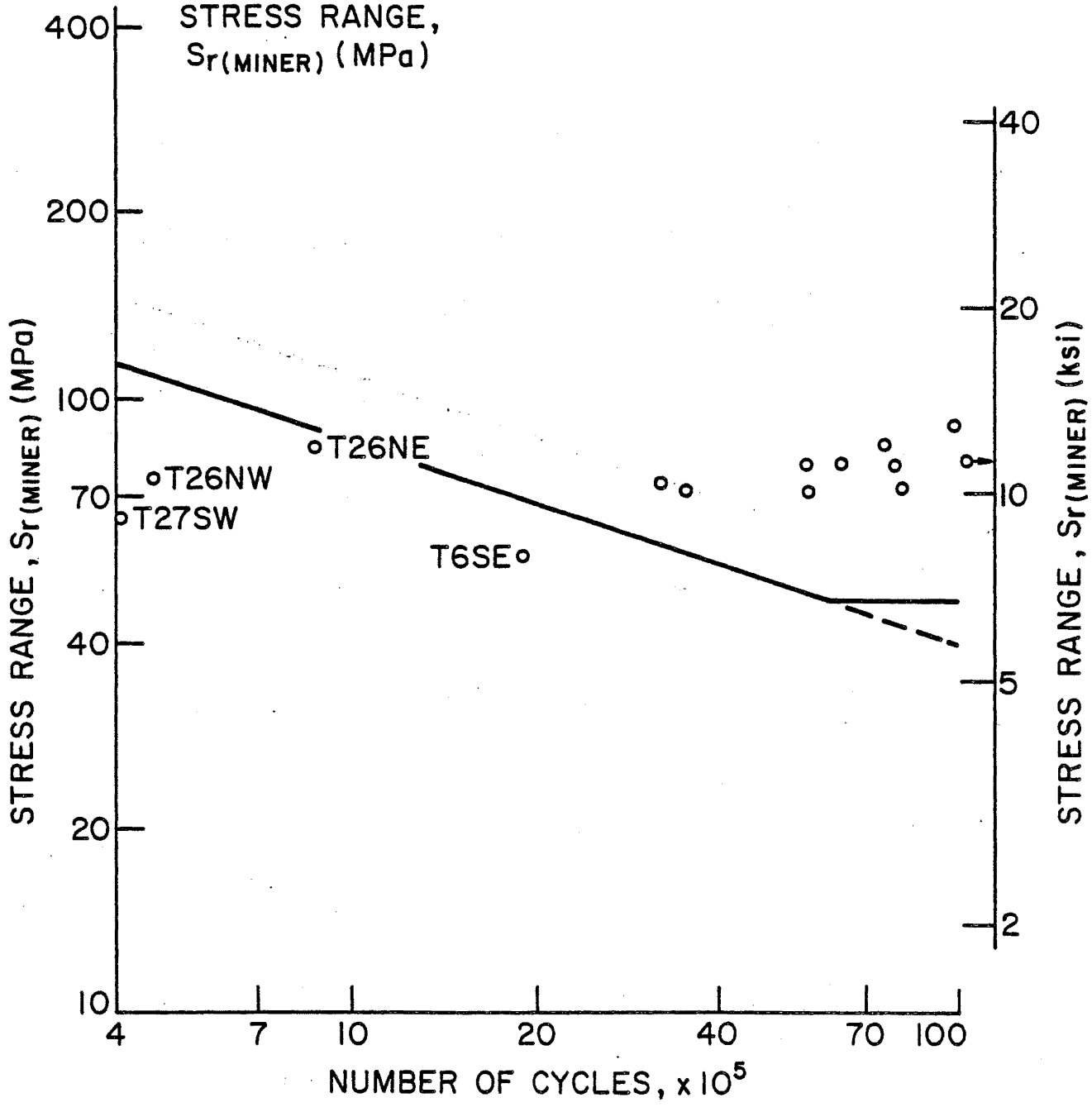

Fig. 26 S-N Values Using Rainflow Counting and Truncating Stresses at 48 MPa (Cracked Details)

APPENDIX A: DATA REDUCTION - STAGE I

The rules governing the computer program for stage I of the data reduction were as follows.

1. The first value for a particular channel was taken as a datum. Thereafter, if a new value was within the threshold levels of the datum, the new value was averaged with all the previous values to establish a new datum.

2. As soon as the stress excursion emerged from within the threshold levels, a maximum or minimum stress was recorded until not only stress reversal occurred but until the stress excursion crossed the other threshold level.

3. The only exception to the above rule was that if the stress remained within the threshold levels for a period in excess of one second, and then reemerged, the process began anew. This procedure was introduced to account for trucks following each other so closely that the equipment was not switched off.

4. The program allowed storage of up to 18 extreme values. If this number was exceeded, the program run was automatically stopped and the results of the last gage printed out to allow the operator to make a decision on whether or not to increase the threshold levels.

Some examples of the effects of these criteria are shown in Figs. A1, A2 and A3. Figure A1 shows a simple stress excursion which crosses the threshold levels once on the tension side and once on the compression side. Only one stationary point is recorded in each direction. Figure A2 represents a detail which undergoes stress reversal early in the excursion. However, the range is not sufficient for the excursion to exceed the lower threshold value, so again only one stationary point is recorded in each direction. Figure A3 shows the stationary points which would have been recorded if the stress level had remained within the threshold values for a period in excess of one second.

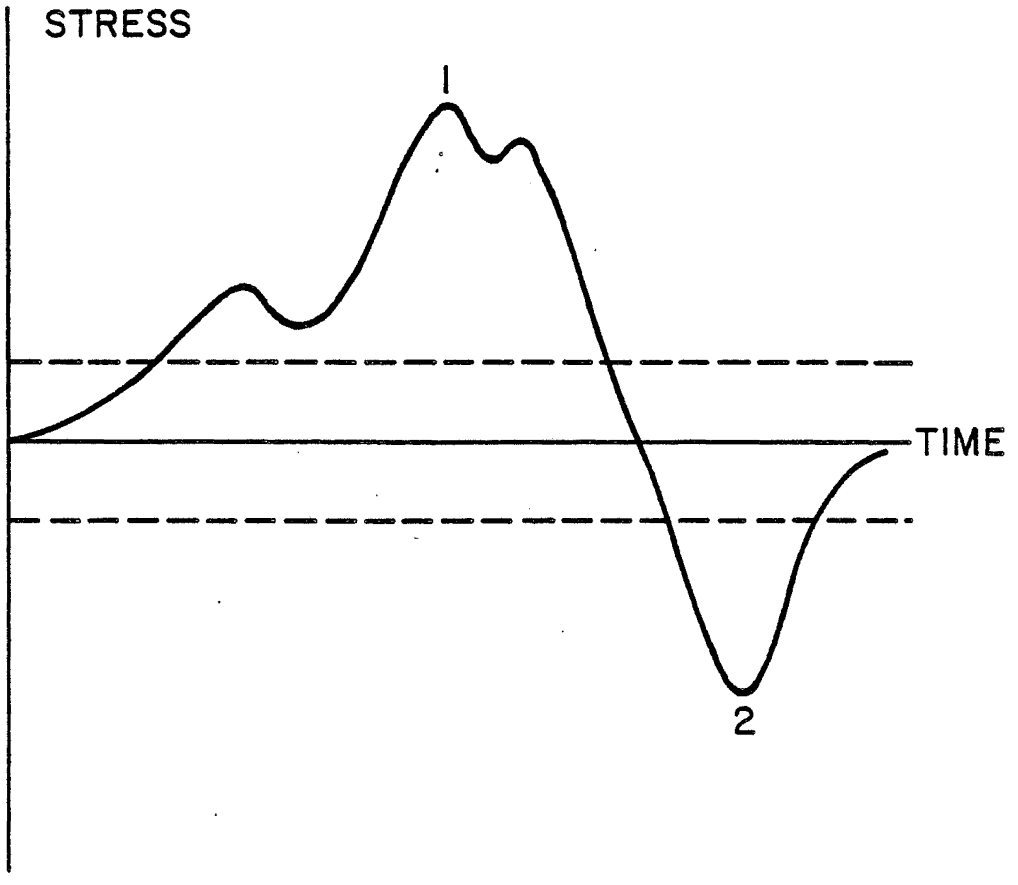

Fig. A1 Simple Stress Excursion with Two Stationary Points

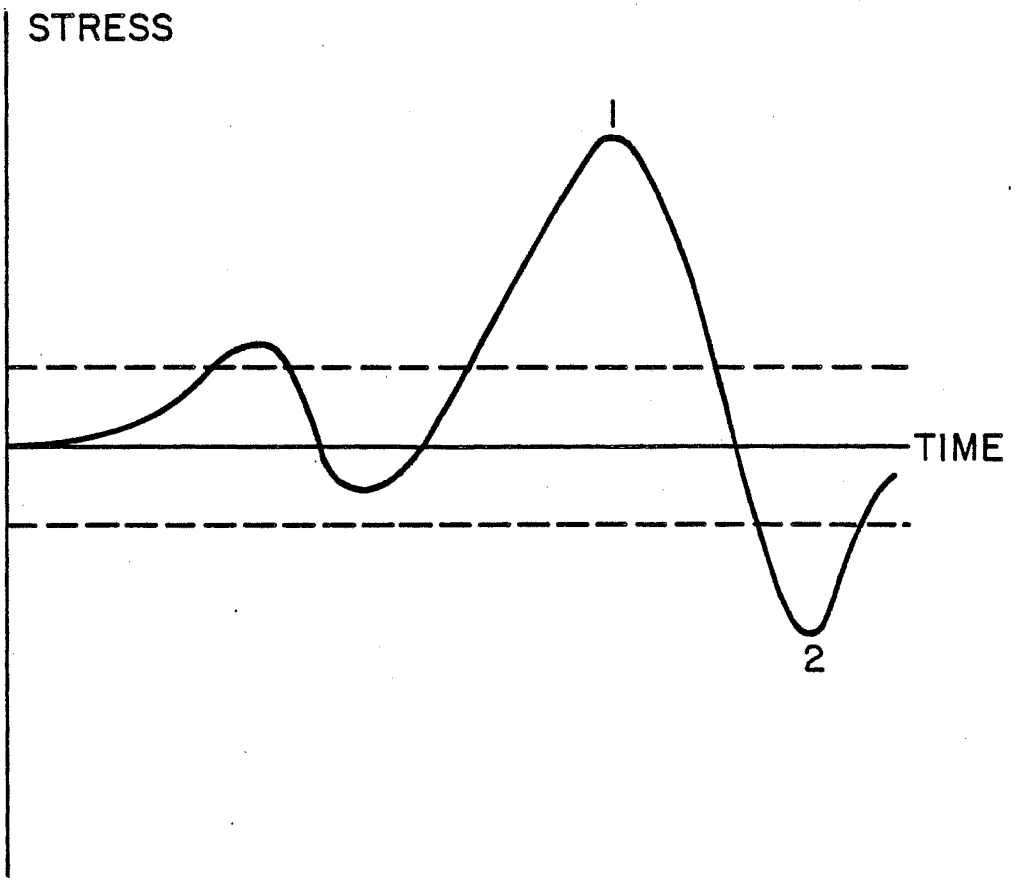

Fig. A2 Complex Stress Excursion with Two Stationary Points

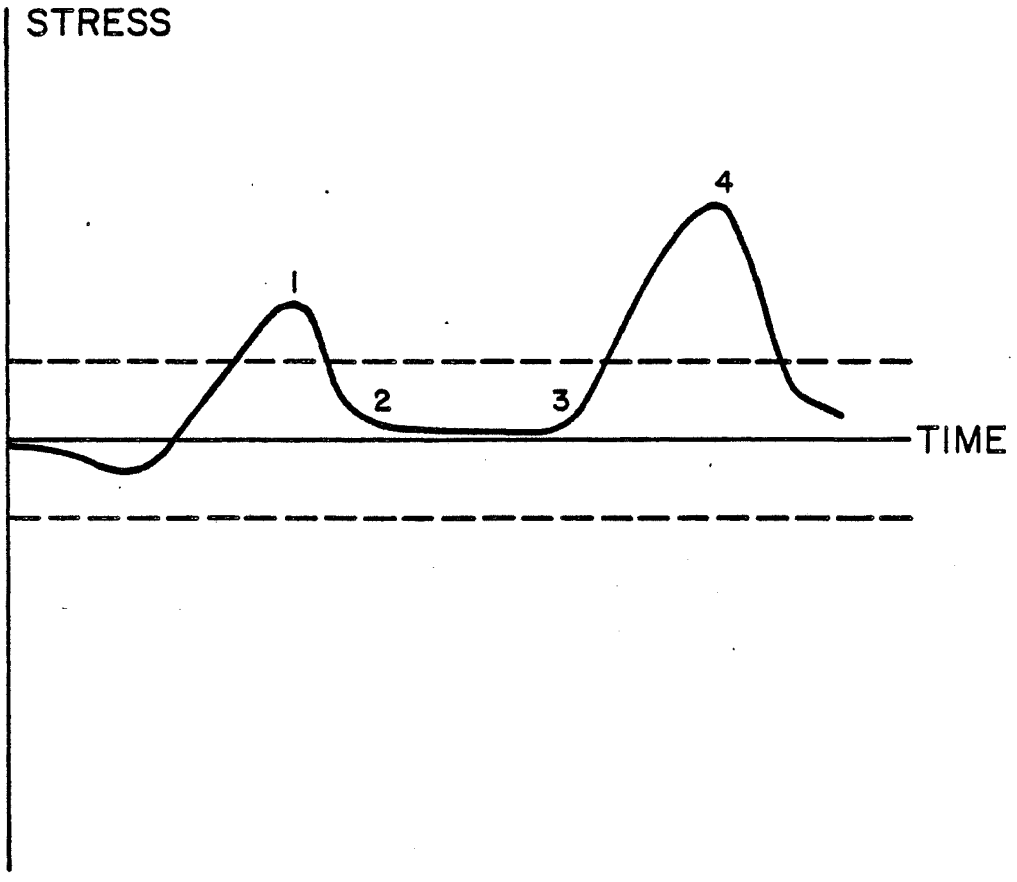

Fig. A3 Stress Excursion Recorded as Two Cycles

APPENDIX B: CYCLE COUNTING PARAMETERS

There are many methods of cycle counting in general use, most of which were developed in response to the needs of a specific application, particularly in the aircraft industry. As many of the methods reflect the characteristics of monitoring instruments, they bear little or no relation to the theory of fatigue crack propagation.

There are three basic types of counting methods, classified according to the characteristics they record. These are methods which count peaks, methods which count ranges and methods which count level crossings. Most of the methods require the record to be plotted relative to some zero or datum level, which is the dead-load stress in the case of highway bridges.

The more common methods are described in detail below.

B.1 Peak Count Method

The several variations of this method all identify the maximum and minimum values of the strain record as the characteristic points. Restrictions may be applied to reduce the number of points such as only counting maximum values above the mean level and minimum values below the mean level or limiting the count to just the maximum values. The effect of this method is to reduce a record to a succession of excursions from the datum level. For example, if the strain record shown in Fig. B1 is counted by recording all the maxima and minima, the resulting record would be that shown in Fig. B2.

A major objection to this method is that small variations of strain are amplified. This effect can be reduced by not counting small strain variations or by using the Mean-Crossing Peak Count Method.

B.2 Mean-Crossing Peak Count Method

This modification of the Peak Count Method, sometimes called the Zero-Crossing Peak Count Method only records the absolute maxima or minima between two successive mean-crossings. Thus, the strain record of Fig. B1 would be reduced to that shown in Fig. B3. However, although the small strain variations are removed, some excursions which are not necessarily small have also been neglected.

Both of the above methods suffer from a very serious drawback. They provide results which are inconsistent with laboratory data using sinusoidally applied loads. For example, n cycles of a sinusoidal strain range of magnitude R would be counted as 2n cycles of range R/2 which clearly incorrectly predicts failure when used in conjunction with the Miner cumulative damage rule.

B.3 Range Count Method

In contrast to the above methods, the Range Count Method counts the ranges between relative maxima and minima in terms of increasing or decreasing ranges. However, no information on peak loads is recorded. For the record shown in Fig. B1, the ranges a-b, b-c, c-d, d-e and e-f would be counted. If small strain reversals are

ignored, the number of ranges may be reduced, for example, to three with values equivalent to a-d, d-e and e-f respectively.

A special, and simplified, case of this method is the Peak to Peak Method which counts only the difference between the absolute maximum and minimum strain recorded during the passage of a single vehicle. Thus, the record of Fig. B1 would be reduced to a single cycle of magnitude d-e.

Neither the Range Count Method nor the Peak to Peak Method provides any information on the peak strains.

B.4 Range-Mean Count Method

This method was developed using fatigue arguments as a basis and differs from the Range Count Method only in that the mean of each range is also counted. Thus, it has an inherent practical drawback in that the distribution obtained is two-dimensional and requires a relatively large number of counters to record the information.

In practice, it is usually necessary to ignore small variations in strain when using the Range Count Method or the Range-Mean Count Method. However, this has a peculiar implication which can be seen with reference to the record shown in Fig. B4. If the record is analyzed without disregarding the small variations, the strain ranges counted will be +3, -1 and +4 respectively. However, if small ranges are disregarded the count becomes simple +6. That is, disregarding small variations leads to a smaller total number of cycles with higher range magnitudes.

B.5 Range-Pair Count Method

Unlike the Range and Range-Mean Count Methods, the results of this method are relatively insensitive to the minimum range magnitude selected. The range is defined to be a strain variation starting from a maximum or minimum strain. Each range pair to be counted in a particular category consists of an increasing strain exceeding the prescribed minimum for that category and the next decreasing strain exceeding the same increment. Small variations are treated as interruptions of larger ranges, and hence their elimination does not significantly affect the count. For example, in Fig. B1 the portion of the record labelled b-c-b' would be considered as a range which is an interruption of the larger range pair of which a-d forms the first half.

As a result of the elimination of the inconsistencies in the simpler methods, the Range-Pair Count Method has had wide acceptance, but this is also partly due to the existence of a relatively simple device known as a "strain range counter" which counts directly by this method.

B.6 Level-Crossing Count Method

This method also developed as a result of readily available automatic counters. The method simple involves the establishment of several strain levels, and counters record the number of times a time-variant strain crosses the level in an increasing direction. The mean levels and the number of peaks cannot be deduced from this method.

B.7 Rainflow Count Method

The outstanding feature of the Rainflow Method is that it is carried out on the basis of the stress-strain behavior of the material being considered. The cycles which are extracted are consistent with those in constant amplitude tests on which the life predictions are invariably based.

Crack growth propagation only occurs if plasticity is present at the crack tip. The strain-time history curve for a detail may be elastic but stress concentration at the detail and the crack tip may introduce stress levels equal to or exceeding the yield stress of the material. The relationship between a nominal strain-time curve and a stress-strain relationship at the crack tip where plasticity has developed is demonstrated by a comparison of Figs. B1 and B5.

It can now be readily seen that the strain time curve can be divided into three half-cycles, a-d, d-e and e-f, and one full cycle, b-c-b'.

The same result can be obtained using the analogy of rain running down a series of pagoda roofs. The stain-time record is drawn with the time axis drawn vertically downwards as shown in Fig. B6. The general rules for counting are then:

1. Rainflow begins at the beginning of the test and successively at the inside of every peak.

2. Flow initiating at a maximum drips down until it comes opposite a maximum more positive than the one from which it started. Similarly, flow initiating at a minimum drips down until it comes opposite a minimum more negative than the minimum from which it started.

3. Rain also stops when it meets rain from the roof above.

4. The beginning of the sequence is a minimum if the initial straining is in tension.

5. The horizontal length of each rainflow is counted as a half cycle at that stain range.

In Fig. B6, rain initiates at a, flows to b, drips to b', flows to d and finally stops opposite e, because e is more negative than a. Rain initiating at c stops at b' where it meets rain dripping from b. Rain initiating at d flows to e and stops at the end of the record, and flow initiating at e flows to f and stops at the end of the recrod.

Hence, these rules can be seen to give identical results to those obtained from a consideration of the stress-strain hysteresis loop.

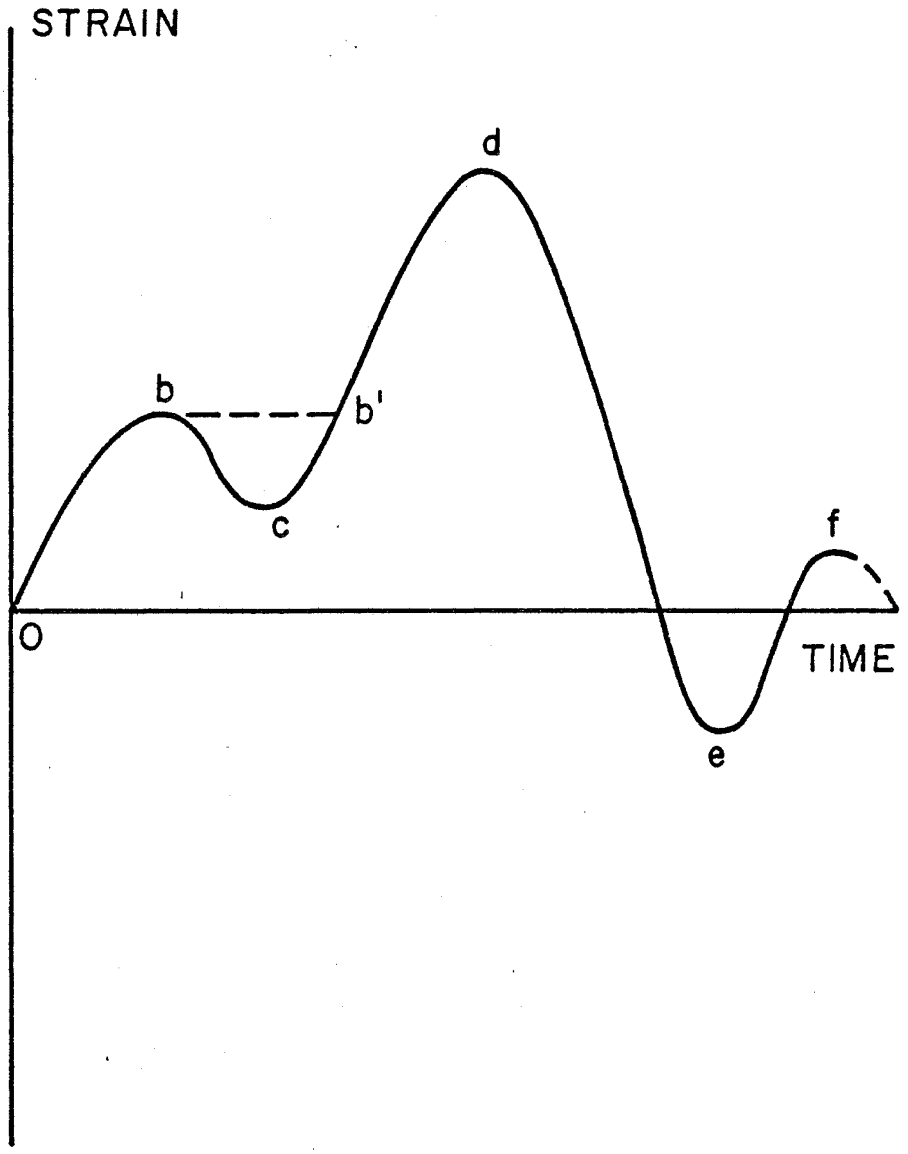

Fig. B1 Sample Strain-Time Record

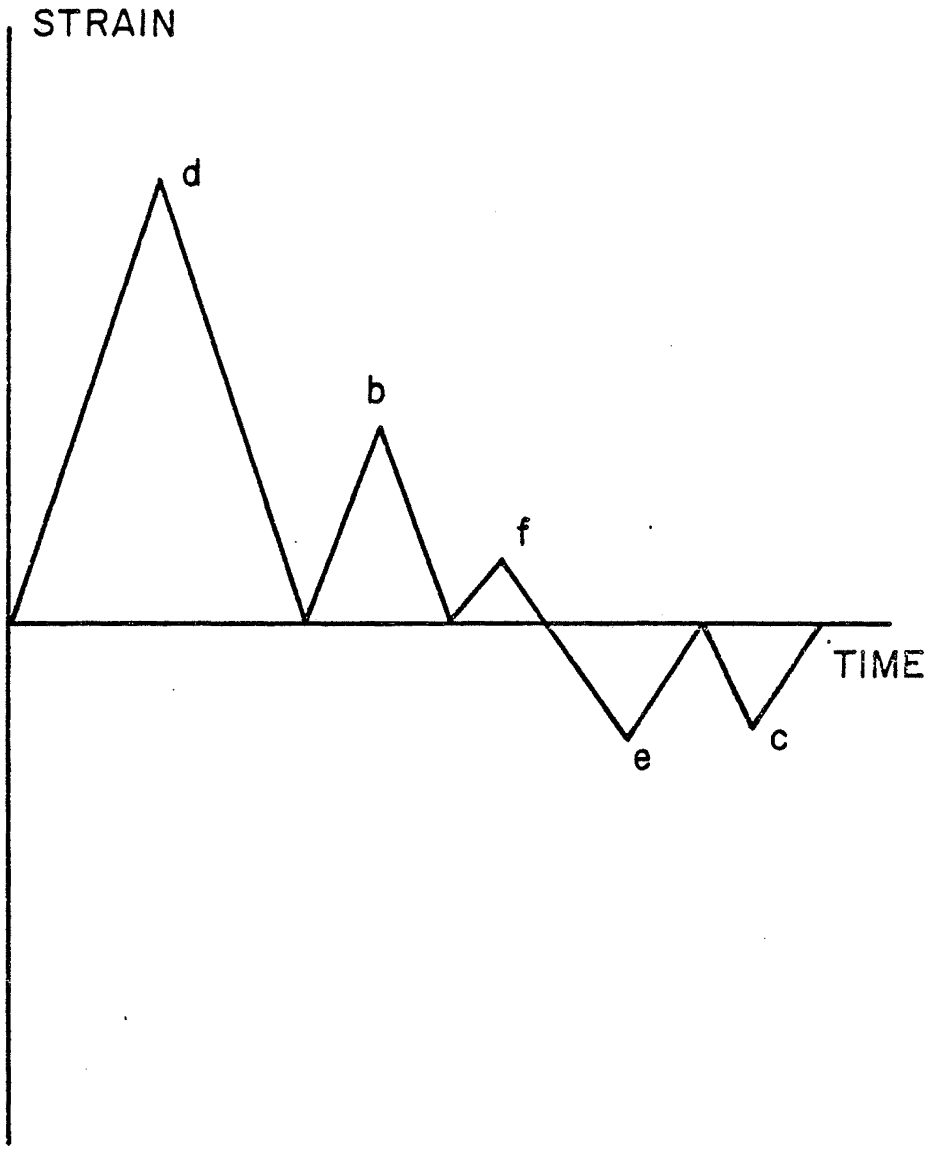

Fig. B2 Effect of Peak Count Method

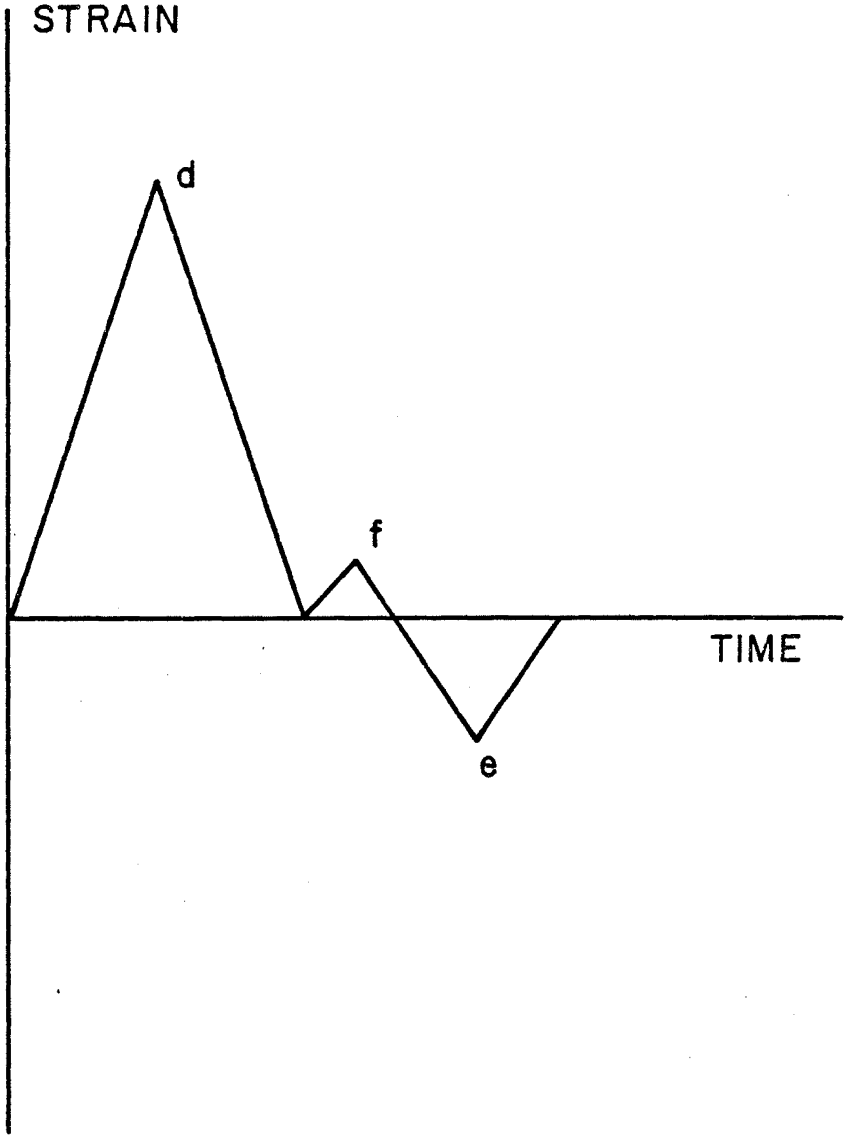

Fig. B3 Effect of Mean-Crossing Peak Count Method

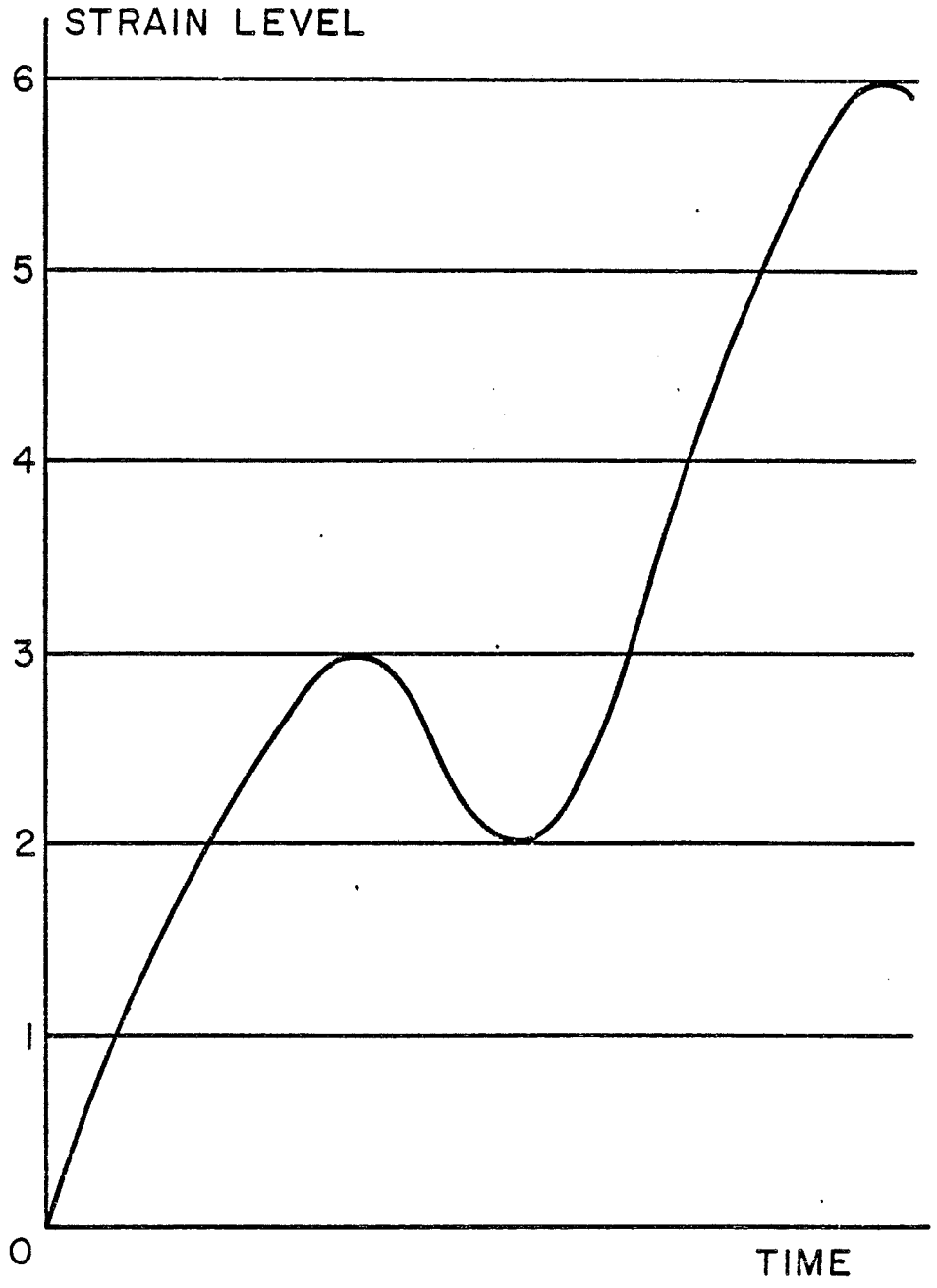

Fig. B4 Effect of Ignoring Small Variations in the Range and Range-Mean Count Methods

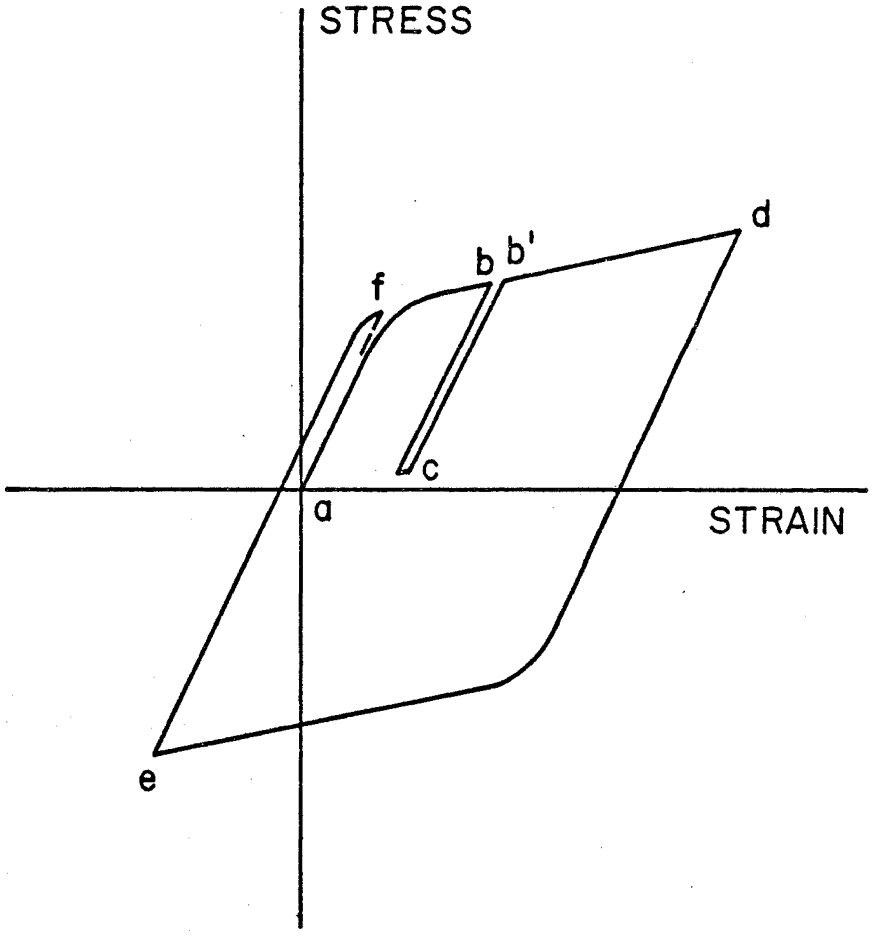

Fig. B5 Stress-Strain Hysteresis Loop for Crack Tip

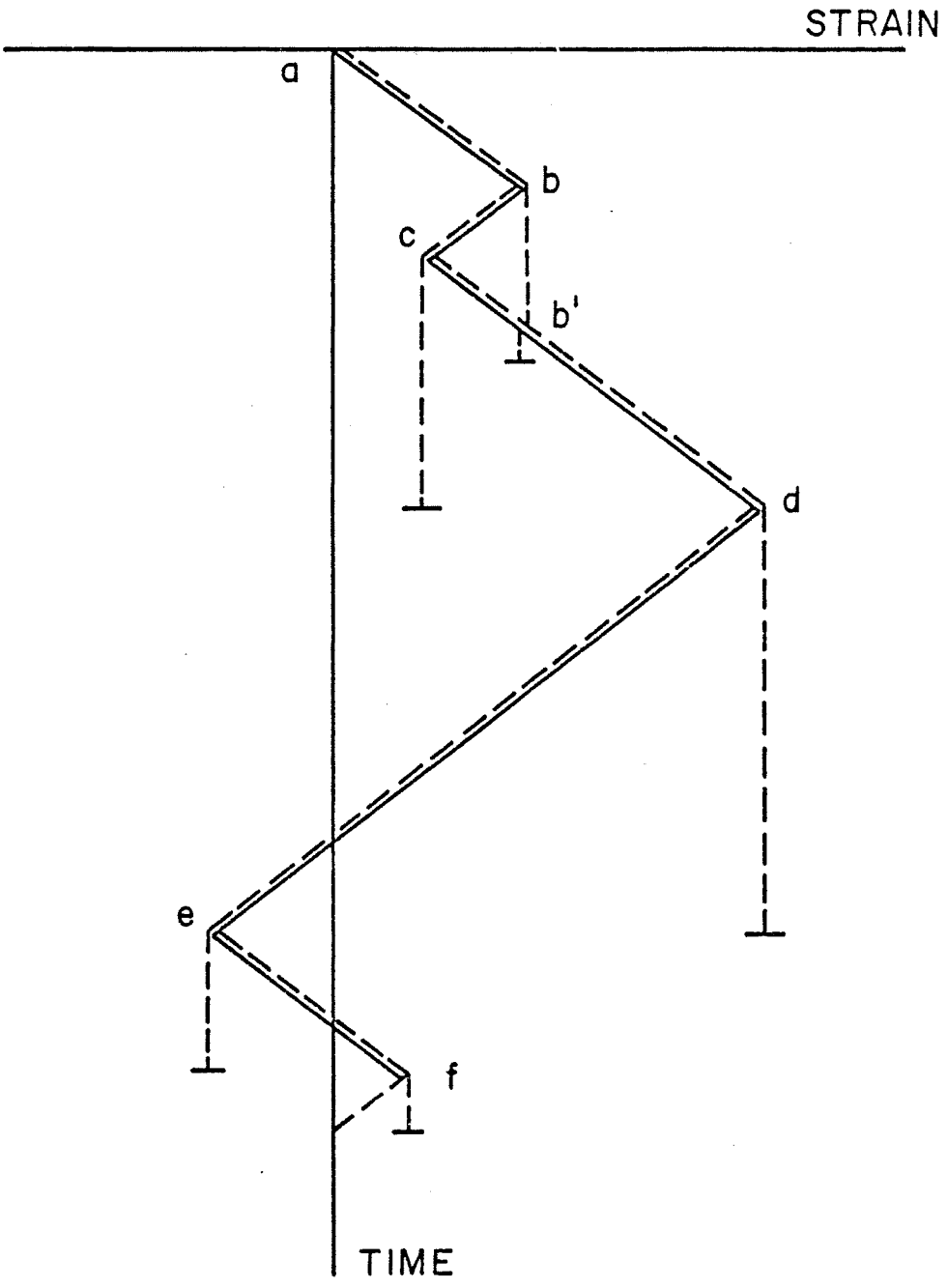

Fig. B6 Rainflow Count Method

APPENDIX C: STRESS RANGE SPECTRA FOR SELECTED DETAILS BY EACH CYCLE COUNTING TECHNIQUE

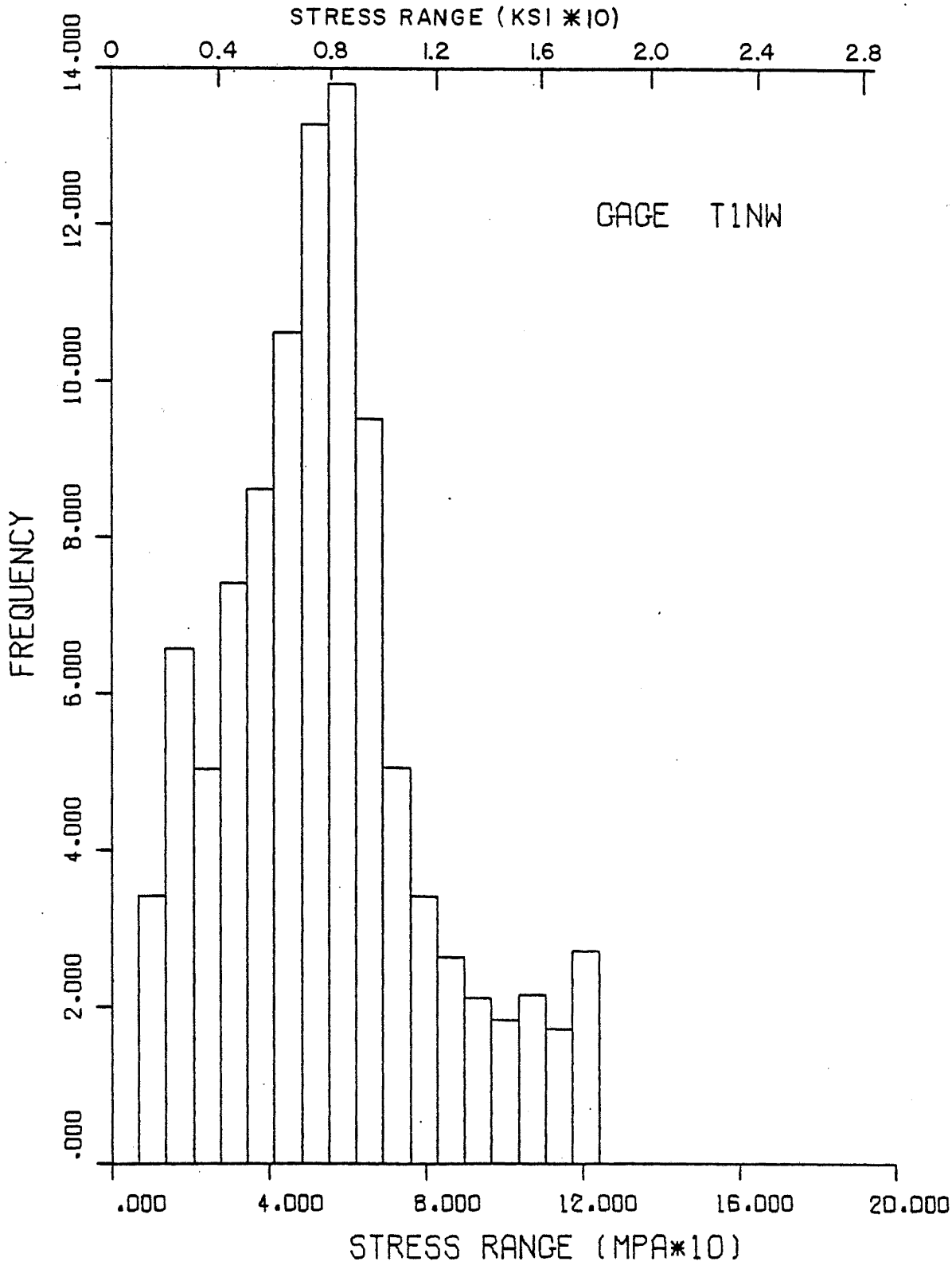

Fig. C1 Stress Range Spectrum for Gage T1NW Using Peak to Peak Counting with Multiple Presence Separation

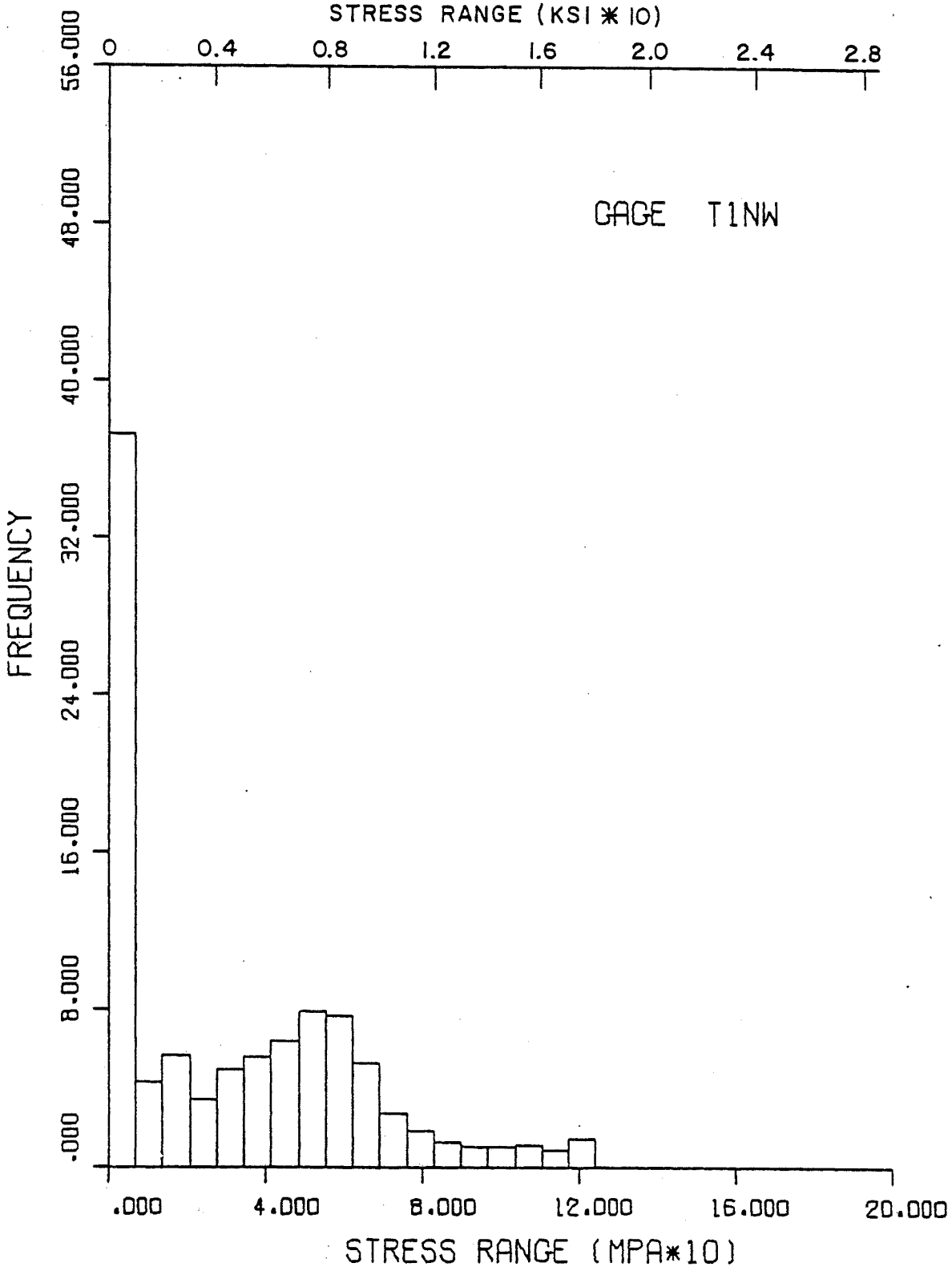

Fig. C2 Stress Range Spectrum for Gage T1NW Using Peak to Peak Counting with Multiple Presence Separation

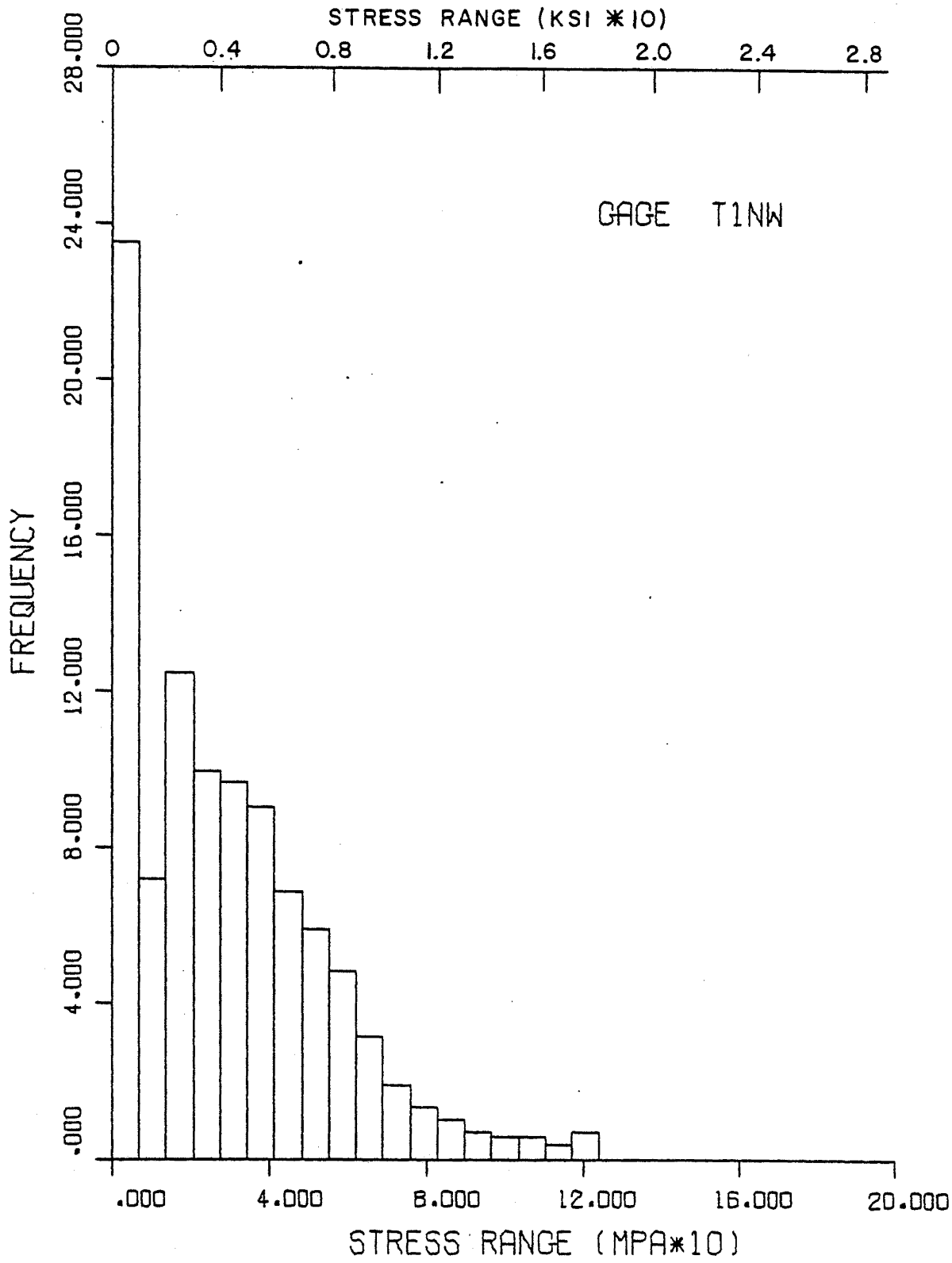

Fig. C3 Stress Range Spectrum for Gage T1NW Using Rainflow Counting

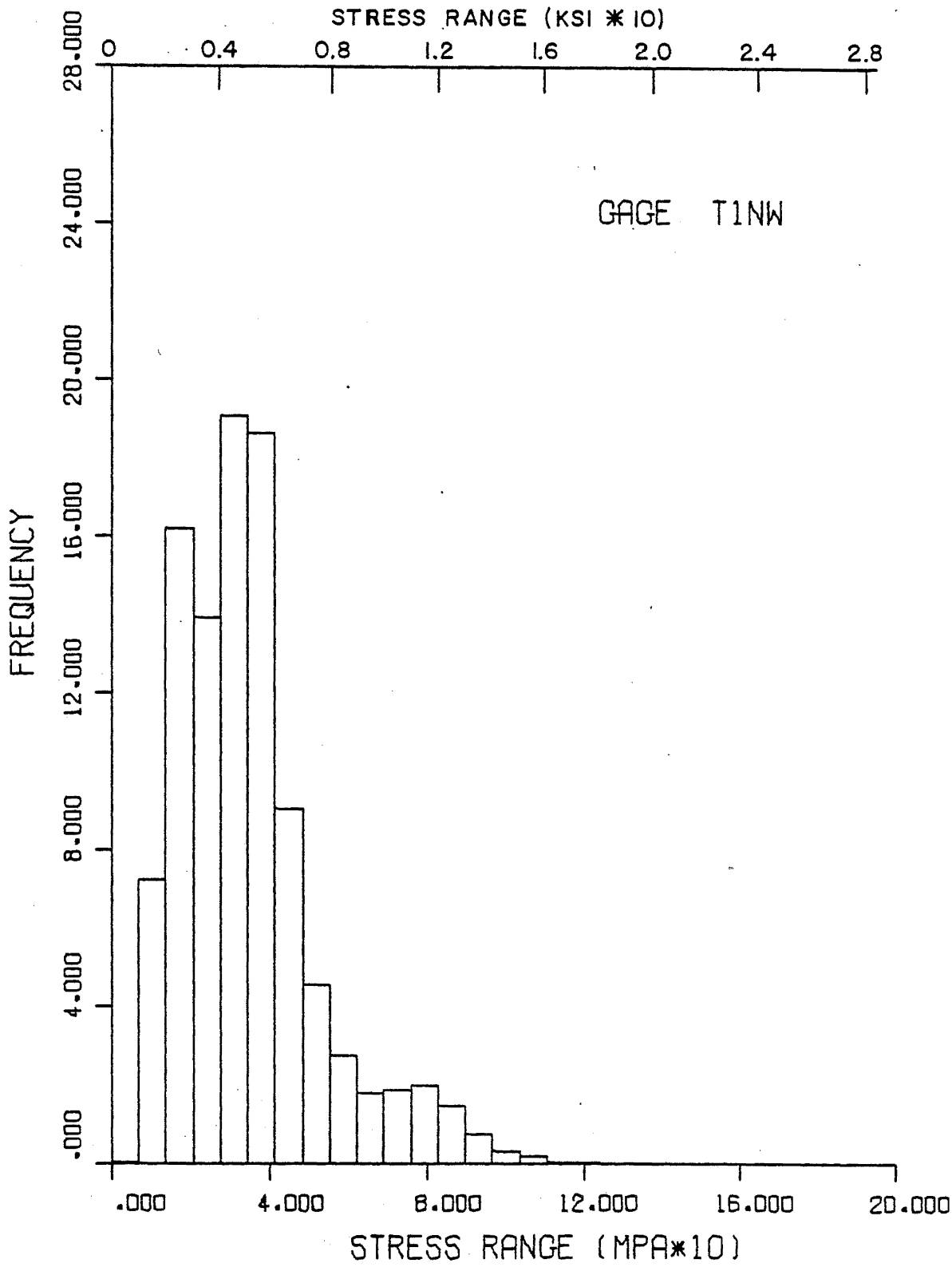

Fig. C4 Stress Range Spectrum For Gage T1NW
Using Modified Rainflow Counting

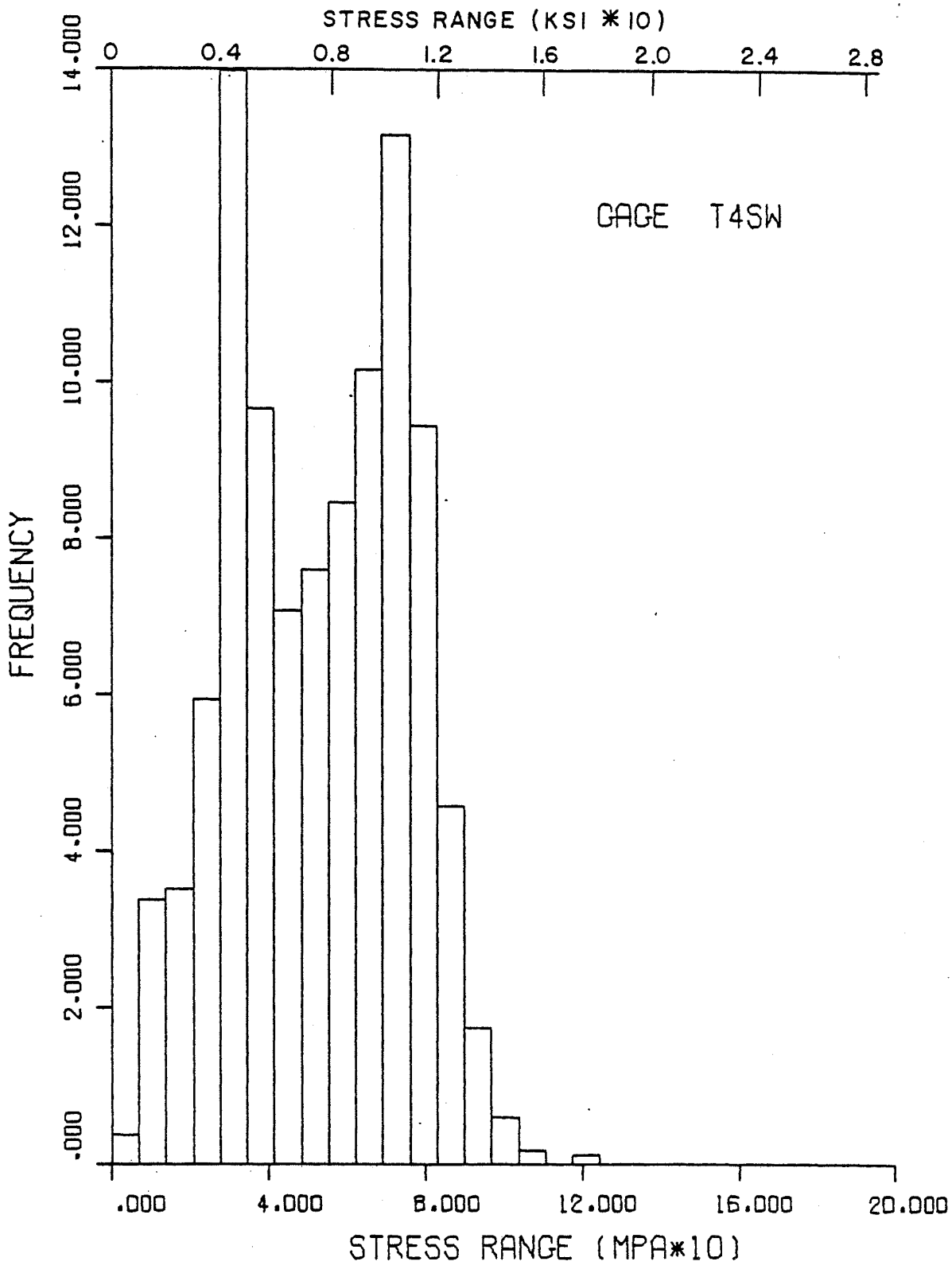

Fig. C5 Stress Range Spectrum for Gage T4SW Using Peak to Peak Counting Without Multiple Presence Separation

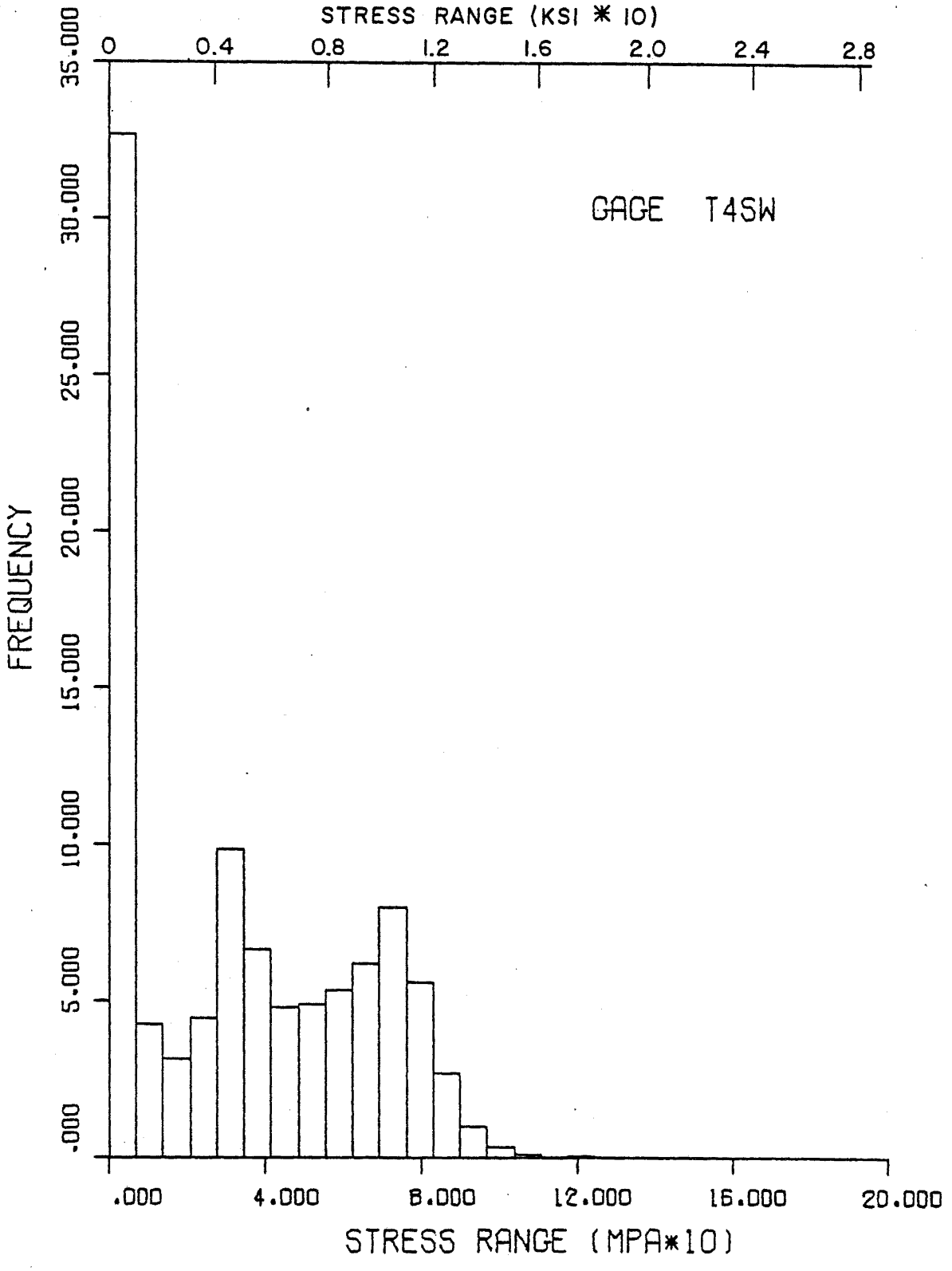

Fig. C6 Stress Range Spectrum for Gage T4SW Using Peak to Peak Counting with Multiple Presence Separation

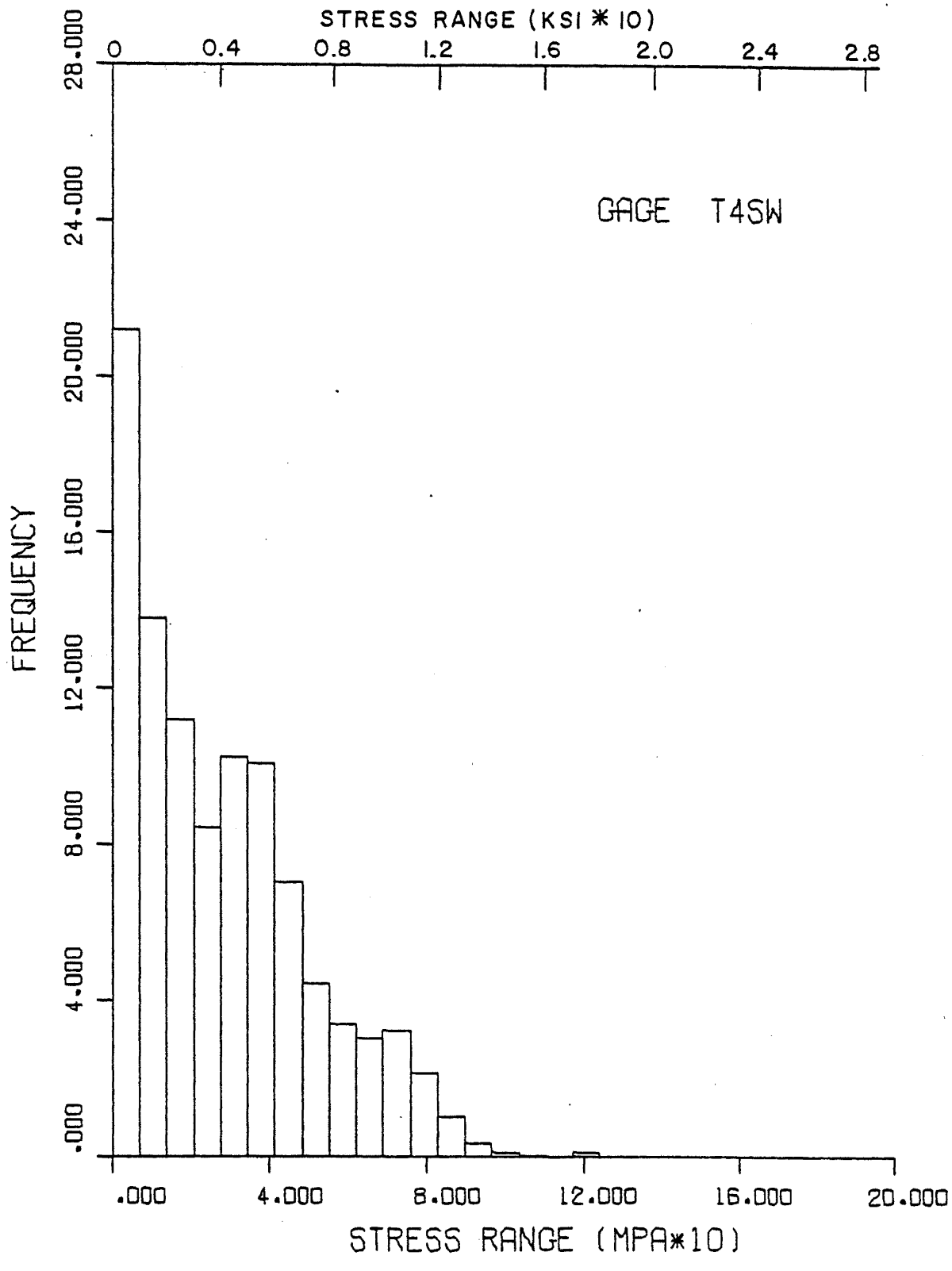

Fig. C7 Stress Range Spectrum for Gage T4SW
Using Rainflow Counting

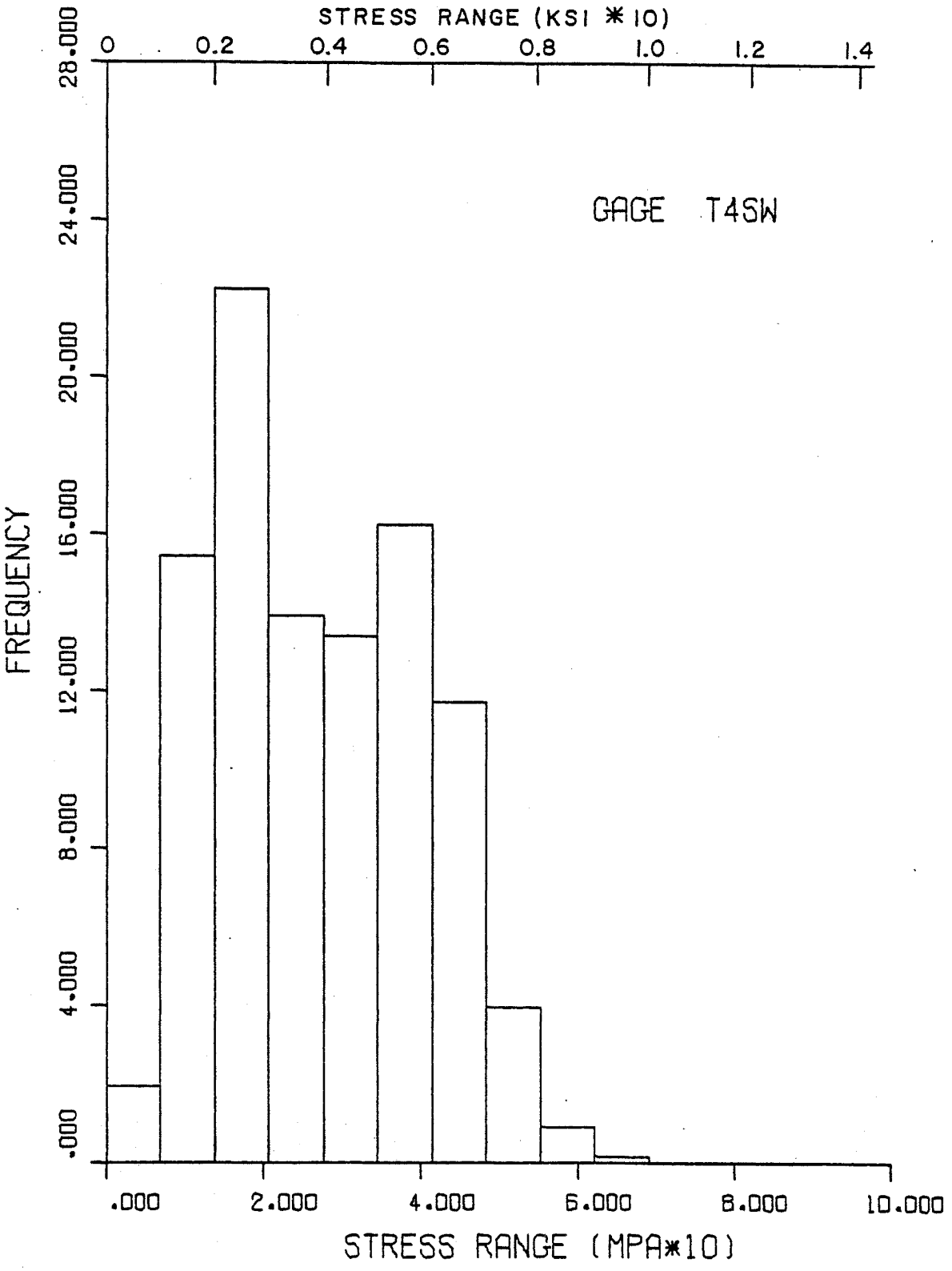

Fig. C8 Stress Range Spectrum for Gage T4SW
Using Modified Rainflow Counting

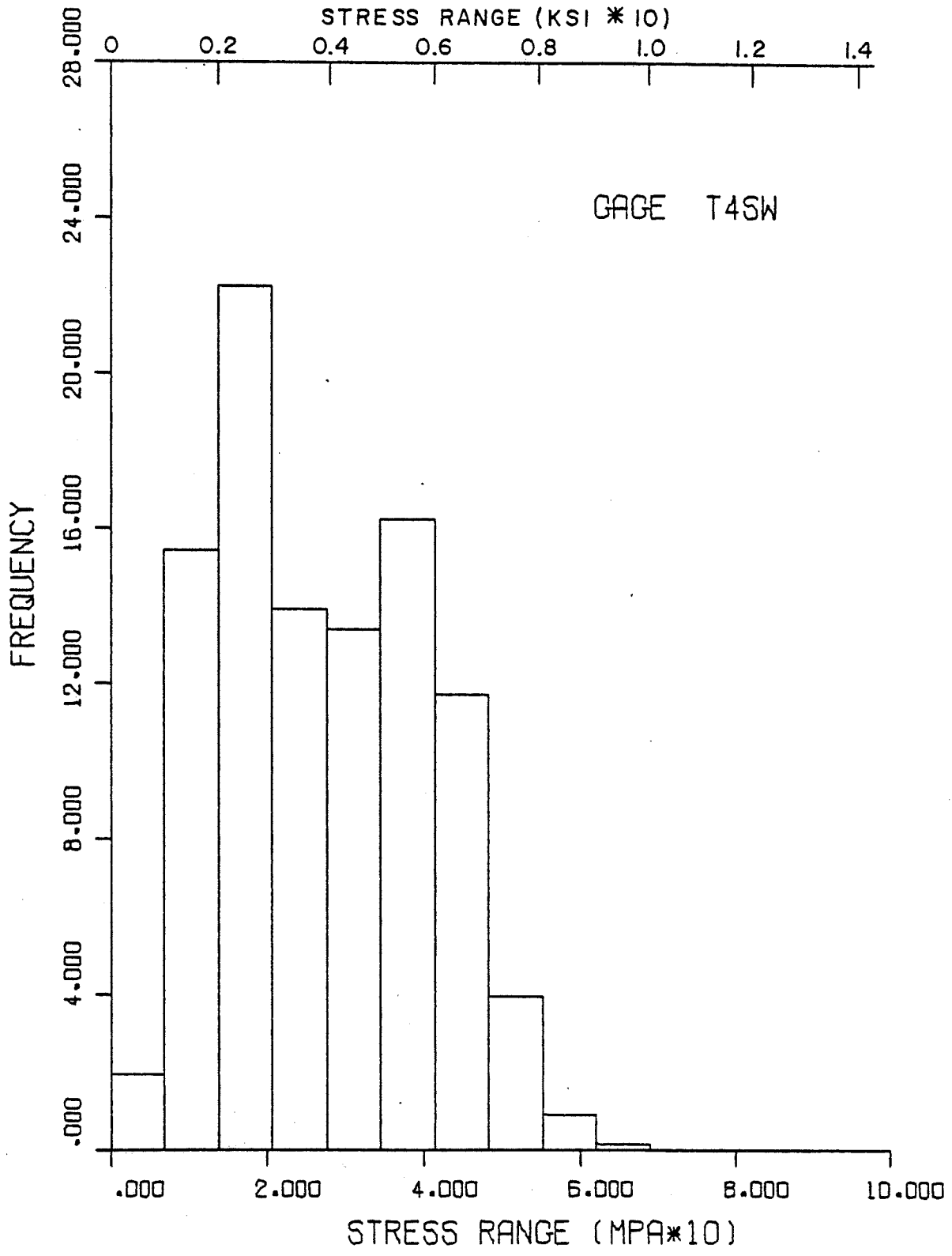

Fig. C9 Stress Range Spectrum for Gage T5SE Using Peak to Peak Counting Without Multiple Presence Separation

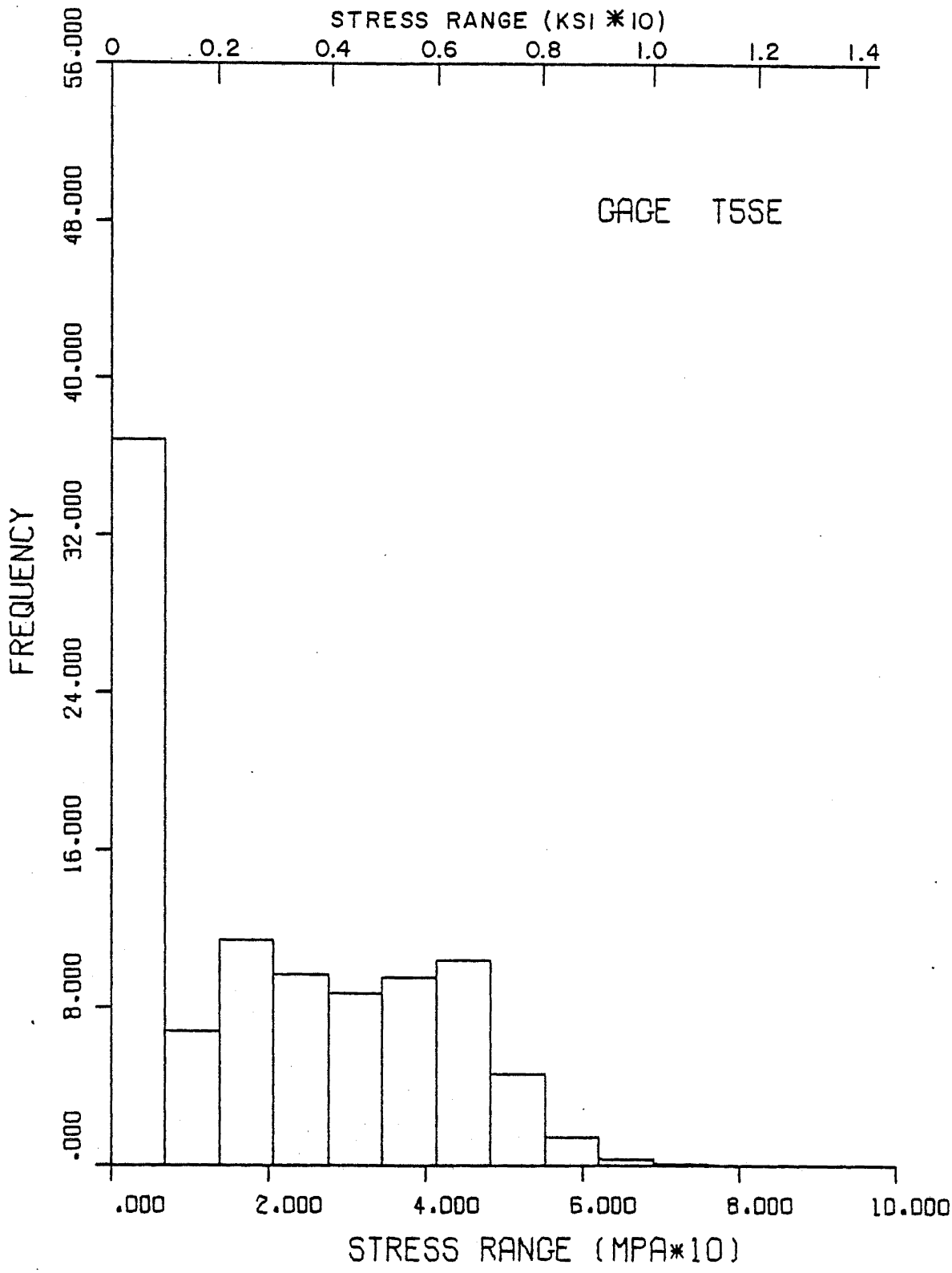

Fig. C10 Stress Range Spectrum for Gage T5SE Using Peak to Peak Counting with Multiple Presence Separation

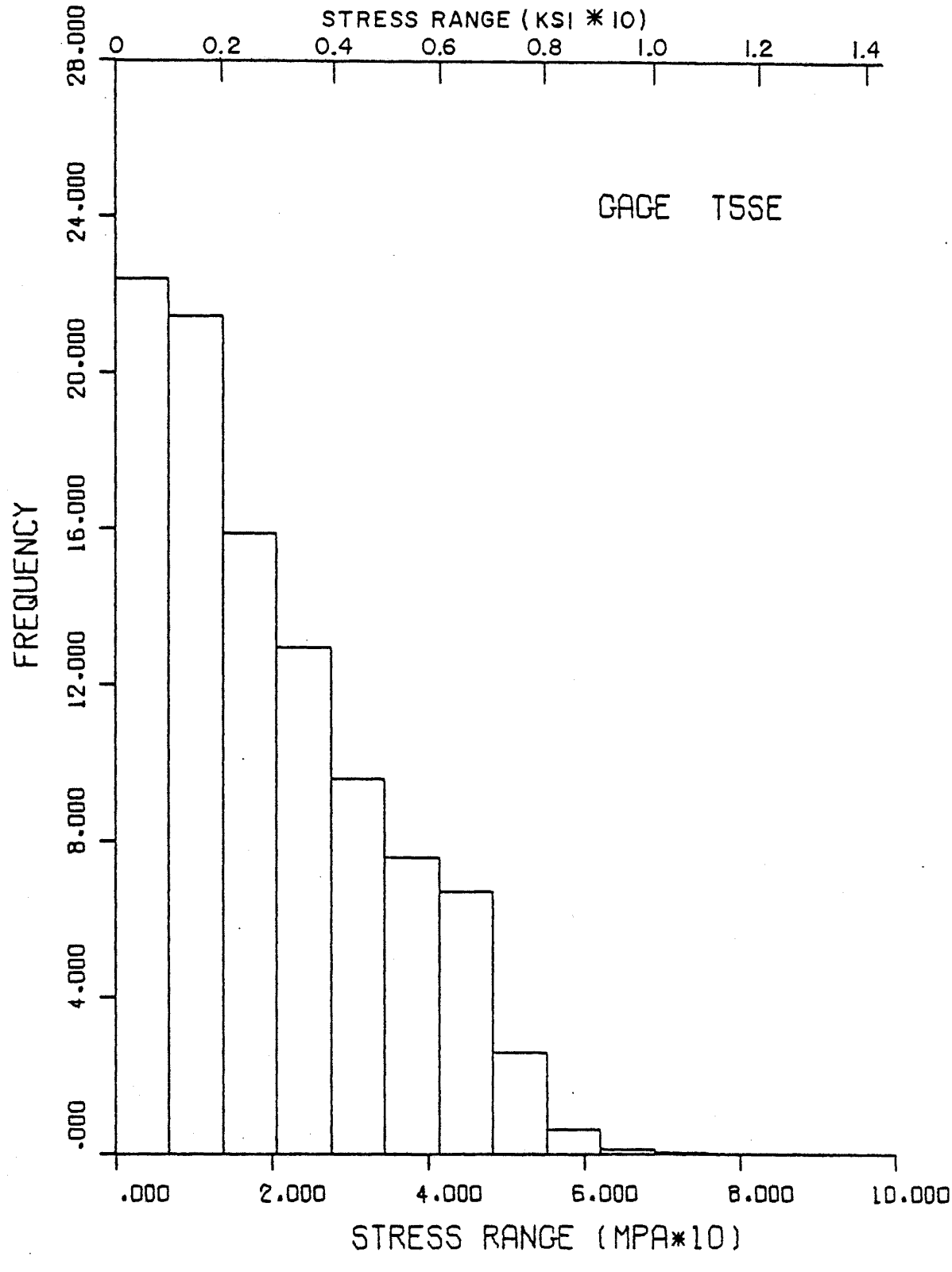

Fig. C11 Stress Range Spectrum for Gage T5SE
Using Rainflow Counting

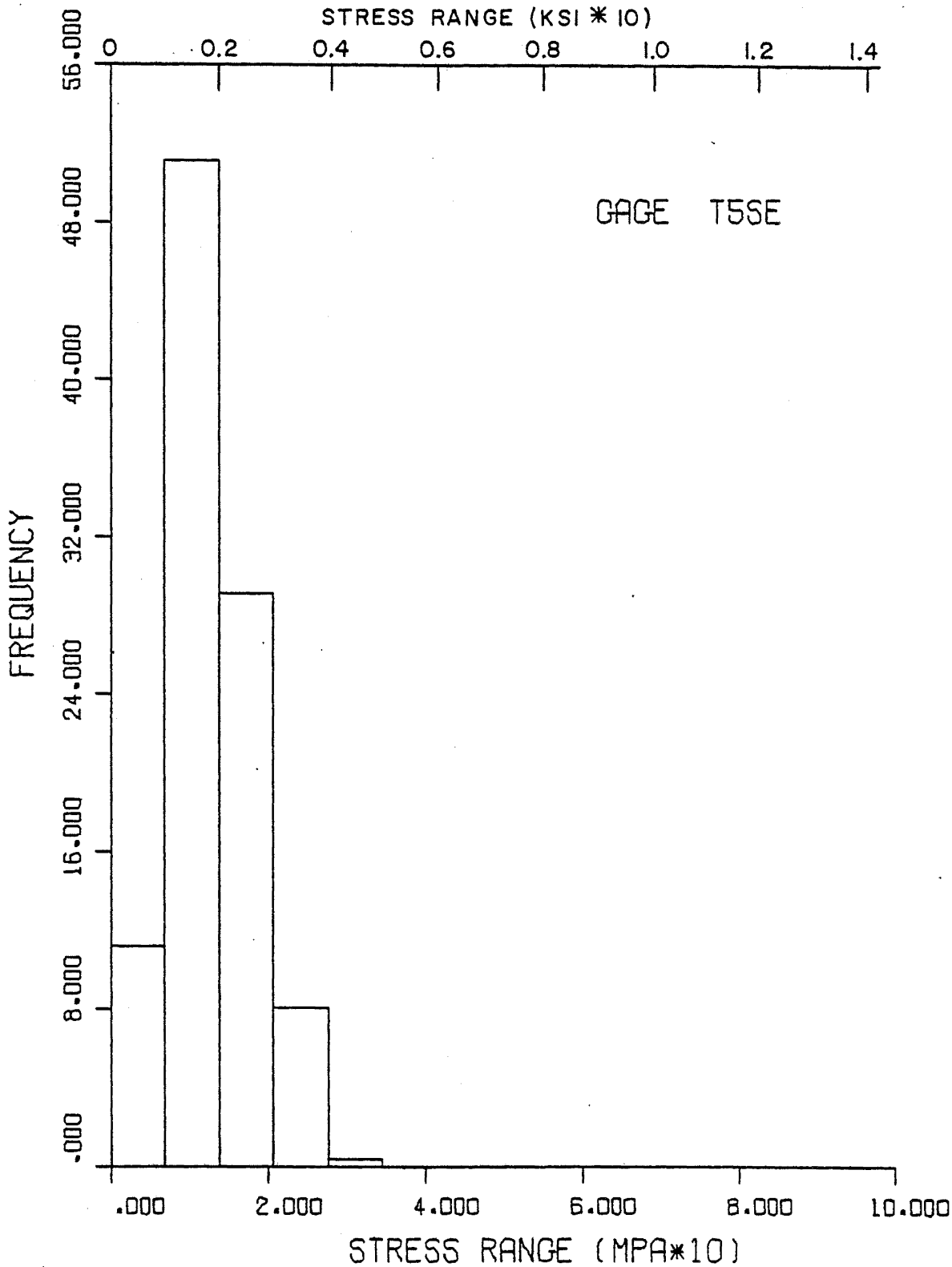

Fig. C12 Stress Range Spectrum for Gage T5SE
Using Modified Rainflow Counting

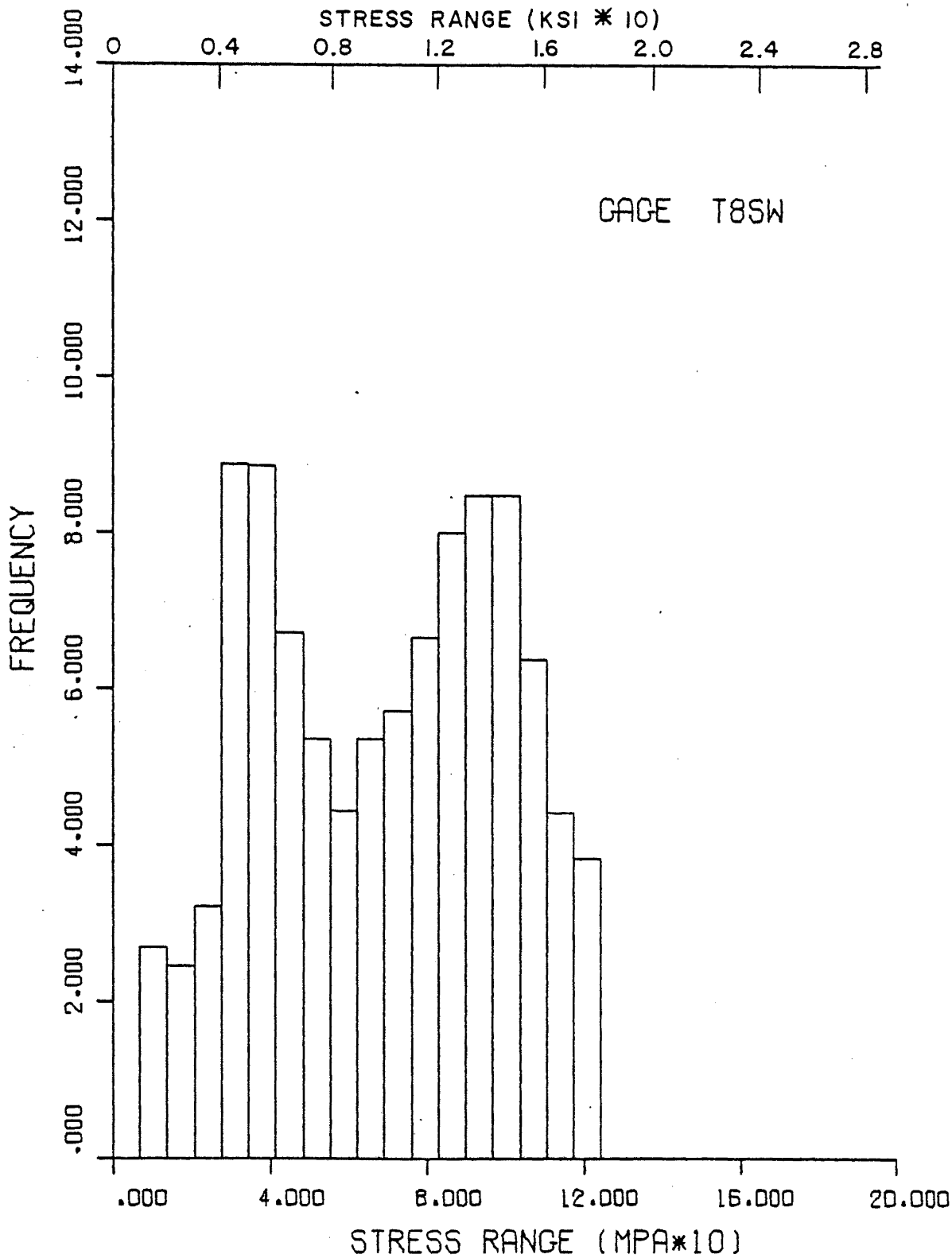

Fig. C13 Stress Range Spectrum for Gage T8SW Using Peak to Peak Counting Without Multiple Presence Separation

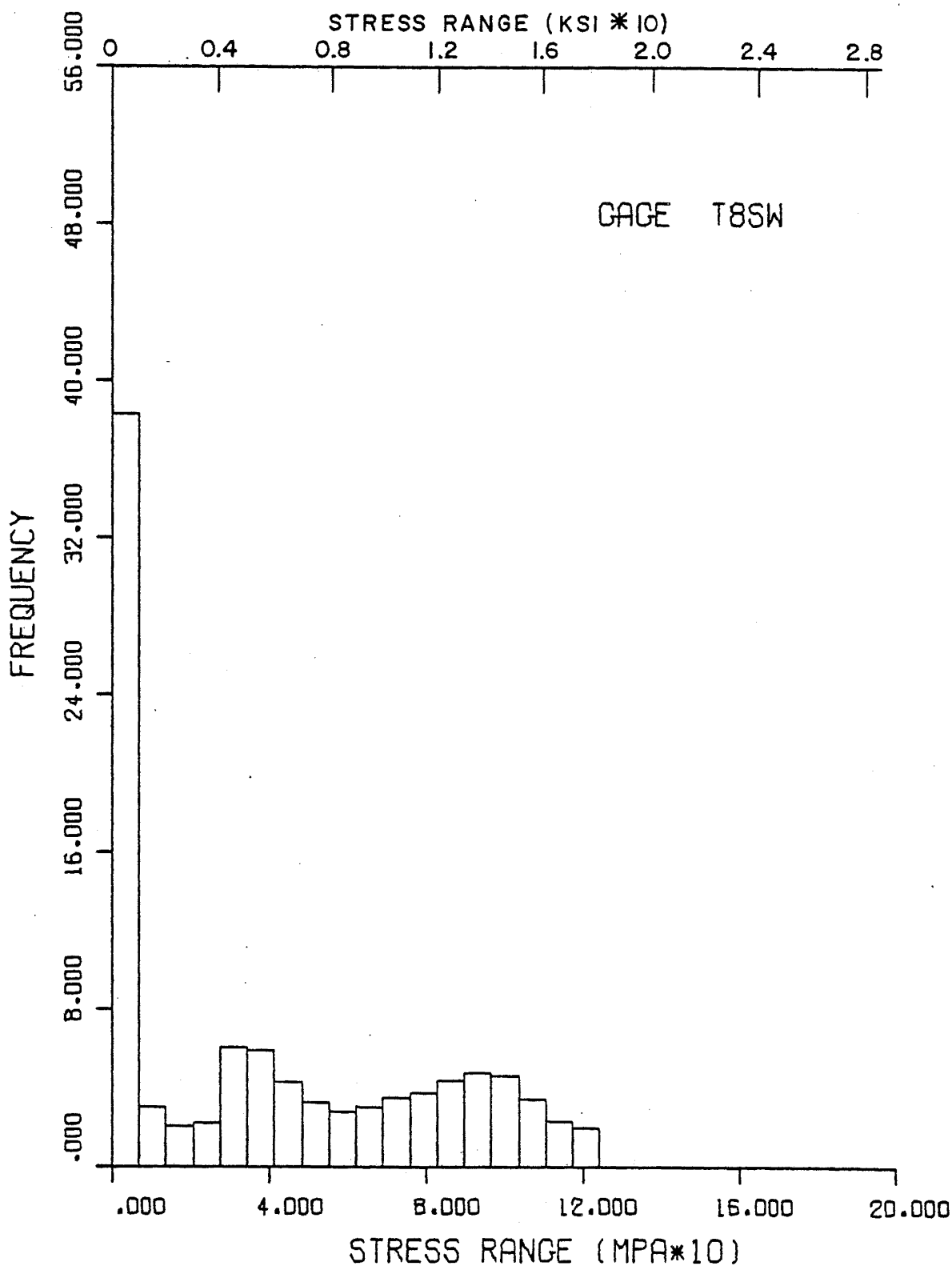

Fig. C14 Stress Range Spectrum for Gage T8SW Using Peak to Peak Counting with Multiple Presence Separation

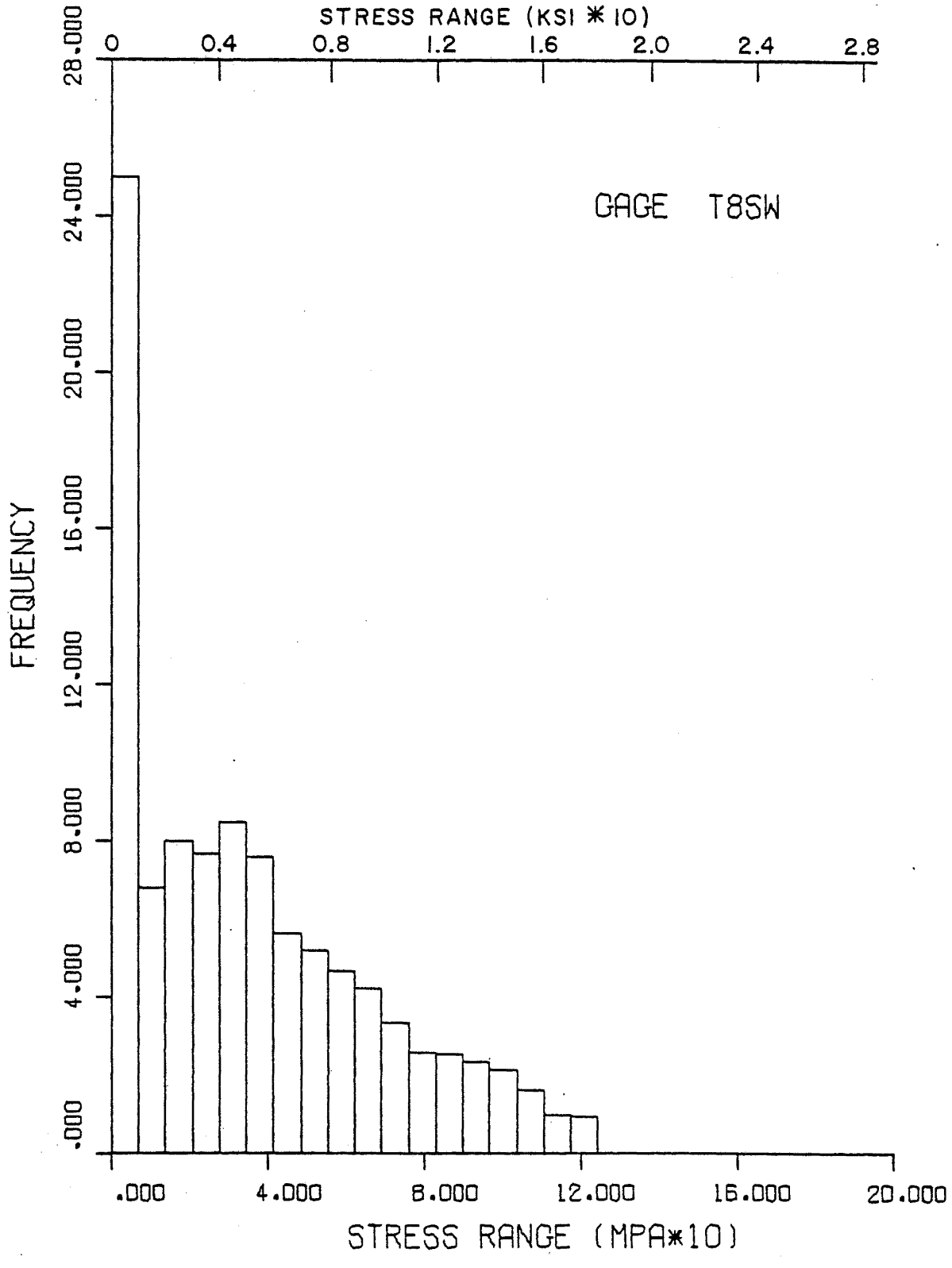

Fig. C15 Stress Range Spectrum for Gage T8SW
Using Rainflow Counting

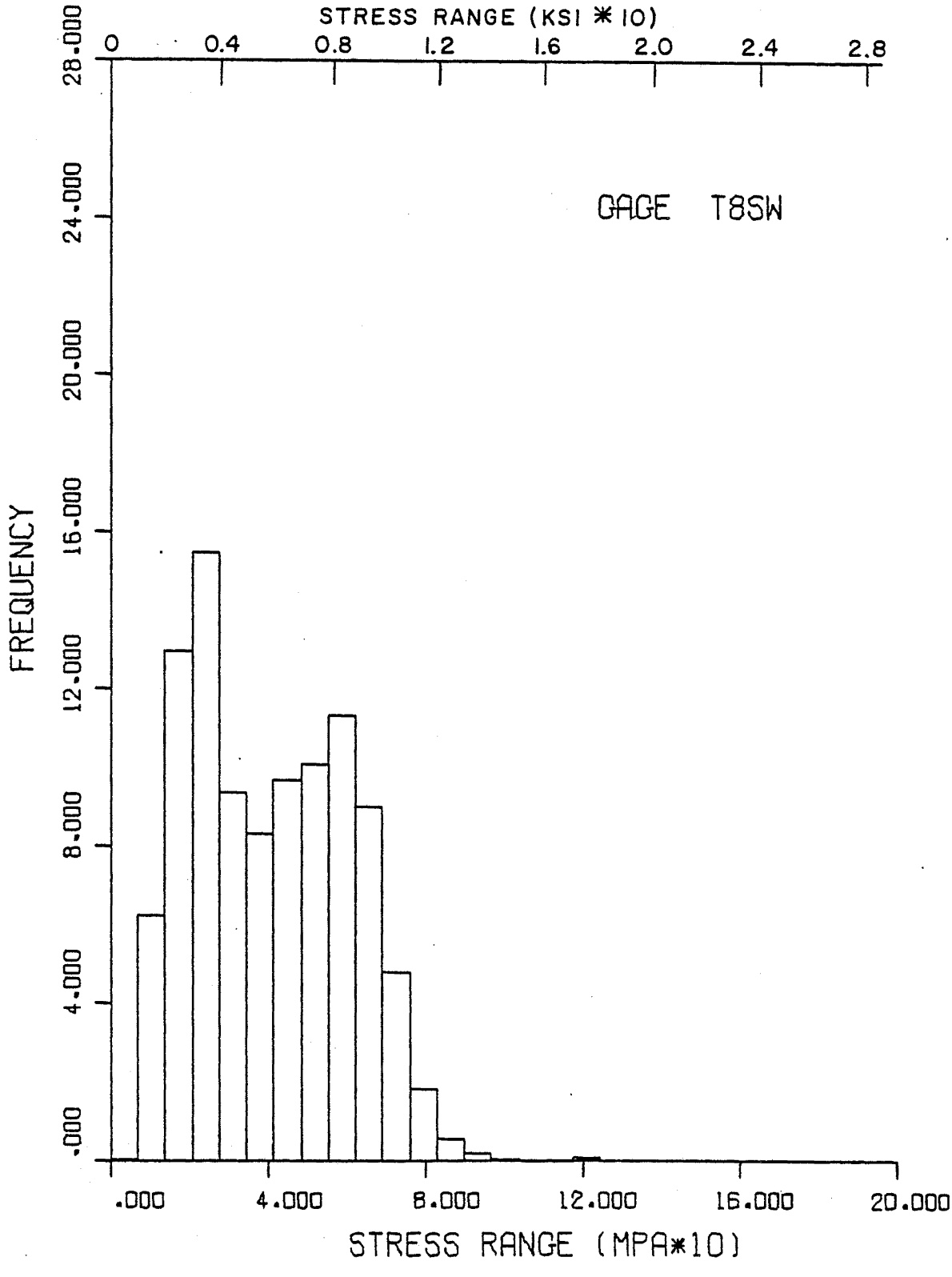

Fig. C16 Stress Range Spectrum for Gage T8SW
Using Modified Rainflow Counting

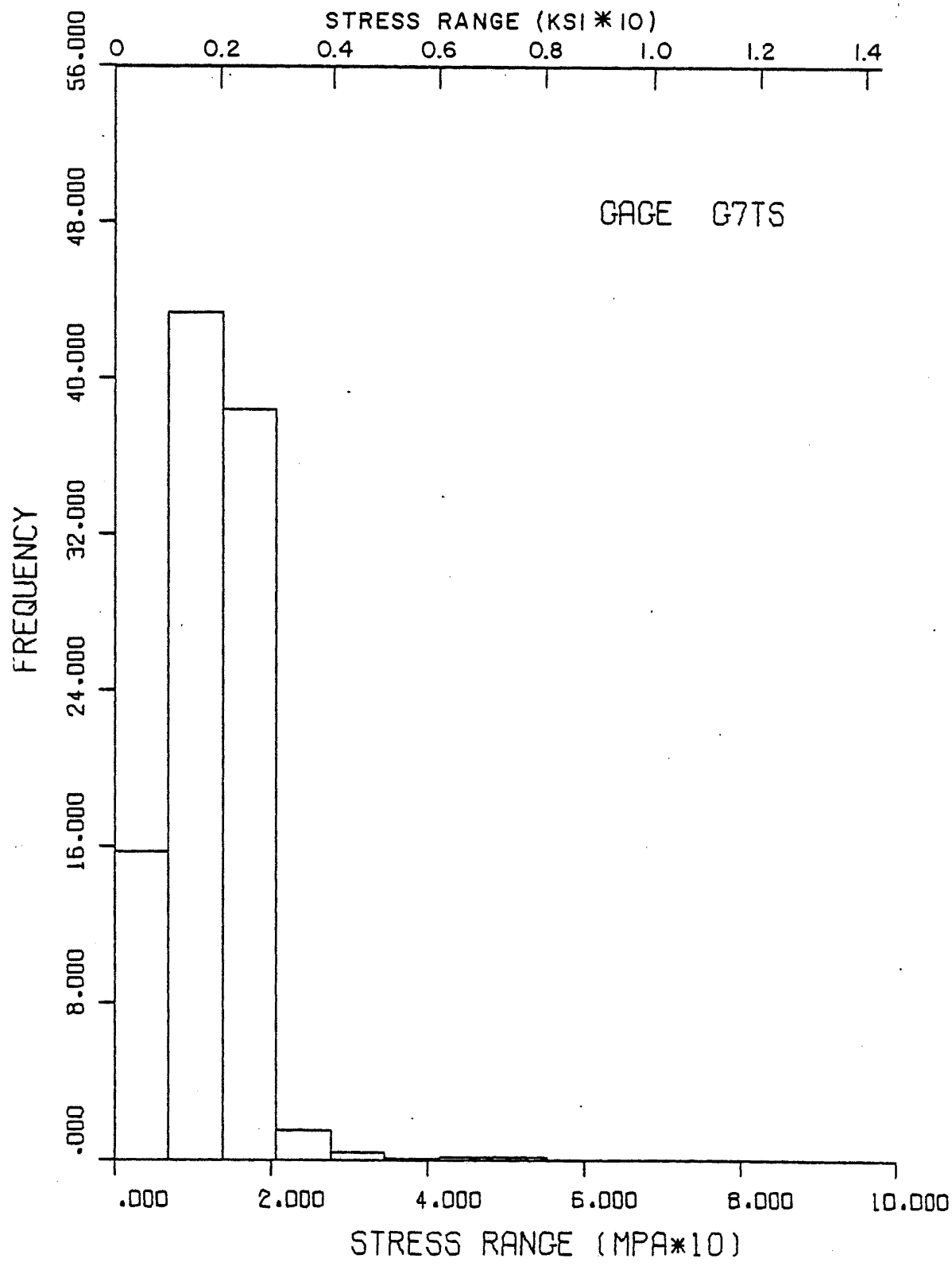

Fig. C17 Stress Range Spectrum for Gage G7TS Using Peak to Peak Counting Without Multiple Presence Separation

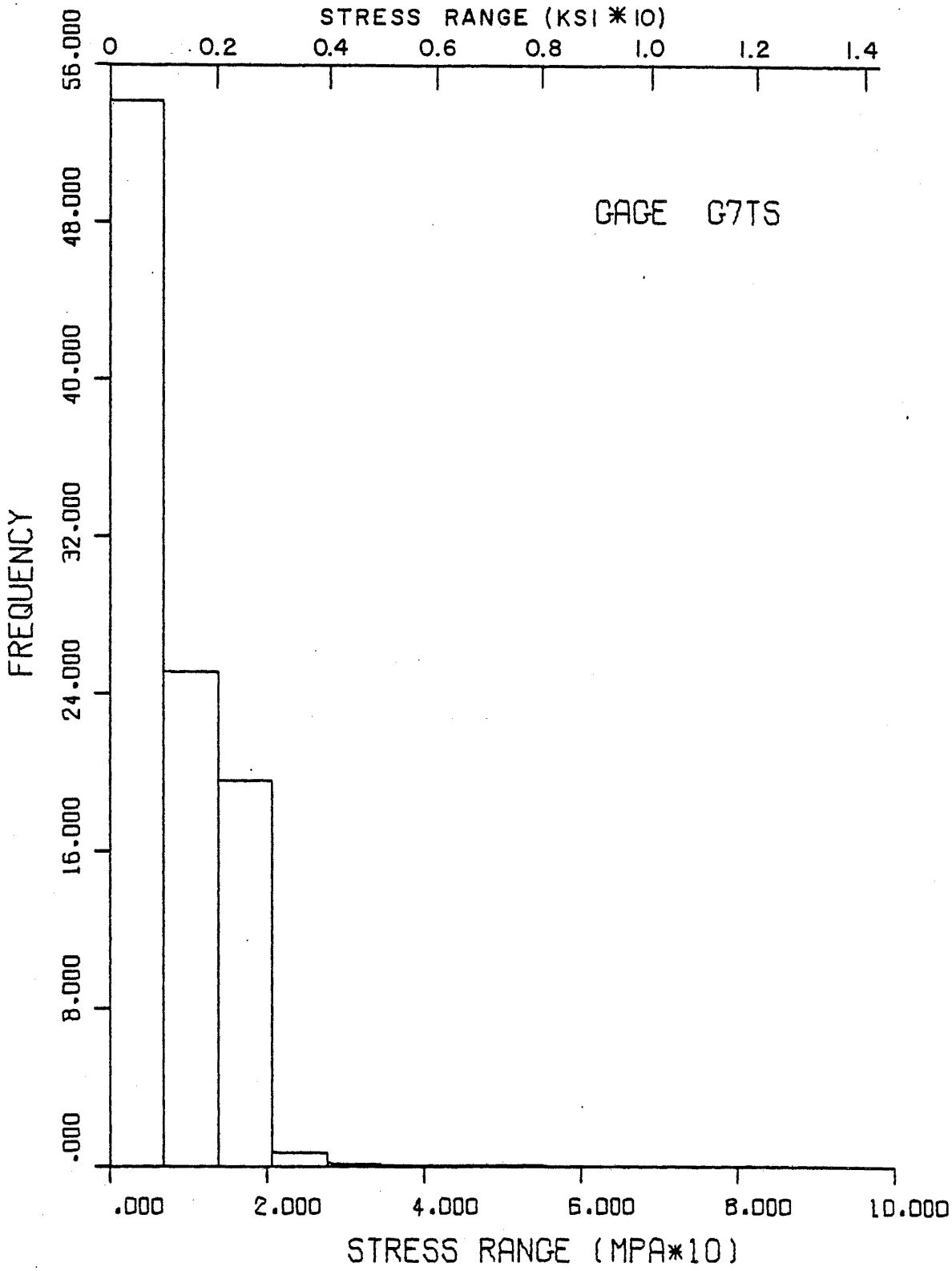

Fig. C18 Stress Range Spectrum for Gage G7TS Using Peak to Peak Counting with Multiple Presence Separation

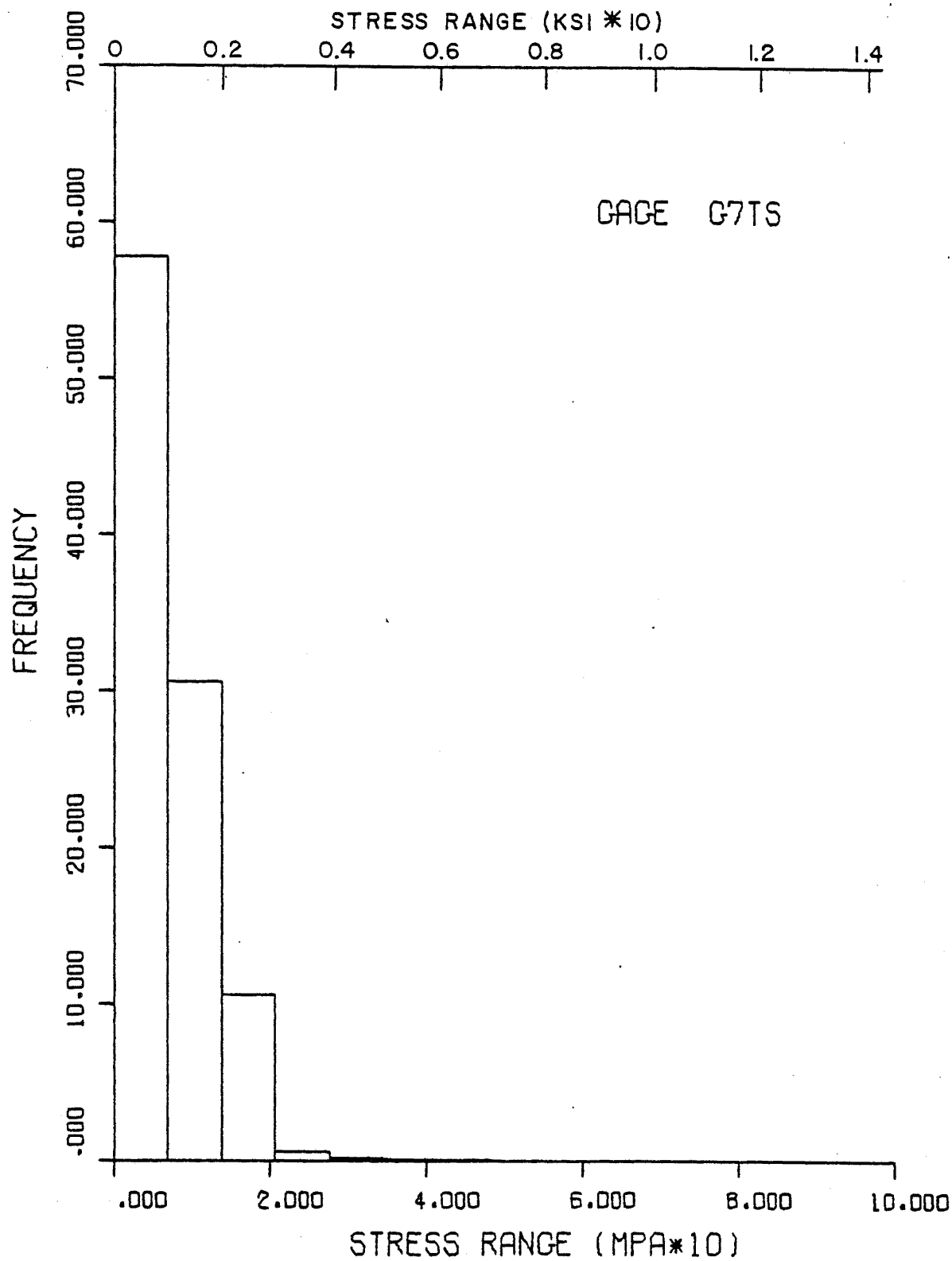

Fig. C19 Stress Range Spectrum for Gage G7TS
Using Rainflow Counting

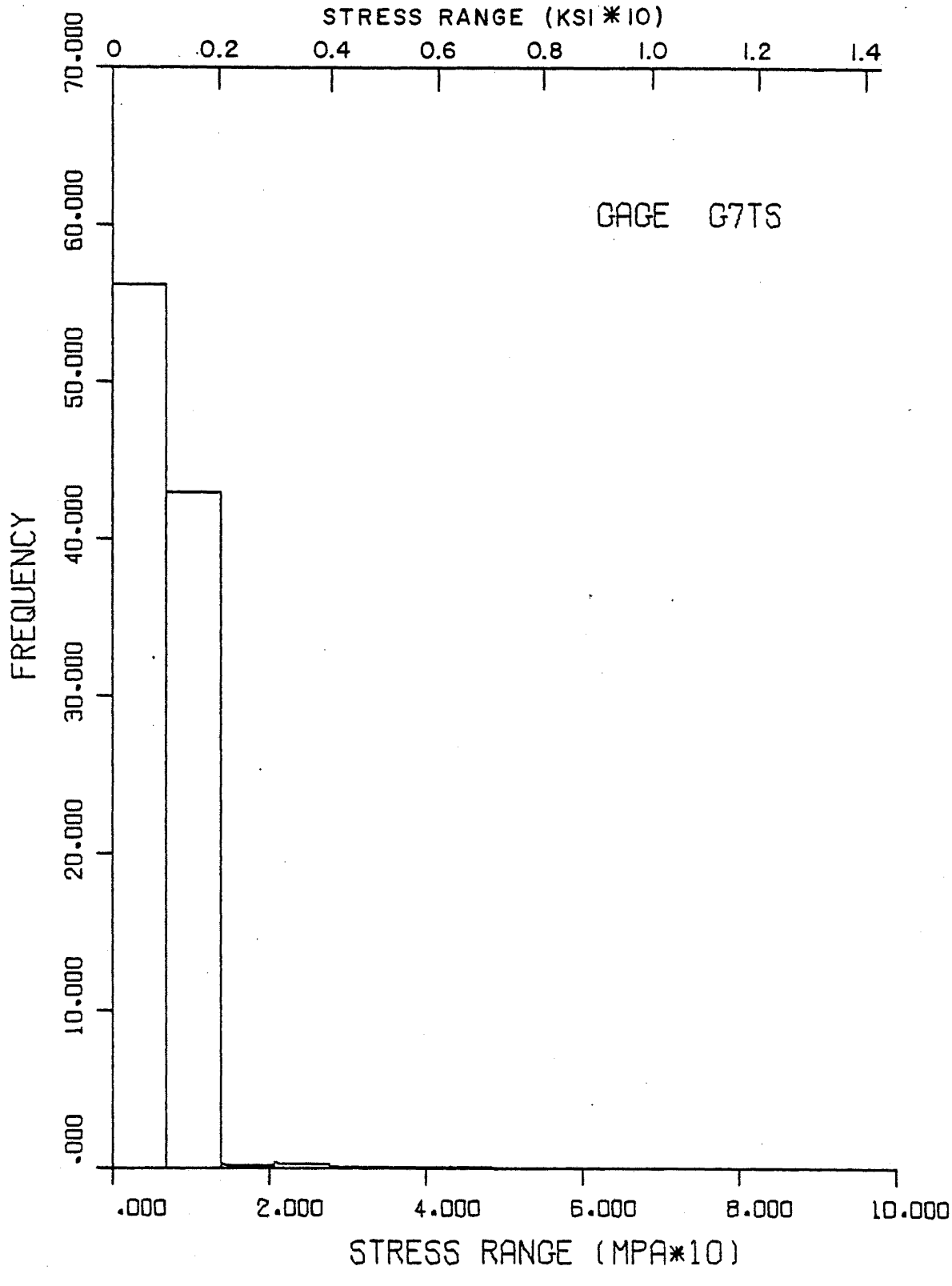

Fig. C20 Stress Range Spectrum for Gage G7TS
Using Modified Rainflow Counting

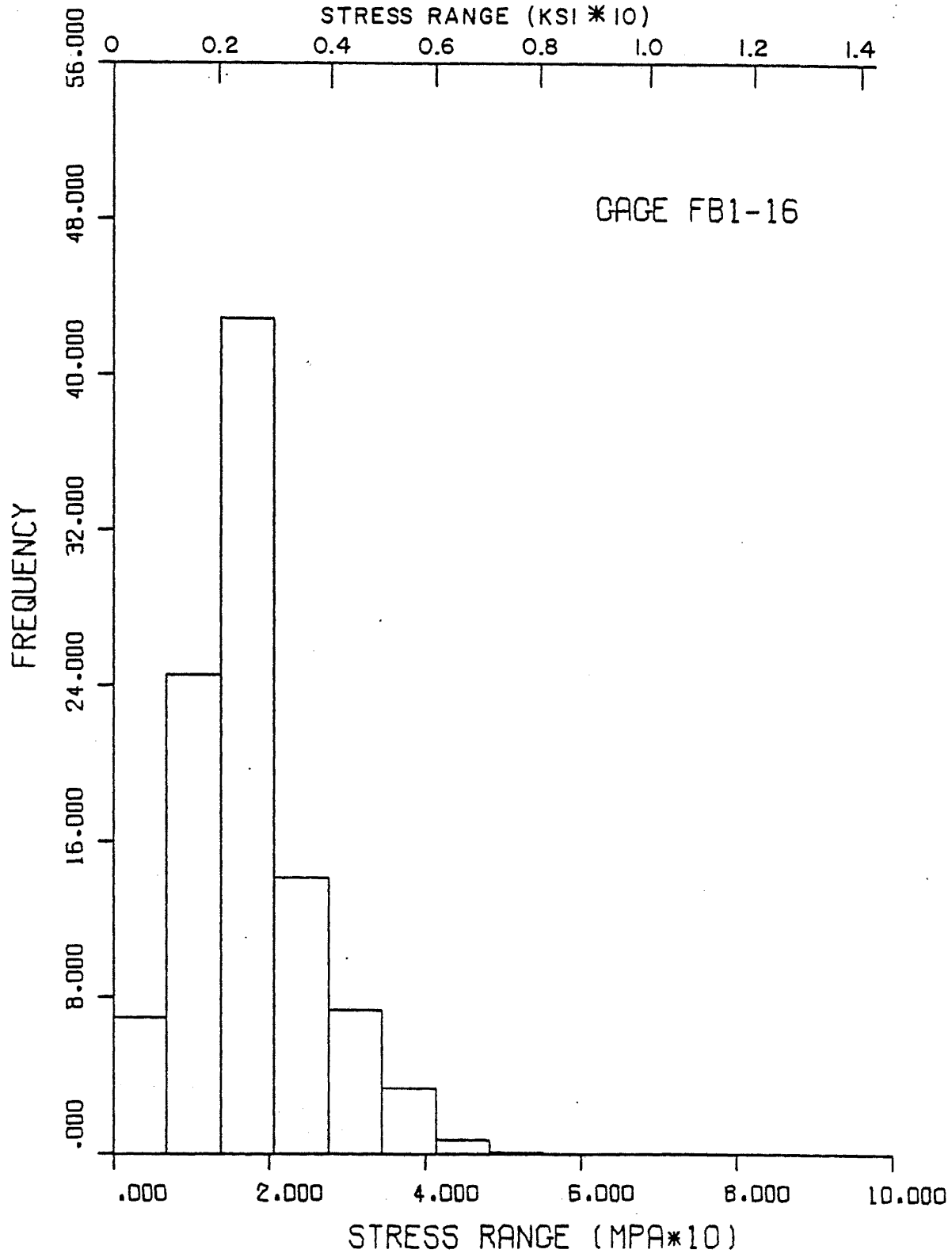

Fig. C21 Stress Range Spectrum for Gage FB1-16 Using Peak to Peak Counting Without Multiple Presence Separation

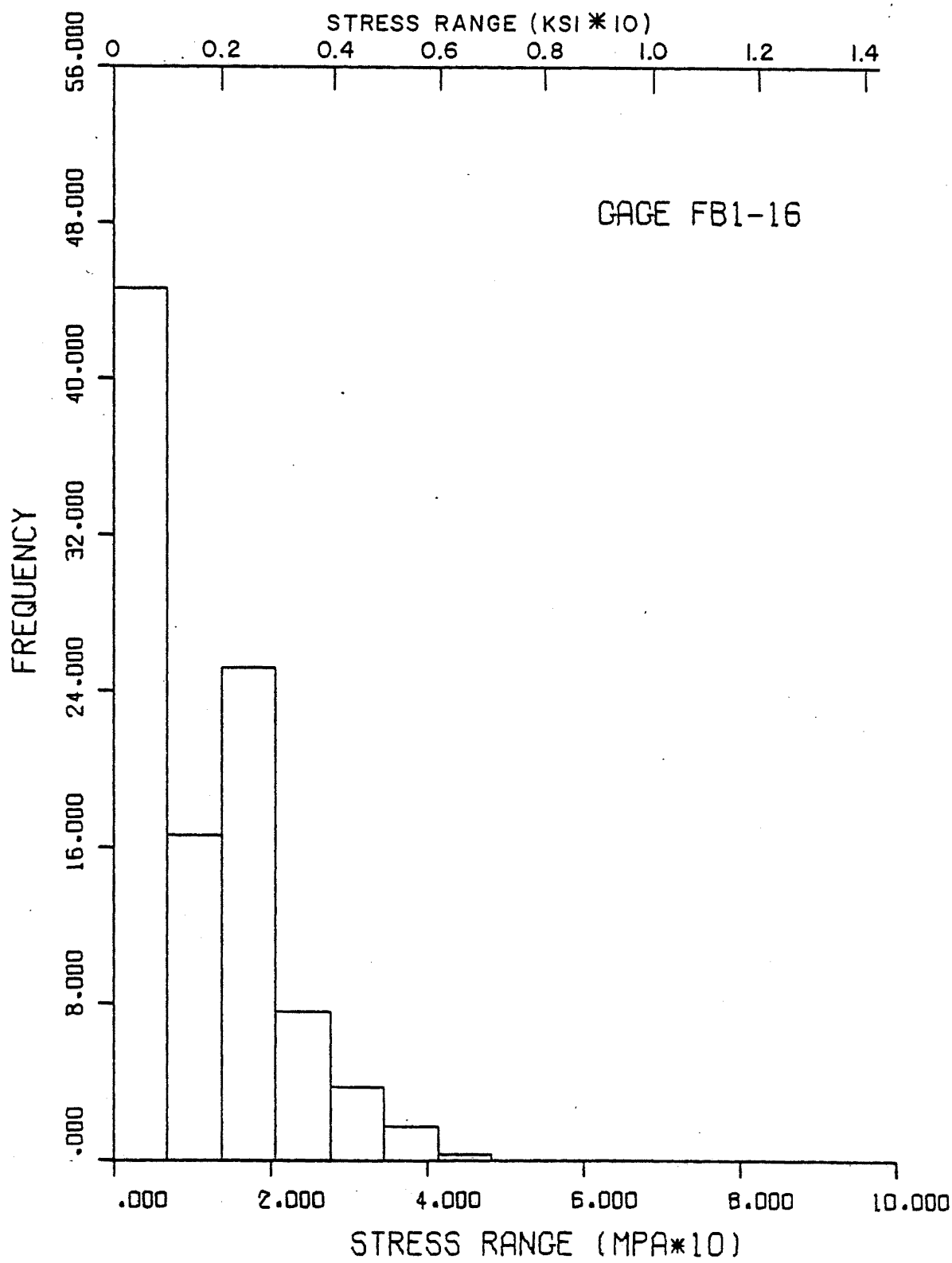

Fig. C22 Stress Range Spectrum for Gage FB1-16 Using Peak to Peak Counting with Multiple Presence Separation

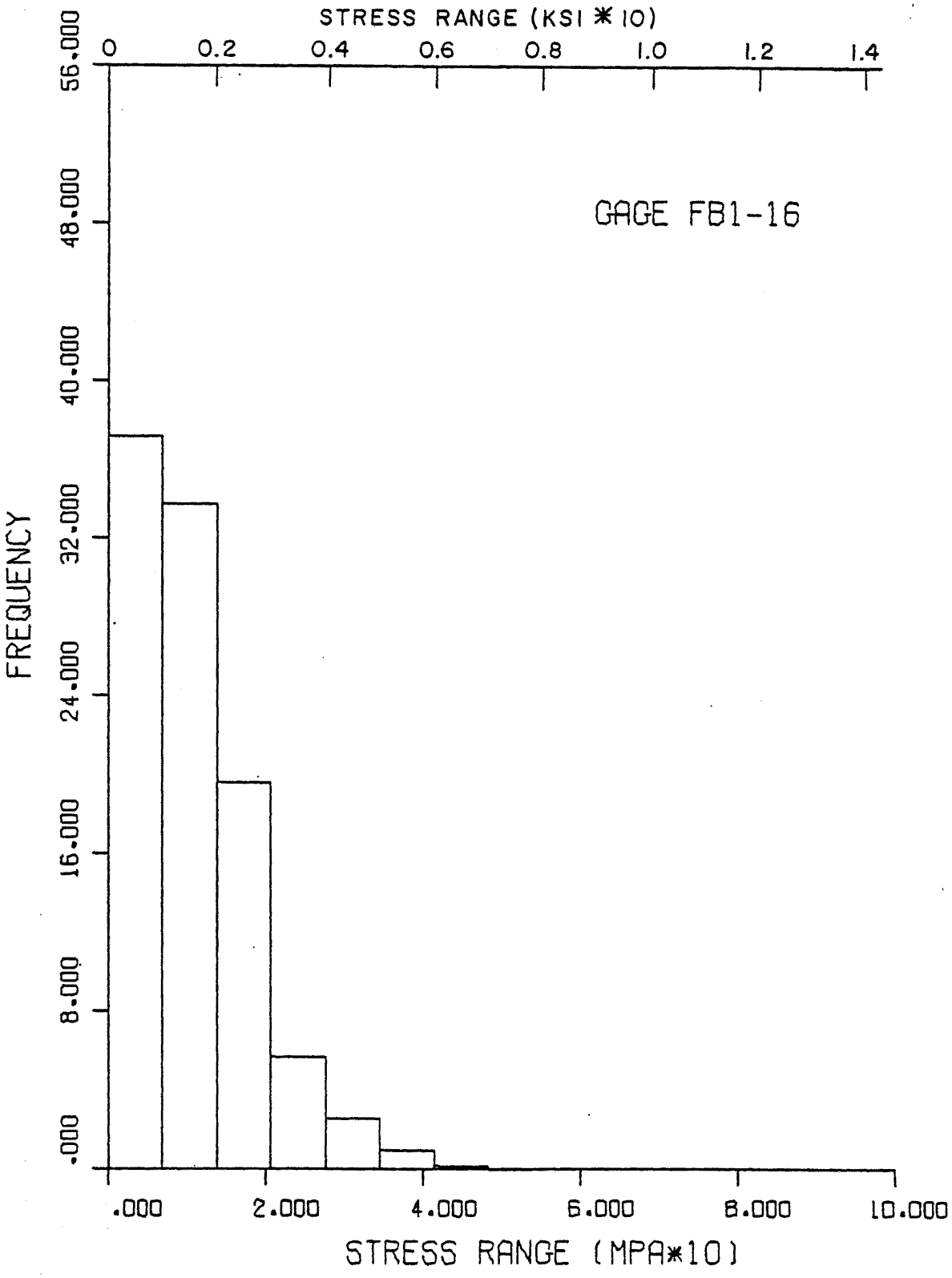

Fig. C23 Stress Range Spectrum for Gage FB1-16
Using Rainflow Counting

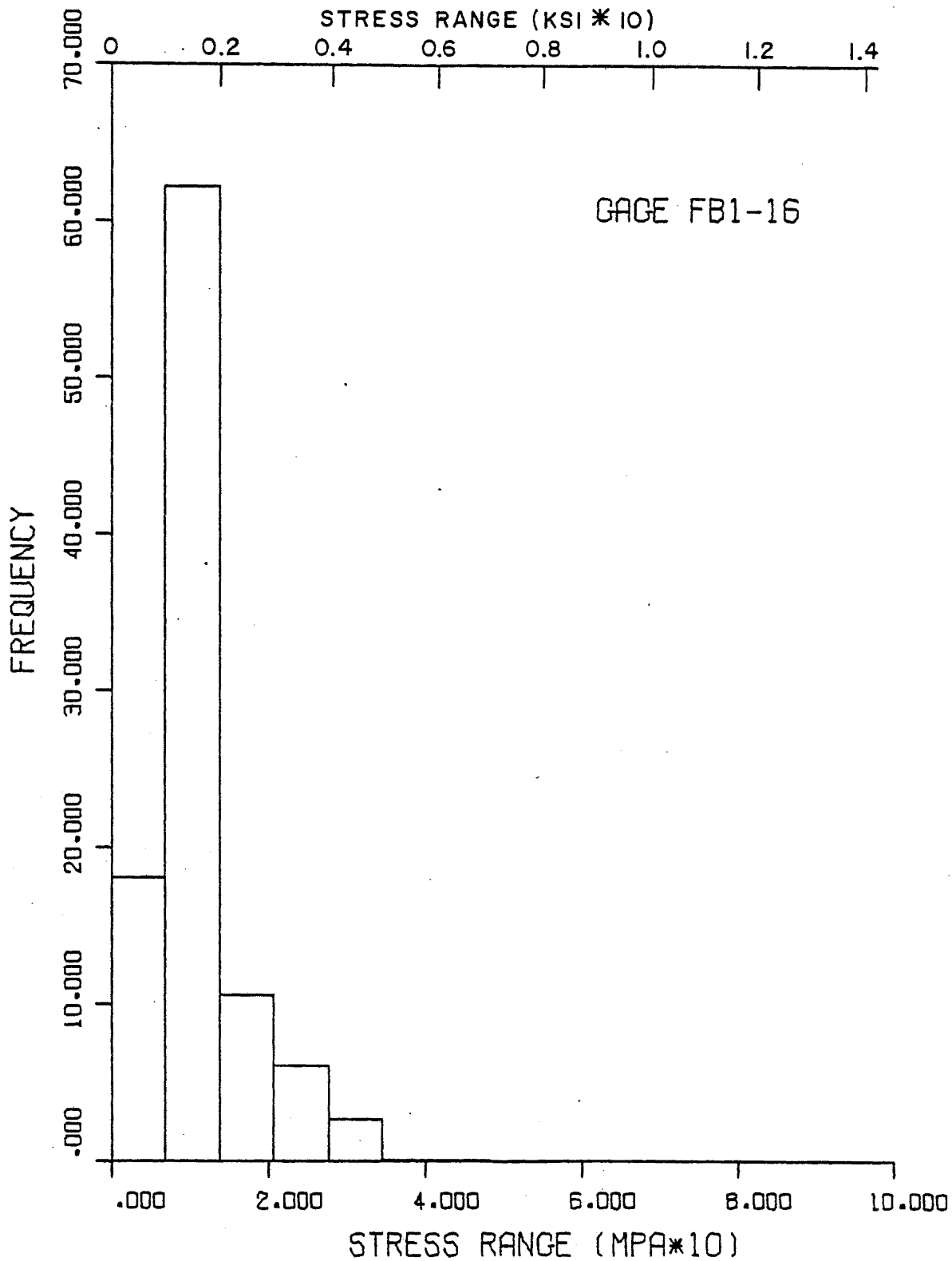

Fig. C24 Stress Range Spectrum for Gage FB1-16
Using Modified Rainflow Counting

APPENDIX D: DERIVATION OF FORMULA TO COMPUTE EFFECTIVE FATIGUE DAMAGE WITH MULTIPLE PRESENCE

Assume that in time, t, N identical trucks cross the bridge, each causing damage d at a detail. Then, the total damage, D, assuming each truck crosses separately is given by

$$D = Nd$$

However, some trucks arrive on the bridge before the last one has left, and the cumulative damage of the two trucks is not 2d, but a factored quantity of 2d, where the factor is a function of the distance between the trucks.

If all possible distances between the trucks that result in multiple presence is divided into discrete intervals, let the number of trucks whose distance behind the truck in front is in the i^{th} interval be n_i. Then, the proportion of trucks whose distance behind the truck in front is in the i^{th} interval is given by:

$$p_i = n_i/N$$

Let the total damage caused by two trucks separated by a distance in the i^{th} interval be $2dr_i$.

It is more convenient for the purpose of deriving a formula, to consider that the leading truck causes damage d, and that the second truck causes damage $f_i d$, such that:

$$d + f_i d = 2dr_i$$

Therefore, $(1 + f_i)\, d = 2dr_i$

and $$f_i = 2r_i - 1$$

Knowing that a fraction p_i of the trucks causes damage $f_i d$, the total damage without ignoring the effect of multiple presence is given by:

$$D_{MP} = \Sigma\ (p_i N)\ (f_i d) + (1 - \Sigma\ p_i)\ Nd$$

$$= Nd\ (\Sigma\ p_i f_i + 1 - \Sigma\ p_i)$$

$$= D\ (\Sigma\ p_i f_i + 1 - \Sigma\ p_i)$$

Hence, the ratio of real to assumed damage is given by:

$$R_F = D_{MP}/D = \Sigma\ p_i f_i + 1 - \Sigma\ p_i$$

Putting $f_i = 2r_i - 1$,

$$R_F = \Sigma\ (2r_i - 1)\ p_i + 1 - \Sigma\ p_i$$

That is, $R_F = 2\ \Sigma\ r_i p_i - 2\ \Sigma\ p_i + 1$

11. REFERENCES

1. Csagoly, P. F., Campbell, T. I. and Agarwal, A. C.
   BRIDGE VIBRATION STUDY, Ministry of Transportation and Communications Report No. RR181, Ministry of Transportation and Communications, Ontario, Canada, 1972.

2. Cudney, G. R.
   THE EFFECTS OF LOADING ON BRIDGE LIFE, Highway Research Record No. 253, Highway Research Board, National Academy of Sciences - National Research Council, Washington, D.C., 1968.

3. Daniels, J. H. and Fisher, J. W.
   FIELD EVALUATION OF TIE PLATE GEOMETRY, Fritz Engineering Laboratory Report No. 386.4, Lehigh University, Bethlehem, Pennsylvania, 1974.

4. Erb, D. P.
   FATIGUE STRENGTH OF TACK WELDED TIE PLATES, Fritz Engineering Laboratory Report No. 386.8, Lehigh University, Bethlehem, Pennsylvania, 1975.

5. Fisher, J. W.
   BRIDGE FATIGUE GUIDE: DESIGN AND DETAILS, Institute of Steel Construction, New York, New York, 1977.

6. Fisher, J. W., Albrecht, P. A., Yen, B. T., Klingerman, D. J. and McNamee, B. M.
   FATIGUE STRENGTH OF STEEL BEAMS WITH TRANSVERSE STIFFENERS AND ATTACHMENTS, NCHRP Report No. 147, Highway Research Board, National Academy of Sciences - National Research Council, Washington, D.C., 1974.

7. Fisher, J. W., Frank, K. H., Hirt, M. A. and McNamee, B. M.
   EFFECT OF WELDMENTS ON THE FATIGUE OF STEEL BEAMS, NCHRP Report No. 102, Highway Research Board, National Academy of Sciences - National Research Council, Washington, D.C., 1970.

8. Fisher, J. W. and Viest, I. M.
   FATIGUE LIFE OF BEAMS SUBJECTED TO CONTROLLED TRUCK TRAFFIC, Paper presented to the International Association for Bridge and Structural Engineering, Seventh Congress, Rio de Janeiro, August 1964.

9. Fisher, J. W., Yen, B. T. and Daniels, J. H.
FATIGUE DAMAGE IN THE LEHIGH CANAL BRIDGE FROM DISPLACEMENT INDUCED SECONDARY STRESSES, Fritz Engineering Laboratory Report No. 386.5, Lehigh University, Bethlehem, Pennsylvania, 1976.

10. Fisher, J. W., Yen, B. T. and Marchica, N. V.
FATIGUE DAMAGE IN THE LEHIGH CANAL BRIDGE, Fritz Engineering Laboratory Report No. 386.1, Lehigh University, Bethlehem, Pennsylvania, 1974.

11. Galambos, C. F. and Armstrong, W. L.
ACQUISITION OF LOADING HISTORY DATA ON HIGHWAY BRIDGES, Public Roads, Vol. 35, No. 8, U. S. Department of Transportation, Washington, D.C., 1969.

12. Galambos, C. F. and Heins, C. P.
LOADING HISTORY OF HIGHWAY BRIDGES, COMPARISON OF STRESS RANGE HISTOGRAMS, Highway Research Record No. 354, Highway Research Board, National Academy of Sciences - National Research Council, Washington, D.C., 1971.

13. Matsuiski, M. and Endo, T.
FATIGUE OF METALS SUBJECT TO VARYING STRESS, Paper presented at the Kyushu district meeting of the Japan Society of Mechanical Engineers, Japan, March 1968.

14. Miner, M. A.
CUMULATIVE DAMAGE IN FATIGUE, Journal of Applied Mechanics, Vol. 12, September 1945.

15. Moses, F. and Pavia, A. P.
PROBABILITY THEORY FOR HIGHWAY BRIDGE DESIGN STRESSES - PHASE II, Department of Civil Engineering, Case Western Reserve University, Cleveland, Ohio, 1976.

16. Slockbower, R. E. and Fisher, J. W.
FATIGUE RESISTANCE OF FULL-SCALE COVER-PLATED BEAMS, Fritz Engineering Laboratory Report No. 386.9, Lehigh University, Bethlehem, Pennsylvania, 1977.

17. Watson, P. and Dabell, B. J.
CYCLE COUNTING AND FATIGUE DAMAGE, Paper presented at Society of Environmental Engineers Symposium on "Statistical Aspects of Fatigue Testing," University of Warwick, England, February 1975.

18. American Association of State Highway and Transportation Officials
1977 INTERIM SPECIFICATIONS, BRIDGES, Washington, D.C.

19. Schijve, J.
THE ANALYSIS OF RANDOM LOAD-TIMES HISTORIES WITH RELATION TO FATIGUE TESTS AND LIFE CALCULATIONS, Fatigue of Aircraft Structures, Pergamon Press, London, England, 1963.

20. Webber, D.
WORKING STRESSES RELATED TO FATIGUE IN MILITARY BRIDGES, Stresses in Service, Institute of Civil Engineers, London, England, 1966.

12. ACKNOWLEDGMENTS

The research reported in this thesis was conducted at Fritz Engineering Laboratory, Lehigh University, Bethlehem, Pennsylvania. The Director of Fritz Laboratory is Dr. Lynn S. Beedle and Dr. David A. VanHorn is the Chairman of the Department of Civil Engineering. The work was part of a study on high cycle fatigue of welded bridge details sponsored by the Pennsylvania Department of Transportation and the Federal Highway Administration of the U. S. Department of Transportation.

Many members of the support staff at Lehigh University gave invaluable assistance in Fritz Laboratory. Mrs. Ruth Grimes typed the manuscript and Mr. Douglas Wiltraut drafted the figures. At the Lehigh University Computer Center the Operations Division under Mr. John H. Morrison and the User Services Division under Mr. Robert A. Pfenning were always ready to offer advice on computing problems. Some of the data reduction was done by Messrs. William L. Allan, Stephen W. Bilan and Dawit Abraham.